KINEMATIC-STABILITY OF MOBILE ROBOT MOVING ON A ROUGH TERRAIN

By
Amjad Ibrahim Massad

Supervisor
Dr. Khaldoun Tahboub

Co-supervisor
Dr. Musa Abdalla

Submitted in Partial Fulfillment of the Requirements for the Degree of Master of Science in Industrial Engineering

Faculty of Graduate Studies
University of Jordan

April, 2005

This thesis (Kinematic Analysis of Mobile Robot Moving on a Rough Terrain) was successfully defended and approved on 28th of April 2005.

Examination committee	**Signature**
Dr. Khaldoun K. Tahboub, Chairman **Assistant Professor of Industrial Engineering**	……
Dr. Musa D. Abdalla, Co-supervisor **Assistant Professor of Mechatronics Engineering**	……
Dr. Mahmoud A. Barghash, member **Assistant Professor of Industrial Engineering**	……
Dr. Mohammad I. Kilani, member **Assistant Professor of Mechanical Engineering**	……
Dr. Mohannad M. Al-Ata, member **Assistant Professor of Mechatronics Engineering** **(Jordan University of Science and Technology)**	……

Dedication

To my mother

Acknowledgement

I would like to express my sincere and deep appreciation to my supervisor Dr. Khaldoun Tahboub who helped and provided me with a truly outstanding cooperation for achieving this work.

Also, I would like to thank Dr. Musa Abdalla for his help, support and encouragement.

Table of contents

List of Tables

List of Figures

NOMENCLATURE

$\|\mathbf{a}\|$	The magnitude of tipover mode axis vector.
$\mathbf{a}_i$	Tipover mode axis vector.
$\hat{\mathbf{a}}_i$	Unit norm tipover mode axis vector for a given ground contact point.
abs (ϕ)	Absolute magnitude of the friction angle.
$\mathbf{C}$	Center of mass.
$\mathbf{c}_i^{IG}$	Coordinate vector.
d_{ij}	Normal distance.
d_t	A distance.
$\mathbf{F}$	External load.
$\boldsymbol{F}_i$	A normal force.
F_{in}	Contact force in the normal direction.
F_{it}	Contact force in the tangential direction.
$\|\mathbf{f}^*\|$	The magnitude of the net force.
$\mathbf{f}_{dist}$	Any other external disturbance force acting directly on the vehicle.
$\mathbf{f}_{grav}$	The gravitational loads.
$\mathbf{f}_i^*$	The new net force vector for a given ground contact point.
$\hat{\mathbf{f}}_i^*$	The unit norm of the new net force vector for a given ground contact point.
$\mathbf{f}_{IG}$	A vector force.

$\mathbf{f}_{\text{inertial}}$	The inertial force.
$\mathbf{f}_{\text{manip}}$	The loads transmitted by the manipulator to the vehicle body.
$\mathbf{f}_{ni}$	Equivalent force couple for a gain ground contact point.
$\mathbf{f}_{r}$	Net force vector.
$\mathbf{f}_{\text{support}}$	The reaction force of the vehicle support system.
$\vec{f}_i$	A position vector of point f_i .
f_i^*	A position vector of point $\vec{f}_i$.
$\mathbf{G}$	Position dependent.
g	Acceleration of gravity.
$\boldsymbol{\Delta h}$	Difference in height.
h_i	A distance.
h	A distance between two points.
$\|\mathbf{I}\|$	The magnitude of tipover axis normal vector.
$\hat{\mathbf{I}}$	A unit norm vector.
$\mathbf{I}_i$	Tipover axis normal for a given ground contact point.
L	An arbitrary vector line.
$\mathbf{1}$	3×3-identity matrix.
m_i	A mass.
$\mathbf{n}_i$	The component of net moment that acting about the c.m for a given ground contact point.
$\mathbf{n}_r$	The net moment acting about the c.m.
O	Center of mass.

$\mathbf{P}_i$	The location of the i^{th} ground contact point.
PE	Potential energy.
$\mathbf{p}_c$	The location of the vehicle center of mass.
p_c	Center of mass point.
$\overrightarrow{p_i p_j}$	A distance vector.
Q	A constant.
$\boldsymbol{R}_i$	An arc radius.
R	Reaction force.
R	A constant.
r_i	A ratio represents the square of tangential force relative to the normal force.
S_{ix}	Zero pitch screw axes parallel to x-axis.
S_{iy}	Zero pitch screw axes parallel to y-axis.
S_{iz}	Zero pitch screw axes parallel to z axis.
$\dot{s}$	Path velocity.
$\ddot{s}$	Path acceleration.
$\mathbf{t}_{tip}$	The time until tipover.
$\tan(\phi)$	Tangent of the friction angle.
$\mathbf{V}$	A perpendicular vector.
$\mathbf{W}$	External load wrench vector.
W_i	The work.
χ_i^{IG}	Coefficient (a contact component).

X_{IG}	A Cartesian coordinate.
y_1^{IG}	Coefficient (a contact component).
Y_{IG}	A Cartesian coordinate.
α	Overall force-angle stability measure.
α	An angle.
$\dot{\vartheta}$	Rate of change of angle.
$\dot{\alpha}$	Time rate of change of dynamic or static of overall force-angle stability measure.
β	An angle.
η_i	The angle between the net force vector and tipover axis normal for a given ground contact point.
μ	The coefficients of friction at the contact points.
σ_i	Sigma that produces the appropriate sign of the angle measure associated with each tipover axis.
Φ	An inclination angle.
ϕ	A friction angle.
ω_{ij}	Rotational velocity.

KINEMATIC ANALYSIS OF MOBILE ROBOT MOVING ON A ROUGH TERRAIN

By
Amjad Ibrahim Massad

Supervisor
Dr. Khaldoun Tahboub

Co-supervisor
Dr. Musa Abdalla

Abstract

Mobile robots are increasingly being used in rough-terrain situations such as military, planetary exploration, scientific discoveries and work assistance. It has been noted that the mobile robots are exposed to be unstable during its movement on the rough-terrains and they may tipover. Accordingly, mobile robots will not be able to perform the missions in appropriate way.

Many factors and variables that affect on stability had been studied in order to form enough knowledge about the probability of turnover from a kinematic point of view. The factors that were studied are surface inclinations, height of the center of mass and the numbers of wheels. The model of this thesis was

simulated using Simulink that is a part of MATLAB software. A proposed multiple shapes and types of the grounds were generated in three-dimensions.

The force-angle stability measure of a mobile robot had been implemented from a previous work and simulated in this research. The kinematic stability measure was applied on four-wheel and three-wheel mobile robot. Several types of surfaces and terrains were introduced to the program in order to investigate the mobile robot kinematic stability. Mobile robots with invert pendulum installed inside their bodies were implemented in order to improve rough-terrain mobility by repositioning their center of mass. The simulation approach and results were good for determining the stability of mobile robots before and after repositioning their center of mass.

Generally, the way to assess stability margin of mobile robots is by concentrating on the minimum stability angle for robot wheels. It was noticed and concluded that kinematic stability is reduced due to decreasing number of mobile robot wheels (for a specific wheels layouts) or increasing the height and the surface inclination. Adjusting the location of the center of mass prevents tipover and improves the stability.

Introduction

1 General Introduction

The mobile robots that operate in field environments will be required to perform tasks on uneven terrain that may cause the system to approach or near approach dangerous tip over instability. To achieve stability for any mobile system while moving on an inclined surfaces or arbitrary rough terrain, an appropriate measure of the tip over stability margin must be defined different definitions of a stability margin measure were developed to assist in avoiding tip over in an automatic systems, or to provide an indication to human operators that tip over may approximately occur (Papadopoulos and Rey, 1996).

Teleported or fully autonomous mobile manipulators or rovers operating in field environments (nuclear, military, and aerospace industries) would require a monitoring of the tip over stability margin. Previous researchers' work was mainly concerned with the vehicle center-of-gravity (c.g.) height and system mass (i.e. heaviness) in order to determine the static machine lateral stabilities (Papadopoulos and Rey, 1996).

While moving through terrain, onboard sensors provide the robot with local accurate information, which robots must use to safely move at speed where the dynamical effects are under control. The requirements are accounting for and determining the physical properties such as inertia and electromechanical properties like steering response when the mobile robot speed is high. If speed

increases, robotic safety and instability margins will generally decrease (Borenstein, 1995).

In this research, an effective tip over stability measure model (the force-Angle stability measure) is adopted because it has a simple graphical interpretation and easear computation in order to enhance the rovers moving on uneven terrain (Papadopoulos and Rey, 1996).

This research aims to adopt a method for kinematic stability for a mobile robot when it moves on inclined surfaces and rough terrains, and then applying this method through simulation on three types of mobile robots:

1. Four-wheel mobile robot.
2. Three-wheel mobile robot (one wheel on the front side and two wheels on the rear side).
3. Three-wheel mobile robot (one wheel on the rear side and two wheels on the front side).

Based on the geometrical distribution of the robot wheels and the force angle stability criterion the three mentioned cases were simulated via simulink in Matlab. Ready derived closed form kinematic equations were used to relate the robot's center of mass and its distributed wheels.

Suggested surfaces such as flat, inclined surfaces with multi degrees of inclination angles and many randomly rough terrains were used in the computer simulation. The method and model will be based on considering gravitational forces due to rover weight and the gravity is assumed to pass through the center of mass of mobile robots.

The basic idea of this adopted technique is measuring the robot's stability in order to be able to obviate the tipover if it may occur. Tipover occurs when the wheels of a robot loose contact with the ground or when moving on steep inclined surfaces. In the static or quasi-static kinematic-stability cases, this occurs when the extension of net forces vector that passes through the center of the mass of a robot falls outside of its base support.

In the static case, stability angles are computed for each tipover axis, which is the angle between the gravitational force vector and the tipover axis normal. The minimum overall stability angle that leads to a stable kinematic control system for a mobile robot was of a great interest. However, in the dynamic case, the analysis are more complicated as robot inertia forces may accelerate the tipping over or may help prevent it even when the projection of the gravity force falls outside of the base support.

In this work, we have restricted the simulation on the quasi-static stability because the principle of work for such robots needs a low ground speed during movement. Accordingly, dynamical forces do not have a large effect on the system behavior.

When the mobile robot looses its stability, it is required to reposition the center of mass of the robot in order to prevent the tipping over. An invert pendulum with a known mass may be installed on the robot body in order to enhance the robot stability.

2 Problem statement and objectives

The proposed mobile robot in the following sections is assumed to be a rover with variable number of wheels supported and connected to the mobile robot body by shoulders and legs. It is required to move on various types of terrains and surfaces that can be regular and flat, or in the other extreme irregular and rough.

During traveling, the rover is exposed to be kinematically unstable with a possibility to turn over due to moving on steep inclinations or climbing on stones and rocks. There are many parameters that affect stability and the probability of turnover from a kinematics point of view.

Our attention in this work will be focused on three main parameters that affect kinematic-stability of mobile robots. These parameters are:

1. The effect of height variable (the height between the center of mass and the ground level) on mobile robot stability.
2. Ground inclination angle (degrees) and its effectiveness on rover stability.
3. Effectiveness of number of rover wheels for a specific wheels distribution and layouts on the stability and mobility with respect to the surfaces and terrains.

The three mentioned parameters effects are to be studied and implemented using computer simulations. Multiple shapes and types of virtual grounds will be generated such as slope less flat surfaces, inclined surfaces, and rough surfaces with hills and valleys.

Since the rover may move through different areas on the rough terrain, some places and positions of the rover will be stable and others their kinematic stability will be compromised.

Matlab engineering software from Math works incorporation will be used to simulate the whole process. Matlab powerful graphics capabilities and unlimited computational power and resources make it the best candidate for this work.

The objectives of the research are as follows:

a) Evaluating some previous used strategies for stability-based kinematic of mobile robots and vehicles.
b) Formulation and implementation of force-angle stability model that can generate the kinematic-stability measure for a mobile robot. Hence, constructing a three-dimensional rough terrain with respect to reference point in order to perform and monitor the rover stability.
c) Improving the performance of the system by building a comprehensive computer program (simulator), and introducing to this program new formulas in order to compute exactly the center of mass location and repositioning the center of mass for the mobile robot in three-

dimensions, so the probability of robot's tipping over can be computed and monitored properly.

d) Analysis of the results by conducting a performance evaluation and comparative analysis for many variables.

3 Organization of the thesis

The thesis is organized and laid out as follows:

The introduction, it contains a general introduction about mobile robot moving on rough terrain and its kinematic-stability measure, with short review for problem basics and its applications and the problem statement and objectives.

Background and literature survey provides previous works. It contains an introduction to kinematic stability and its importance in robotics, energy stability level, and center of mass controlling. It gives an overview of kinematic and dynamic stability, i.e. basic theories, concepts, definitions, advantages and differences among traditional methods. And it describes mobile robot stability approaches and methodologies. The major adopted algorithm is represented in this section, since it provides a description of the problem formulation and solution methodology for kinematic stability of mobile robots, method for measuring the stability angle.

Problem solving methodology includes the steps for solving the problem when the mobile robot is stable and the equations for determining the location of

center of mass. It includes also a method for reconfiguration the center of mass when the mobile robot looses its stability in order to prevent tipping over.

Discussion and results gives detailed computer implementation of the problem. Its function is to transform the manual formulation into applicable simulation program. Matlab generated results are presented and discussed.

Summary, conclusions and recommendations. It gives an explanation and analysis of the results and provides study to the effects of varying kinematic-stability parameters. In addition, recommendations for future extension were proposed.

Background And Literature Survey

1 Introduction

Vehicle systems, which have superior mobility characteristic, are desired in application that requires off-road motion capability. These fields include military application, mining and planetary exploration, and the vehicle may be required to posses varying levels of autonomy. (Sreenivasan and Wilcox, 1994).

For Example, an unmanned planetary mission requires robotic vehicle that have the capability to perform autonomously for long durations. This autonomy is required due to the fact that the speed-of-light, round-trip communication delay to planets is very high and making it impossible for a human operator to direct the robotic. These vehicles must be equipped with excellent sensing and intelligent guidance capabilities. The over all performance of an autonomous vehicle can be improved by maximizing the mechanical mobility characteristic of the vehicle. (Sreenivasan and Wilcox, 1994).

1.1 Stability definitions

Ghasempoor and Sephri (1995) stated that the local stable workspace at any time depends on the linkage configuration, velocities and accelerations of the moving links as well as loading. They defined a basis for determining the energy stability margin.

Definition 1: The equilibrium plane associated with a particular edge of a support boundary is plane containing the edge and with an orientation with respect to the vertical plane such that if the body is rotated around the edge until the center of gravity falls in this plane, the net moment of all present forces and moment around the edge becomes minimum in absolute sense (Ghasempoor and Sephri, 1995).

Definition 2: The energy stability level associated with a particular edge of a support boundary is equal to the work required to rotate the vehicle body (which is subjected to gravitational as well as external and inertial forces / moment) a bout the edge, until the center of gravity reaches the equilibrium plane. The minimum of energy stability levels associated with each edge of the support boundary is the energy stability margin (Ghasempoor and Sephri, 1995).

Messuri and Klein (1985) adopted from developed series definitions and theorems concerning the static stability of a legged machine. The following definitions were the basis for determining if a vehicle is statically stable:

Definition 1: the support pattern associated with a given support state is the convex polygon, in a horizontal plane, which contains the vertical projection of all the supporting feet.

Definition 2: "the magnitude of the static stability margin for an arbitrary support pattern is equal to the shortest distance from the vertical projection of the center of gravity to any point on the boundary of the support pattern. If the pattern is statically stable, the stability margin is positive. Otherwise it is negative".

Definition 3: The support associated with a given support state consist of the line segment which connect the tips of the support feet that form the support pattern.

Definition 4: The energy stability level associated with a particular edge of a support boundary is equal to the work required to rotate the body center of gravity, about that edge, to the position where the vertical projection of the body center of gravity lies a long that edge of the support boundary.

2 Literature survey

A review of the recent approaches is presented in (Sreenivasan And Wilcox, 1994). Their research was in stability and traction control of an actively actuated micro-rover. They addressed the issue of enhancing mobility of actively actuated vehicles by the use of optimal force distribution and controlling the location of the center of the mass of the vehicle body. Their actively actuated vehicles also possessed the ability to vary their configuration and that capability can be used to locate the center of mass of the system to further enhance mobility by providing sufficient traction and ensuring vehicle stability during difficult vehicle maneuvers.

Some of the mobility issues that are relevant to autonomous vehicles include obstacle climbing, ditch crossing, and self- recovery of the vehicle from an overturn failure. An obvious approach to improving the obstacle-climbing and ditch- crossing ability of a vehicle is to increase the size of the vehicle to proportionately reduce the scale of terrain obstacles encountered. This approach has the limitations of increasing the initial cost and the power requirements of the vehicle (Sreenivasan and Wilcox, 1994).

Sreenivasan and Wilcox (1994) dealt with an actively actuated vehicles refer to vehicles that possess independent actuators for the suspension and the locomotion degrees of freedom. Using the actuators can influence the contact forces at the vehicle-terrain contact points. It was assumed that (Gofor) had the capability to vary his geometry to accommodate for terrain obstacles.

A measure of machine stability for moving base manipulator was conducted by (Ghasempoor and Sepehri , 1995), they presented a scheme to monitor the potential of tipping over for moving base manipulators. They extended a method to quantitatively include the effect of all factors relevant to the stability of moving base manipulator. These factors included vehicle top heaviness, rugged terrain conditions, inertial and external reactions arising from the manipulation of the implement. Their research was directed to teleoperated heavy – duty hydraulic machines that are used in forestry and construction industries.

A dynamic motion planning of autonomous vehicles was conducted by (Shiller and Yu-Rwei, 1991), they presented a method obtaining the geometric path and vehicle speeds that minimize motion time considering vehicle dynamics, terrain topography, obstacles and surface mobility for planning the motions of autonomous vehicle moving on a general terrain. Several constraints between the vehicle and ground are considered to ensure vehicle dynamic stability along the path.

These constraints are (Shiller and Yu-Rwei, 1991): (a) limits on engine torque, (b) limits on the coefficient of friction (sliding constraint), (c) positive contact between the vehicle and ground (contact constrain), and (d) tip-over. The tip over constraint was obtained by expressing the condition for which the vehicle is about to tip over in term of path velocity and acceleration $s, \dot{s}, \ddot{s}$,

and terrain topography. Shiller and Yu- Rwei (1991) had a limiting case for this constraint occurs when the entire weight shifts to one side of the vehicle, and the wheels on the other side are about to lose contact with ground. As seen from Figure (1), if the vehicle is about to tip over counter clockwise (CCW), then the total reaction force R is applied on the left wheel, and the friction force f_y points downward, as shown (the friction force can be applied in the other direction, but then the vehicle will not tip over (CCW). The vehicle will not tip over (CCW) if the resultant moment created by the reaction and the friction forces around its center of mass is positive.

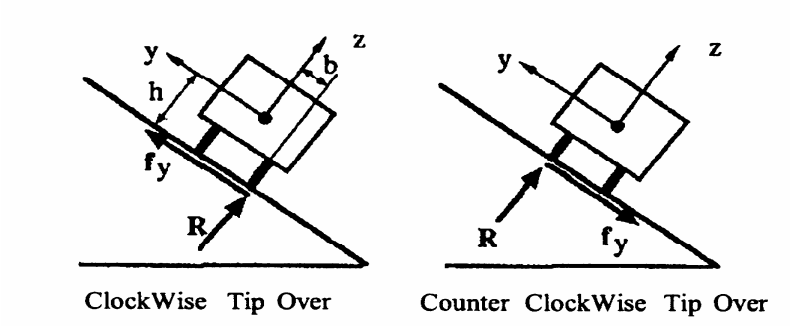

Figure (1): Tip over constraint (R and f_y) when the entire weight shifts to one side of the vehicle. (Shiller and Yu- Rwei, 1991).

Ghasempoor and Sepehri (1995) defined three steps to calculate the energy stability level; finding the equilibrium plane, calculation of the work required to rotate the center of gravity to the equilibrium plane and finally calculation of the work done by destabilizing forces and moments other than gravity loading during the same rotation of the machine. They noted that the gravity

force is conservative while all other destabilizing forces and moments are non-conservative. That leads to conclude that the amount of work depends on the path traveled.

A displacement analysis of an actively articulated wheeled vehicle configuration with extensions to motion planning on uneven terrain was conducted by (Sreenivasan and Waldron, 1996), They presented a displacement analysis of actively articulated wheel vehicles on uneven terrain. The used vehicle in this search has the ability to adapt to variation in the terrain and they can influence the forces at the wheel – terrain contact locations. They possessed special mobility capabilities such as obstacle climbing and self – recovery from an over – turn failure. The displacement analysis led to multiple solutions due to the inherent no linearity in the position kinematics equations. Geometric reasoning had been used to identify the particular configuration that represents the correct vehicle geometry on the terrain.

A simple dynamic model was used by (Shiller and Yu- Rwei, 1991) to demonstrate the approach. Except for the tip over constraint, the reaction and friction forces were translated to the mass center to avoid solving explicitly for the reaction forces at the contact points.

Sreenivasan and Waldron (1996) pointed out that the uneven terrain is, in general, a complex nonlinear surface. And the position kinematics problem

becomes difficult if the terrain is characterized by nonlinear functions. A piece – wise planar was assumed to achieve a simplification. They presented a kinematics analysis that assumes the vehicle and the terrain are rigid. In the presence of the compliance or soft soil, the obtained solutions can be used as initial conditions of a dynamic simulation that uses these effects to obtain more accurate solutions.

Failures such as the interference of the vehicle with the terrain on with itself and the inability of the vehicle to get over large obstacles or to cross wide ditches are geometric failures. Failures such as lifting of a wheel off the ground due to negative contact forces normal to terrain, or large slip rates due to large tangential to normal contact force ratios at the wheel terrain contact points are force failures.

For a vehicle comprised of "n" modules, (Sreenivasan and Waldron, 1996) showed that the mobility of the vehicle is "3+n". And by knowing the values of these "3+n" motion coordinates had been solved using the "2n" wheel-terrain contact constraints. A polynomial system of degree eight had been solved to obtain the configuration of the master module (middle module), and a polynomial system of degree thirty two had to be solved to obtain the configurations of each of the other modules.

Another research that dealt with the stability measurement was presented by (Davidson and Schweitzer, 1990); they measured the margin of static stability by using normalized values for virtual power. Each value takes in consideration the motion about an axis of rotation that is associated with one made of potential ever overturning. Static stability was treated for spatial positioning of the feet and for both three and four feet in contact the ground.

Davidson and Schweitzer (1990) included the external reaction loads at the tool and the load from a tethering cable – winch arrangement. They included also the inertial loads from a heavy tool such as an excavating arm in a quasi – static manner. They calculated the values for normalized virtual power with relation to a geometrical description of stability of the vehicle as if it were operating on level ground.

Sreenivasan and Waldron (1996) stated that it is necessary to obtain appropriate paths for the system to follow to reach its goal points on the terrain. The selection of a path may be based on considerations such as system safety. And the planning algorithms shall be required to look for geometric failures and force failures.

Davidson and Schweitzer (1990) had utilized screw-mechanics and geometry to develop (1) an algorithm for computing, in real time, the instability of

four-legged vehicles on very rough terrain, and (2) a two-dimensional graphical display of their proximity. They pointed out when a vehicle would become unstable by sliding down the hill, or by a combination of sliding and rolling as a result of soil failure, then more sophisticated treatment would be required.

Another stability method, which was utilized to maintain stability of a vehicle during moving on rough-terrain, was presented by (Messuri and Klein, 1985). This research used a legged vehicle, which offers the potential of increased mobility for traversing rough-terrain, and, by using an improved stability measure, which can be automatically optimized. They took in consideration the effect of constraints on the kinematical limits of individual legs that leads to a scheme for automatic body regulation. So they incorporated an automatic body regulation schemes into the vehicle control algorithm to provide a high degree of vehicle maneuverability so as to reduce the operator's burden.

A physics-based planning for planetary exploration was conducted by (Farritor and Dubowsky, 1998) presented a planning methodology based on a physics-based model of the rover and environment. They developed a plans that allow a rover to perform a mission while considering constraints such as power, actuator, wheel slip and vehicle stability limits.

Farritor and Dubowsky, (1998) stated that the requirement of any model is determing the rover attitude and configuration as a function of the terrain. This needs to calculate the load distribution on the wheels, the rover's stability, actuator outputs, etc. in their work, the rover's configuration, position and attitude was fully defined by ten parameter: three for the position (x,y,z) in the fixed frame of the body, three for attitude (yaw, roll and pitch angles respectively) and four for the configuration of the rocker-bogie mechanism.

Messuri and Klein (1985) studied the ability to find the position to which the body center of gravity could be moved in order to obtain the maximum energy stability margin for a given configuration, i.e. moving to the highest level on the energy stability margin surface. They applied the following definition: An optimally stable position is any position in the plane of the body at which the energy stability margin would be maximal if the center of gravity were moved to that position.

Farritor and Dubowsky, (1998) used in their work quasi-static force balance to determine if the rover will tip, if the wheels will slip, if the rover will slide, the amount of energy consumed and actuator saturation. The previous information is critical to determine the fitness of an action plan. Their implemented force analysis assumed that the ground couldn't apply to a large moment, in any direction, to the wheels. They stated that their assumption

prevents the three-dimensional force analysis from becoming highly statically indeterminate.

3 Formulations

3.1 General Formulations

Sreenivasan and Wilcox (1994) denoted the contact points by P_i and the local normals at P_i were denoted by the unit vector n_i, see Figure (2).

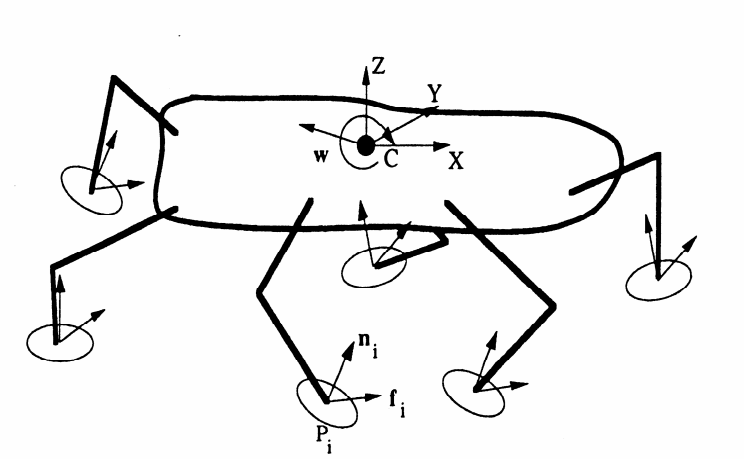

Figure (2): Forces distribution in an activity actuated vehicle. (Sreenivasan and Wilcox, 1994).

The contact force vectors were denoted by f_i and c in the center of mass of the system. The dynamic equation of vehicle was written as follows:

G f = W. ……(1)

Where **G** is a position dependent 6×3n matrix (n = Number of contact points), **f** is the 3n×1 contact force vector, and **W** is the 6×1 external load wrench vector consisting of the commanded inertial forces and torques and the weight of the system.

G = $[S_{1x}\ S_{1y}\ S_{1z}\ S_{2x}\ S_{2y}\ S_{2z}\ldots\ldots\ldots\ S_{nx}\ S_{ny}\ S_{nz}]$ where $S_{ix,}$ S_{iy} and S_{iz} are the Zero pitch screw axes parallel to the x, y and z axes passing through the point P_i.

f = $[\ \mathbf{f}_1^T\ \mathbf{f}_2^T\ \ldots\ldots\ \mathbf{f}_n^T\ ]^T$. The control issue involved computation of the contact force vector **f** for a desired wrench **W**. They determine the ratio of the tangential contact force component on the plane orthogonal to $n_{i,}$ and the normal contact force component along n_i, at $P_{i,}$ was denoted by r_i. Therefore, $r_i = [\text{norm}\ \{\ \mathbf{f}_i - (\ \mathbf{f}_i^T\ n_i\ )\ n_i\ \}\ /\ \mathbf{f}_i^T\ n_i\ ]$.

They formulated the force distribution problem, from the point of view of vehicle traction and stability as follows:

1. Minimizing the maximum force ratio r_i to improve traction. The forces were constrained by the six equality constraints in the previous dynamic equation.
2. They ensured that the normal components of the contact force vectors, $(f_i^T n_i)$, is positive. And this was required to maintain vehicle stability because the terrain cannot support negative normal forces.

The ability to vary the mass and the force distribution in Sreenivasan's actively actuated vehicles can be exploited by using the following scheme:

1. They identified the set of contact points P_i where the normal vectors n_i were "suitable" from the point of view of traction. They had chosen n_i that have a large component along the load wrench **W**. Then, moving the center of mass of the system **C** as close to these contact points. And this redistribution of mass was very useful when the vehicle is trying to negotiate an obstacle. They explained that the contact points on the obstacle would have "unsuitable" normal vectors. So the center of mass should be moved toward the contact points that are not on the obstacle. Sreenivasan's and Wilcox assumed that there are no limits on the location of **C** with respect to P_i. Also they explained that if **W** is a pure force, **C** could be chosen such that **W** passes through the point that has the most suitable normal. And that is a marginal stability condition because that leads to zero normal forces at all other contact points. Hence, *there is a trade – off between the traction requirements and vehicle stability.* The location of **C** has to be chosen so that sufficient traction and stability is achieved.

2. When the desired location of **C** is identified, the matrix **G** is fixed. The desired contact forces can be obtained by using the under constrained force distribution equation, and by solving an optimization problem wherein the maximum r_i is minimized.

Sreenivasan and Wilcox (1994) explained in their research force distribution that act on the Gofor wheels which operating on an uneven terrain, see Figure (3). They assumed that the contact normals are the same at the two front wheels. In their work the friction coefficient was assumed to be the same at all the contact points. They defined F_{in} is the contact force along the terrain normal vector at the point contact and F_{it} is the contact force in the tangential direction at the point of contact. The vector $\mathbf{f}_{iG}$ represents the vector sum of inertia and gravity forces. They simplified a dynamic model of the vehicle by obtaining the combined masses of the wheels and the forks onto the body. They stated that this simplification is justified because typically the vehicle body carries a major of the onboard sensing and computing hardware and is expected to be much heavier than the wheels and the forks. Point O represents the center of mass of the body and the lumped masses.

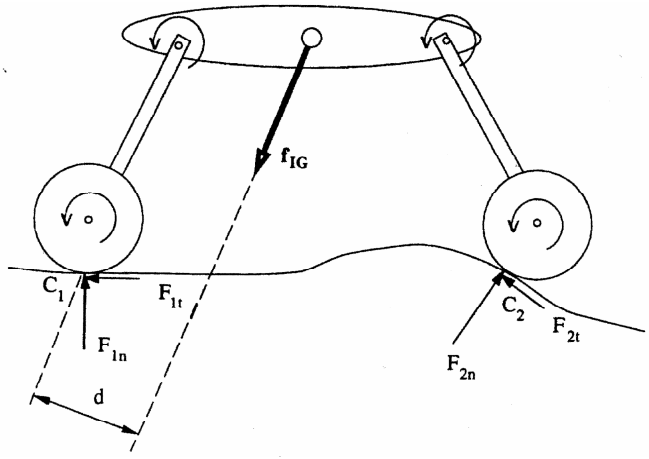

Figure (3): Force distribution.(Sreenivasan and Wilcox, 1994).

The dynamic equations of the vehicle in figure (3) was formulated by (Sreenivasan and Wilcox, (1994) as follows:

$$\mathbf{G\,f = W} \ldots\ldots\ldots\ldots\ldots\ldots \quad (2)$$

Where, **G** is a 3×4 matrix the elements of which are a function of position. $\mathbf{f} = [\mathbf{F}_{1t,}\ \mathbf{F}_{1n,}\ \mathbf{F}_{2t,}\ \mathbf{F}_{2n}]^T$, and **W** is a 3 ×1 vector composed of the inertial and gravity forces. Equation (2) represented three equations in the four unknown contact forces. Therefore, there is a degree of freedom involved in the solution of the unknown **f** from Equation (2).

Sreenivasan and Wilcox (1994) presented two mobility issues of the vehicle:

1. Overall vehicle stability (Keeping it from toppling over).
2. Slipping at the contact points.

Their work introduced a definition to reduce the slip at the contact points; the ratio of the tangential to the normal force has to be minimized. Refer to Figure (4) which give atypical variation of slip rates with respect to the ratio of the tangential to normal forces. They let the square of the ratio $(F_{it} / F_{in})^2 = r_i$

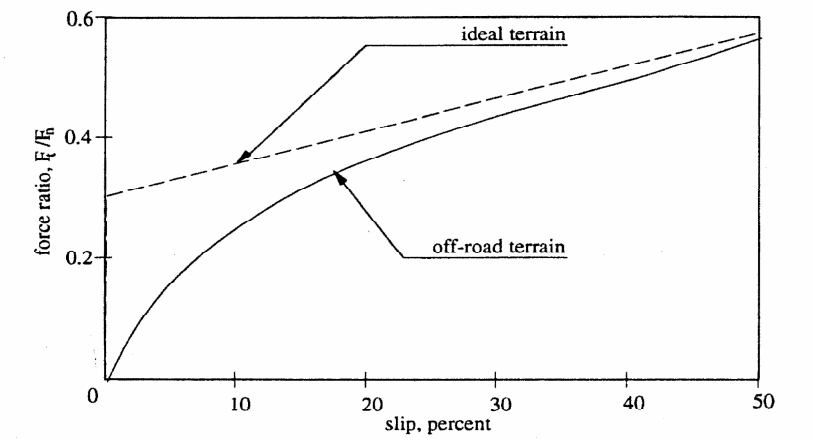

Figure (4): Variation of percentage slip with respect to the contact force ratio. (Sreenivasan and Wilcox, 1994).

In their work, two manners were proposed to minimize the slip for a given terrain and a desired kinematics state of the vehicle:

1. Control of center of mass (CCM): they proposed that the vehicle configuration, is changed so that a large part of the vehicle forces are supported by the contact point that has the "best" contact normal. And they stated that the best contact normal refers to the normal vector that has the largest component along the vector $\mathbf{f}_{IG}$. So in Figure (3), the best contact normal is the normal vector at $\mathbf{C}_1$. Therefore, the fork joint positions have to be changed so as to minimize d, the perpendicular distance from point $\mathbf{C}_1$ to the point $\mathbf{f}_{IG}$. They pointed out that if the vector of $\mathbf{f}_{IG}$ goes beyond point $\mathbf{C}_1$ (negative d), the vehicle becomes unstable. Which means that improving traction leads to lowered stability and vice- versa. And if d is Avery small positive number, the slip is

minimized. And for a desired kinematics state, the matrix **G** and the vector **W** are fixed.

2. Optimal force distribution: for the fixed values of **G** and **W.** the researchers noted that there are a one infinity set of solutions for **f** from equation (2), and the optimal solution is the particular vector **f** that minimizes the maximum of the square of the ratios $\mathbf{r}_i$. They proposed $\mathbf{\Phi}(\mathbf{f}) = \max_i \{\mathbf{r}_i\}$.

The optimization problem was stated as follows:

Minimize $\mathbf{\Phi}(\mathbf{f})$ with the equality constraint $\mathbf{G\,f = W.}$

They verified that the optimal solution of the above problem satisfies the equality $\mathbf{r}_1 = \mathbf{r}_2$. They considered force distribution in finger grasping with three points of contact. But in this problem the application was applied to the two contact points. Following to that, the optimal **f** can be obtained by solving the three scalar linear equations by Equation (2) along with the nonlinear constraint.

$(F_{1t} / F_{1n}) = (F_{2t} / F_{2n})$. ……(3)

Then Sreenivasan and Wilcox noted that $\mathbf{f}' = [\ F_{1t},\ F_{1n},\ F_{2t}\ ]^T$. And they proposed $\mathbf{g}_i$ represent the ith column of matrix **G**, and let $\mathbf{G}' = [g_1,\ g_2,\ g_3]$. Then Equation (2) was rearranged to obtain the following:

$$\mathbf{G}'\mathbf{f}' = \mathbf{w} - \mathbf{g}_4 F_{2n} \qquad \text{.....(4)}$$

They showed that unless $\mathbf{C}_1$ and $\mathbf{C}_2$ are coincident (a trivial case), the matrix $\mathbf{G}'$ is nonsingular. Therefore, Equation (4) was used to solve for F_{1t}, F_{1n} and F_{2t} in terms of F_{2n} to obtain:

$$F_k = p_k F_{2n} + q_k \qquad \text{.....(5)}$$

Where k =1t, 1n, and 2t. Equations (3) and (5) led to the following:

$$\left\{\frac{p_{1t}F_{2n} + q_{1t}}{p_{1n}F_{2n} + q_{1n}}\right\} = \sigma\left\{\frac{p_{2t}F_{2n} + q_{2t}}{F_{2n}}\right\}, \sigma = \pm 1 \qquad \text{.....(6)}$$

Equation (6) yields four solutions for F_{2n}. The values of F_{1t}, F_{2n}, and F_{2t} were calculated from Equation (5). A solution set that includes negative values of F_{1n} or F_{2n} is undesirable because negative normal force cannot be generated at the contact points. Sreenivasan and Wilcox concluded the evaluation of the optimal contact force that are required to generate the desired kinematics state of vehicle, Sreenivasan and Wilcox (1994) investigated the marginally stable vehicle geometries, and vehicle geometries that lead to marginal traction. As shown in Figure (5), the coordinate system $x_{IG} - y_{IG}$ (frame IG) is such that y_{IG} is along the vector F_{IG} and the origin is at O. This research proposed the angle ε_i, which represents the angle of inclination between the contact normal at $\mathbf{C}_i$ and the axis y_{IG}. They used CCM; an improvement in

over all traction was achieved. They assumed an ideal slip model, the a necessary condition for zero slip at the two contact points in that the friction angle at the contact points must be larger than at least one of the two ε_i. Even if this condition is not met, CCM along with optimal force distribution can be used to minimize slip at the wheels.

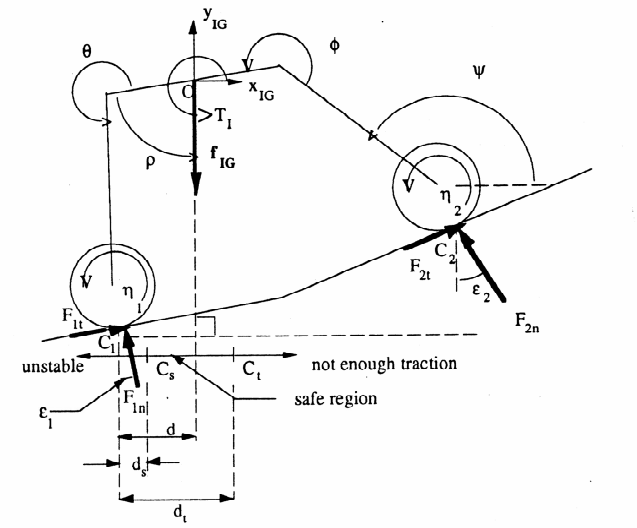

Figure (5): Stability versus traction. (Sreenivasan and Wilcox, 1994).

Sreenivasan and Wilcox (1994) mentioned a trivial case was the contact normals at C_1 and C_2 are parallel. In this situation, CCM does not lead to improve traction. So during a time step, if the two angles ε_i are equal, CCM is not employed for that time step. They concluded that optimal force distribution is still performed. The ideal slip model was assumed and the coefficients of friction at the contact points were assumed to be μ. The angle of iclination of the vector $\mathbf{f}_{IG}$ with the body is ρ. They let $\mathbf{c}_i^{IG}$ be the

coordinate vector of point C_i in frame IG. They let also $\mathbf{c}_i^{IG} = [x_i^{IG}\ y_i^{IG}]^T$ and $\mathbf{f}_{IG}$ be the norm of the vector $\mathbf{f}_{IG}$. The dynamic equations for the vehicle system were as follows:

$$F_{1t}\cos(\varepsilon_1) - F_{1n}\sin(\varepsilon_1) + F_{2t}\cos(\varepsilon_2) - F_{2n}\sin(\varepsilon_2) = 0 \quad \text{.....(7)}$$

$$F_{1t}\sin(\varepsilon_1) + F_{1n}\cos(\varepsilon_1) + F_{2t}\sin(\varepsilon_2) + F_{2n}\cos(\varepsilon_2) = f_{IG} \quad \text{.....(8)}$$

$$\{F_{2t}\sin(\varepsilon_2) + F_{2n}\cos(\varepsilon_2)\}x_2^{IG} - \{F_{2t}\cos(\varepsilon_2) - F_{2n}\sin(\varepsilon_2)\}y_2^{IG} + \{F_{1t}\sin(\varepsilon_1) + F_{1n}\cos(\varepsilon_1)\}x_1^{IG} - \{F_{1t}\cos(\varepsilon_1) - F_{1n}\sin(\varepsilon_1)\}y_1^{IG} + T_I = 0 \quad \text{..... (9)}$$

Sreenivasan and Wilcox verified that if the center of mass O is located such that $\mathbf{f}_{IG}$ passes through C_t, then the vehicle configuration was assumed to be one of the marginal traction. The difference between the X_{IG} coordinate of C_t and C_1 is the distance d_t. The variable d_t is to be evaluated (refer to Figure (5)). The coefficient of y_1^{IG} and y_2^{IG} are contact components along the x_{IG} direction. These forces are expected to be small and they are equal and opposite to each other (from Equation (7)). And that means the moments contributed by the terms y_1^{IG} and y_2^{IG} are expected to be small. But they assumed y_1^{IG} and y_2^{IG} to be constant and equal to their values at the current time step, in the evaluation of d_t. CCM was assumed to be performed by actively controlling the position of one actuator and by locking the other actuator.

For the configuration of Figure (5). Sreenivasan and Wilcox made the fork angle θ vary to control the value of *d*. the fork angle ϕ was kept constant. So the variation of x_1^{IG} is much larger as compared to x_2^{IG} during one time step and x_2^{IG} was assumed to be constant, and equal to its value at the current time step during their analysis. The previous assumptions, Equations (7) – (9) represent three linear equations in the five unknowns F_{1t}, F_{1n}, F_{2t}, F_{2n} and x_1^{IG}. Sreenivasan and Wilcox implemented two conditions to satisfy the marginal traction:

$$F_{1t} = \sigma_1 \mu F_{1n} \qquad F_{2t} = \sigma_2 \mu F_{2n}$$

Where σ_1, $\sigma_2 = \pm 1$. For marginal traction, $r_1 = r_2 = \mu^2$ (according to Eq. (10)).

They stated that in a situation where one of the two r_i is equal to μ^2, and the other is not equal to μ^2 (say, equal to μ'^2), then using optimal force distribution, the value of the two r_i can be made equal to a value ν^2 that lies between μ^2 and μ'^2. Equations (7)-(10) are five equations in the five unknowns F_{1t}, F_{1n}, F_{2t}, F_{2n} and x_1^{IG}. Substitute Equation (10) in Equations (7) and (8):

$$\{\sigma_1 \mu \cos(\varepsilon_1) - \sin(\varepsilon_1)\}F_{1n} + \{\sigma_2 \mu \cos(\varepsilon_2) - \sin(\varepsilon_2)\}F_{2n} = 0 \quad \ldots\ldots(11)$$

$$\{\sigma_1 \mu \sin(\varepsilon_1) - \cos(\varepsilon_1)\}F_{1n} + \{\sigma_2 \mu \sin(\varepsilon_2) + \cos(\varepsilon_2)\}F_{2n} = f_{IG} \text{.....(12)}$$

Equations (11) and (12) can be used to solve for F_{1n}. The two equations are invertible provided det (**H**) $\neq 0$, where:

$$\mathbf{H} = \begin{bmatrix} \sigma_1 \mu \cos(\varepsilon_1) - \sin(\varepsilon_1) & \sigma_2 \mu \cos(\varepsilon_2) - \sin(\varepsilon_2) \\ \sigma_1 \mu \sin(\varepsilon_1) - \cos(\varepsilon_1) & \sigma_2 \mu \sin(\varepsilon_2) + \cos(\varepsilon_2) \end{bmatrix}$$

Case 1 ($\sigma_1 = \sigma_2 = \sigma$):

For this case, det (**H**) = (μ^2+1) sin($\varepsilon_2 - \varepsilon_1$). Therefore **H** is singular only if $\varepsilon_2 = \varepsilon_1$. And that is the trivial situation where CCM is not relevant.

Case 2 ($\sigma_1 = -\sigma_2 = \sigma$):

H is singular only if $\tan(\varepsilon_2 - \varepsilon_1) = \frac{2\sigma\mu}{\mu^2 - 1}$. Let $\mu = \tan(\phi)$, where ϕ is the friction angle. Then, for $\tan(\varepsilon_2 - \varepsilon_1) = \sigma \tan(2\sigma)$, **H** is singular. And that lead to the following condition for singularity of **H:**

$$(\varepsilon_2 - \varepsilon_1) = \text{abs}(2\phi) \text{ .....(13)}$$

Marginal stability represents a situation where the vehicle begins to topple over (Sreenivasan and Wilcox, 1994). And this is equivalent to zero contact

force components at one of the two contact locations. They had implemented the configuration of Figure (5):

$$F_{2t} = F_{2n}. \quad \ldots\ldots\ldots\ldots\ldots\ldots\ldots\ldots(14)$$

Equations (7) – (9) and (14) represent 5 equations in the five unknown $F_{1t,}$ F_{1n}, F_{2t}, F_{2n} and χ_1^{IG}. These equations can be solved to obtain χ_1^{IG}. A safety factor (δ_t) was applied to obtain $d_s = \chi_1^{IG} - \delta_s$. So this characteristic marginal stability. Sreenivasan and Wilcox, (1994) explained that for the vehicle to be stable, and free from slip at the contact points, the previous analysis requires the variable d to be contained in the interval $[d_s, d_t]$.

A general coordinate system was proposed by (Ghasempoor and Sepehri, 1995) as shown in Figure (6). Frame **XYZ** { $\mathcal{M}$} was attached to the vehicle body at point P and it was called machine coordinate system. f_1 , f_2, …., are coordinates contact points. Gravity frame $\overline{XYZ}$ was defined with the origin always at the center of gravity of the machine. In general, the two coordinate systems were separated by a translation and two attitudinal rotations for roll and pitch of the machine frame with respect to the gravity frame.

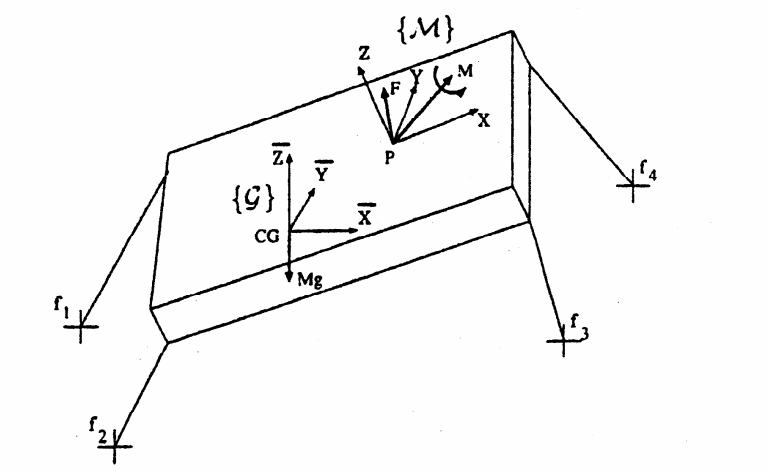

Figure (6): Machine and gravity coordinate frame. (Ghasempoor and Sepehri, 1995).

Referring to Figure (7), f_1 and f_2 were the two adjacent contact points forming one edge of the support boundary as assumed by (Ghasempoor and Sepehri, 1995). $\bar{b}$ is a unit vector in direction of a line connecting f_1 and f_2.

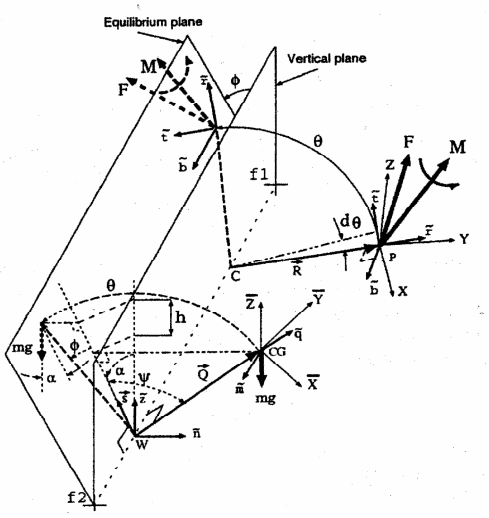

Figure (7): energy stability level calculation.(Ghasempoor and Sepehri,1995).

$\vec{f}_1$ *and* $\vec{f}_2$ are the position vectors of points f_1 and f_2 described in the frame $\{\mathcal{G}\}$

and $\vec{R}$ is a vector orthogonal to $f_1 f_2$, *i.e.,*

$$\vec{R}\ \tilde{b}\ = 0$$

Vector $\vec{f}_1 \boldsymbol{C}$ connecting point $\boldsymbol{C}$ to point f_1 was defined as

$$\vec{f}_1 \boldsymbol{C} = \boldsymbol{\lambda}\tilde{b}$$

And from the relation

$$\vec{f}_1 + \boldsymbol{\lambda}\tilde{b} = -\ \vec{R}$$

They solved for $\boldsymbol{\lambda}$

$$\boldsymbol{\lambda} = \frac{\left(\left(\vec{f}_1\right)\left(\tilde{b}\right)\right)}{b^2}$$

Where $b^2 = 1$. That's lead to $\vec{R}$ can be found from the following relation,

$$\vec{R}\ = \left(\vec{f}_2\ \tilde{b}\right)\tilde{b}\quad \vec{f}_1 \ldots\ldots\ldots\ldots\ldots\ldots\ldots\ldots(15)$$

$\tilde{t}$ Is a unit vector, which is perpendicular to $\vec{R}$ and can be calculated

From $\tilde{t} = \tilde{b} \times \tilde{r}$

Where $\tilde{r} = \dfrac{\vec{R}}{\left|\vec{R}\right|}$ is a unit vector in direction $\vec{R}$.

Similarly as the previous procedure Q^{-} was computed in the gravity frame $\{\mathcal{G}\}$

From

$$Q^{-} = (\vec{f}_1^{*}\tilde{m})\tilde{} \quad f_1^{*} \qquad \text{.....(16)}$$

Where f_1^{*} and f_2^{*} are the position vectors of points $\vec{f}_1$ *and* $\vec{f}_2$ in frame $\{\mathcal{G}\}$

$\tilde{m}$ Was defined as the unit vector parallel to the line connecting f_1 to f_2 in $\{\mathcal{G}\}$

Coordinate and is given by,

$$\tilde{m} \quad = \frac{\left(\vec{f}_2^{*} - \vec{f}_1^{*}\right)}{\left|\vec{f}_2^{*} - \vec{f}_1^{*}\right|} \qquad \text{.....(17)}$$

They defined in their work an equilibrium plan for a general three-dimensional case.

It was described with an inclination angle of Φ from the vertical plane. The relation holds this plane is (refer to Figure (7)):

$$\sum_{around_{J_1 J_2}} \mathcal{M} \quad = (\vec{F}\,\tilde{t})\left|\vec{R}\right|\vec{M}.^{\rightarrow}\,\tilde{b} + mg\left|Q\right|\cos\alpha\sin\phi = 0\text{.....(18)}$$

They noted that a destabilizing moment has been assigned a positive sign. And from relation (18), angle Φ was found as,

$$\Phi = -\sin^{-1}\frac{(\vec{F}\,\tilde{t})\left|\vec{R}\right|\vec{M}.^{\rightarrow}\,\tilde{b}}{mg\,Q\left|\right|\cos\alpha} \qquad \text{.....(19)}$$

from the previous equation, Ghsempoor and Sepehri defined vectors in the numerator in frame $\{\mathcal{M}\}$ and $\vec{Q}$ in denominator was defined in frame $\{\mathcal{G}\}$.

The angle α in (18) represents the angle that support boundary edge, f_1 f_2 which are made with the horizontal plane, i.e,

$$\alpha = \cos^{-1}\left(\tilde{z}\,\frac{\vec{s}}{|\vec{s}|}\right) \qquad \text{.....(20)}$$

Where $\vec{s} = \tilde{m} \times \tilde{n}$ is a vector perpendicular to f_1 f_2 in the vertical plane. Ghasempoor and Sepehri pointed out that when **M** and **F** are both zero then $\Phi = 0$, and that means the vertical plane is the equilibrium plane.

Equation (19) has a solution only if

$$(\vec{F}\,\tilde{t})|\vec{R}|\vec{M}\cdot\vec{b} \le mg|Q|\cos\alpha\cos\alpha$$

Then the previous condition does not hold it means that the summation of moment around the support boundary edge is negative, representing a situation whereby the body will never be on the verge of instability if rotated around this particular edge of the support boundary. And for such case, the angle Φ is chosen as $\Phi = 90^{\circ}$, where the net moment around the edge of the support boundary is minimum.

Davidson and Schweitzer (1990) considered a four-legged vehicle setting on level ground as shown in Figure (8). They assumed the contact points of the feet are points B, C, D, and E. B and C are two front feet, the external load was the vector **F** which represents the weight of the vehicle and acts through

the mass center G. they represented the modes of static in stability by the rotational velocity vectors ω_{12}, ω_{23}, ω_{34} and ω_{41}. They used the normal distance (d_{12}, d_{23}, d_{34} or d_{41}) between the external load and each axis potential rollover to measure the margin of static stability for that axis. Davidson and Schweitzer stated that when any such distance becomes zero, rollover occurs about the corresponding axis of rotation that joins two of the contacts where the machine touches the ground. They also stated that for the four-legged vehicle, then at a given stance and on level ground, the margin of static stability in the minimum distance d_{ij}, which is associated with that stance.

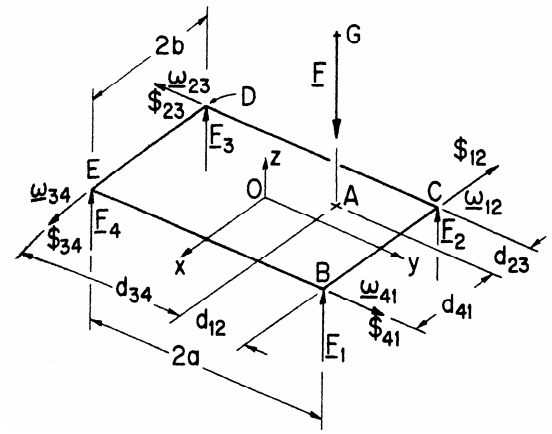

Figure (8): The force system on the four feet of a stationary COWELEV. (Davidson and Schweitzer, 1996).

3.2 Work and Energy Stability Formulations

Ghasempoor and Sepehri (1995) dealt with work calculation for conservative and non-conservative work. Since the weight force is conservative, the work required for rotating the center of gravity around a support boundary edge to the equilibrium plane depends on the vertical displacement of the center of gravity h.

$$W_1 = mg|Q|(\cos\phi - \cos\Psi)\cos\alpha \quad \text{.....(21)}$$

The angle Ψ between $\vec{Q}\vec{s}$ in the vertical plane was calculated from the relation,

$$\Psi = \cos^{-1}\left(\tilde{q}\,\frac{\tilde{s}}{|\tilde{s}|}\right)$$

Where $\tilde{q} = \dfrac{\vec{Q}}{|\vec{Q}|}$, all these vectors were defined in frame $\{\mathcal{G}\}$.

The work done by destabilizing forces and moments during the hypothetical. rotation of the machine over a support boundary edge to the onset of instability, was calculated from

$$W_2 = \int (\vec{F}\,\tilde{t})d_s + \int (\vec{M}\,\tilde{b})d\theta \quad \text{.....(22)}$$

Where $d_s = |\vec{R}| d\theta$. All the vectors now are defined in frame { $\mathcal{M}$ }.

Ghasempoor and Sepehri pointed out that during the hypothetical rotation of the machine over the edge of the support boundary, the direction of external and inertial forces and moments do not change relative to the machine frame { $\mathcal{M}$ }. So the two inner products under the integral sign remain constant and they had

$$W_2 = (\vec{F}\ \tilde{t}) |\vec{R}| \int d\theta + (\vec{M}\ \tilde{b}) \int d\theta$$

Which result in,

$$W_2 = [(\vec{F}\ \tilde{t}) |\vec{R}| + (\vec{M}\ \tilde{b})]\theta$$

Where $\theta = \Psi + \phi$

The energy stability level was calculated for each edge of support boundary, e.g. $f_1 f_2$ is,

Energy stability level $f_1 f_2 = (W_1 - W_2)$.

Therefore at each instant, the energy stability level can be calculated for every edge of the support boundary. The minimum of all energy stability levels is called energy stability margin for that instant.

Messuri and Klein (1985) illustrated the application of their adopted five definitions. They assumed a vehicle that has four supporting legs and is standing on an inclined plane, with a horizontal body as shown in Figure

(10). And Figure (9) shows that support boundary lies in the plane of the incline. Figure (10) shows a geometrical comparison of the energy stability levels for the front and rear edge of the support boundary. They explained that the line segment from point F_1 (rear edge of support boundary) to the point CG (body center of gravity) represent the radius R_1 of an arc which the body central of gravity would trace if the body were rotated about the rear edge of the support boundary.

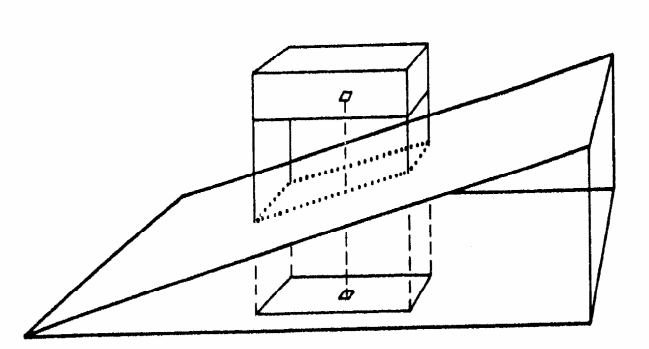

Figure (9): Vehicle standing on an inclined plane with the body horizontal. (Messuri and Klein, 1996).

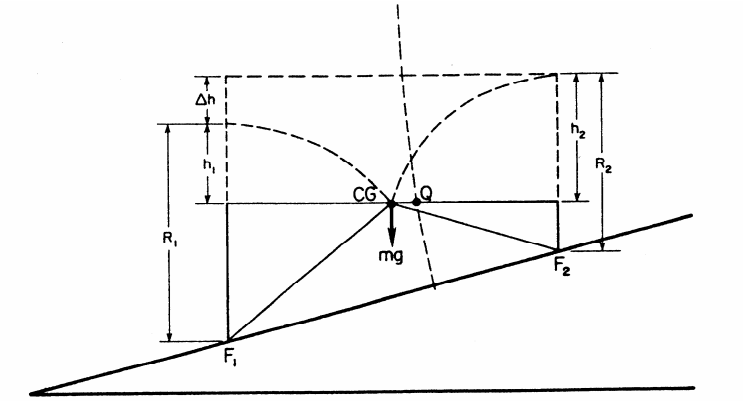

Figure (10): Side view of the configuration in Figure (12), showing a geometrical comparison of the energy stability level for the front and rear edges of the support boundary. (Messuri and Klein, 1996).

They stated that if the body were rotated to the position where the body center of gravity is vertically about the rear edge of the support boundary, then the vehicle would be on the verge of in stability corresponding to zero static stability margin. The change in vertical height through which the body center of gravity is moved from its original position to this position of zero static stability margins is given by the distance h_1. Therefore, the amount of potential energy required to rotate the body center of gravity, about the rear edge of the support boundary, from its original position to the point of zero static stability is mgh_1, where m represents the mass of the vehicle body, and g represents the acceleration due to gravity.

The amount of energy required to rotate the body center of gravity about the front edge of the support boundary, to the point of zero static stability is mgh_2. Since h_2 equals $h_1+\Delta h$, it is required less energy to over turn the vehicle about the rear support legs as opposed to the front support legs.

Messuri and Klein concluded if it were desired to shift the body to a position of greater over all stability, the body should be shifted such that h_1 equals h_2, at which point the energy stability levels for the front edge and rear edge would be equal. And this shift is implemented by coordinated leg motion.

Messuri and Klein (1985) stated that the definition of the energy stability margin requires the consideration of all edges of the support boundary. Also the position of the body and legs, especially in the case of very rough terrain, may not permit a simple geometric solution. There fore, a general equation had been derived which gives a measure of the energy stability level about any given edge of the support boundary. Since the potential energy is given by (PE = mgh), and since the mass m and acceleration of gravity g are constant, it is necessary to find the vertical height h through which the body center of gravity would move if the body were rotated about the given edge of the support boundary to the point of zero static stability margin.

They considered the general situation as shown in Figure (11). Where points F_1 and F_2 represent the footholds of two support feet, and the line segment connecting F_1 and F_2 represents one edge of the support boundary. Plane1 is a vertical plane containing line F_1 F_2. The point CG represents the location of the body center of gravity. Vector $\overline{R}'$ is a vector from line F_1F_2 to point CG, and is orthogonal to line F_1F_2. Unit vector $\hat{Z}$ represent the upward vertical direction. The vector $\overline{R}'$ is obtained by rotating vector $\overline{R}$, about line F_1F_2, until it lies in plane 1. They defined θ as the angle between $\overline{R}$ and $\overline{R}'$, and Ψ as the angle between $\overline{R}'$ and $\hat{Z}$, the vertical height h through which the point CG moves when the vector $\overline{R}$ is rotated to the vertical plane was given by

$$h = |\overline{R}| (1-\cos\theta) \cos\Psi \qquad \ldots\ldots\ldots\ldots\ldots\ldots \quad (23)$$

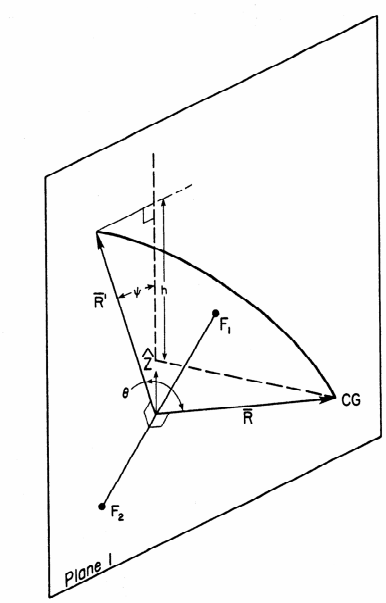

Figure (11): Derivation of the energy stability level equation. (Messuri and Klein, 1996).

Messuri and Klein (1985) pointed out that during operation of the walking vehicle, the location of all the feet can be found with respect to the body center of gravity, and the vector formulation provides simple efficient method of calculating the energy stability margin for any position of the body or legs. And their general formulation (Equation 23) can be applied for any type of terrain condition.

4 Assumptions, Requirements and Solutions

Sreenivasan and Wilcox (1994) verified that their scheme had some limitations. One of them that active control of the vehicle configuration requires the response of the variation of the center of mass to be fast enough to adjust for terrain variations. They stated that this limitation is not a very serious one because the speeds of these vehicles tend to be low in difficult terrain situations (about 5-10 cm/s). And clarified that there are kinematics bounds on the workspace where **C** can be placed with respect to the contact points. Also if the above scheme requires **C** to be outside this bound, **C** can be placed on the boundary of its workspace closest to its desired value to obtain best results. Another limitation is the fact that scheme requires the position kinematics analysis of complex kinematics chains in real time. And this may not be possible in some situations because position kinematics of closed chains tend to be very complex. Finally, the optimization problems arising from the redundancy in force distribution tend to be complex and unsuitable for real – time implementation.

Sreenivasan and Wilcox (1994) stated that in situations where the position kinematics and the optimization problem are complex, sub–optimal solutions that can be implemented in real time have to be investigated.

Sreenivasan and Wilcox (1994) presented their micro rover (Gofor). The vehicle consists of a body, two forks, and four wheel as shown in Figure (12). The four wheels and the two forks are all separately actuated. Each of the two

forks constitutes one actuated degree of freedom (dof). The doted line shown in Figure (12) is the rigid coupling forming the forks can perform complete rotations about its axis without interfering with the body. The body was designed so that the forles can lower the vehicle and the vehicle can rest on its belly. The six-actuator axes are all parallel to each other; if the vehicle is resting on a plane horizontal surface, the actuators all produce torques about axes perpendicular to the vertical plane.

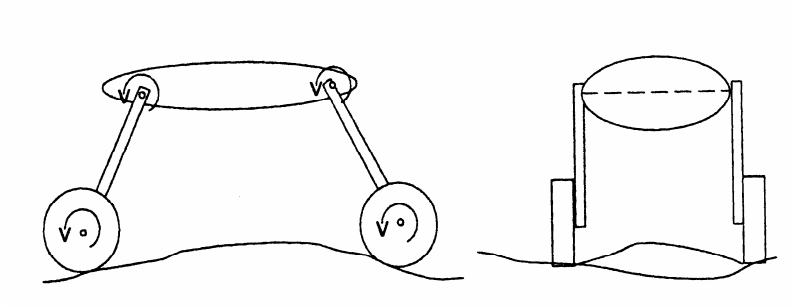

Figure (12): The Gofor on an uneven terrain. (Sreenivasan and Wilcox, 1994).

Sreenivasan and Wilcox (1994) performed a planar study in their research to investigate mobility enhancement. They clarified that their simplified analysis can be used to study the underlying principles of mobility enhancement using active actuation and their basic ideas can be applied to all activity-actuated vehicle. They noted that extensions to more complex systems may require some effort insolvent the nonlinear optimization problem and the position kinematics analysis.

Sreenivasan and Waldron used in their research a multi – modules actively articulated vehicle as shown in Figure (13). Each module consists of a body

and two active wheels. The consecutive modules were connected by active articulations (A_i).

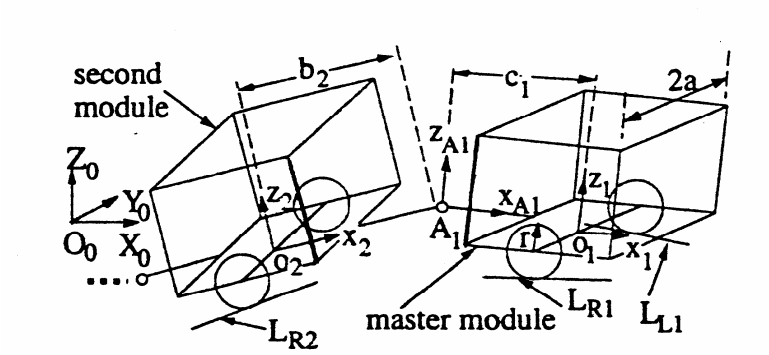

Figure (13): Articulated wheeled vehicle geometry. (Sreenivasan and Waldron, 1996)

Sreenivasan and Waldron (1996) involved a strategy to identify asset of discrete points on the path and solving for the geometric configurations of the vehicle at these points. These configurations can be used to check for geometric or force failure. In there research, if the vehicle configuration at a point on the terrain is found to be unsafe, the vehicle will be required to avoid this point on the terrain by going "around it". The researchers implemented in their work the WAAV, which possesses special mobility features including obstacle climbing, and self-recovery from an accident. The initial, final and intermediate configurations of a WAAV system during and obstacle-climbing maneuver are shown in Figure (14).

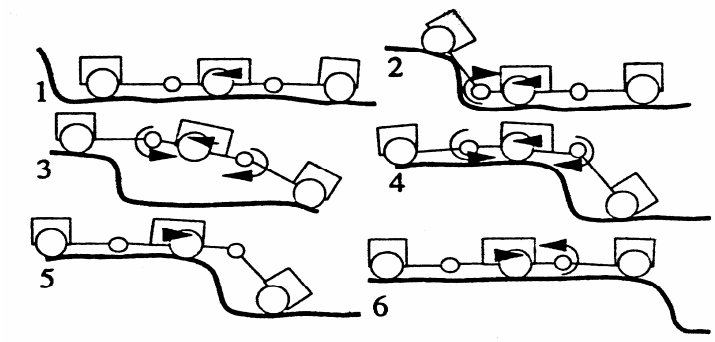

Figure (14): Vehicle climbing an obstacle. (Sreenivasan and Waldron, 1996)

Davidson and Schweitzer (1990) presented a paper concerns an improvement in a class of combined wheeled and legged vehicles (COWELEVs), which are used by the construction and forestry industries in Europe. In their mode, the central frame was kept level, and on - board computer calculates the location of the center of mass in real time. Their measurements were made to determine the instantaneous position of the four legs and their contacts with the ground. In their way the potential stability of the vehicle can be determined for just three supporting legs before the fourth leg is lifted so as to make a step.

Sreenivasan and Wilcox (1994) presented (Gofor) which is an actuated micro-rover vehicle that had a mass of less five kilograms, and had a body whose dimensions are about 0.31m×0.28m×0.08m. It had the ability to recover from overturn, and had interesting mobility characteristic. An

important advantage of micro-rovers is that several of them can be used during a particular application and this reduces the reliability requirements on the vehicles.

Farritor and Dubowsky, (1998) pointed out that the practical constraints of space rover systems, such as weight and power, require mobile robots to travel at slow speeds, approximately 3 cm/s. the dynamic effects are small and a quasi-static model approximates its behavior. Estimates of soil characteristics will be difficult, but are essential for any rational planning approach.

5 Kinematic-Stability problems in Mobile Robots

5.1 Introduction

Future robot vehicles will perform challenging tasks in rough terrain, such as planetary exploration and military missions. (Iagnemma et al., 2003). To understand the complexity of robots and their applications, it is required to form knowledge of electrical engineering, mechanical, industrial and computer engineering in addition to economics and mathematics.

The mobile robots that operate in field environments will be required to perform tasks on uneven terrain that may cause the system to approach or near broach dangerous tip over instability. Definitions of a measure stability margin were developed to avoid tip over in an automatic systems, or to provide an indication to human operators that tip over may approximately occur. (Papadopoulos and Rey, 1996).

A mobile machines or rovers equipped with manipulator arms and controlled by on-board human operators are commonplace systems in the construction mining and forestry industries, see for example Figure (15) (Papadopoulos and Rey, 1996).

When such systems exert and carry large forces and move with heavy payloads, or operate over very uneven or slopped terrain, tip over instabilities may occur causing dangers to the operator, reduce productivity, and risk damaging the machine. The safety and productivity of these mobile machines could be improved by automatic detection prevention of tip over instabilities using supervisory control systems.

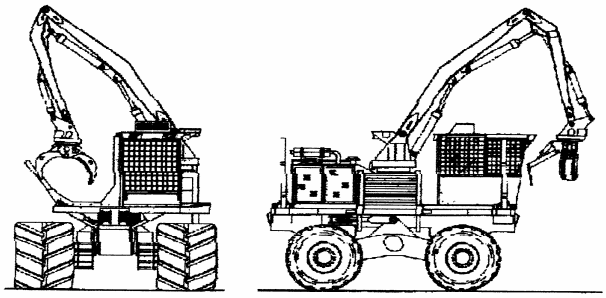

Figure (15): Example mobile manipulator. (Papadopoulos and Rey. 1996)

To achieve stability for any mobile system while moving on an inclined surfaces or arbitrary rough terrain, an appropriate measure of the tip over stability margin must be defined. Teleoperated or fully autonomous mobile manipulators or rovers operating in field environments (nuclear, military, and aerospace industries) would require a monitoring of the tip over stability margin. The previous researchers concerned with vehicle center-of-gravity (c.g.) height and system mass (i.e. heaviness) in order to determine the static machine lateral stabilities (Papadopoulos and Rey, 1996).

In this research, an effective tip over stability measure model (the force-Angle stability measure) is studied which has a simple graphical interpretation and easy computation in order to enhance the rovers moving on uneven terrain.

This model which was developed by Papadopoulos and Rey remain sensitive to top heaviness and applicable to general case of systems operating over uneven terrain and subject to inertial and external forces. The following model does not require any integration make it advantageous to previously proposed measures.

5.2 Background

It is necessary to concern with the stability of the central body, which provides mobility, i.e. the vehicle body or base in order to determine the tip over stability margin of a ground vehicle system. Papadopoulos and Rey (1996) assumed that the vehicle body is nominally in contact with the ground, as would be the case if mobility is provided via wheels, tracks, alternating (statically stable) legged support, or a combination of them.

When a nominally upright vehicle body undergoes a rotation that results in a reduction of the number of ground contact points such that all remaining points lie on a single line (the tipover axis), the tip over (roll over) instability will occur. Then mobility control is lost, and if the situation is not reversed, the vehicle is over turned (Papadopoulos and Rey, 1996).

The low (c.m) height is desirable from stability point-of-view, heaviness on the other hand is stabilized at low velocities and destabilized at high velocities (Papadopoulos and Rey, 1996).

5.3 Force-Angle Stability Measure

Let a two contact point planer system whose center-of-mass (c.m.) is subject to a net force $\mathbf{f}_r$ which is the sum of all forces acting on the vehicle body as shown in Figure (16). The supporting reaction forces do not contribute to a tip over motion instability and they will be ignored from the net force summation. The force vector subtends two angle, η_1 and η_2 with the two tip-over axis normals $\mathbf{I}_1$ and $\mathbf{I}_2$. It can be noticed that the Force-Angle stability measure, α, is given by the minimum of the two angles, weighted by the magnitude of the force vector ($\|\mathbf{f}_r\|$) for heaviness sensitivity (Papadopoulos and Rey, 1996):

$$\alpha = \theta_1 . \|\mathbf{f}_r\| \quad \text{.................................... (24)}$$

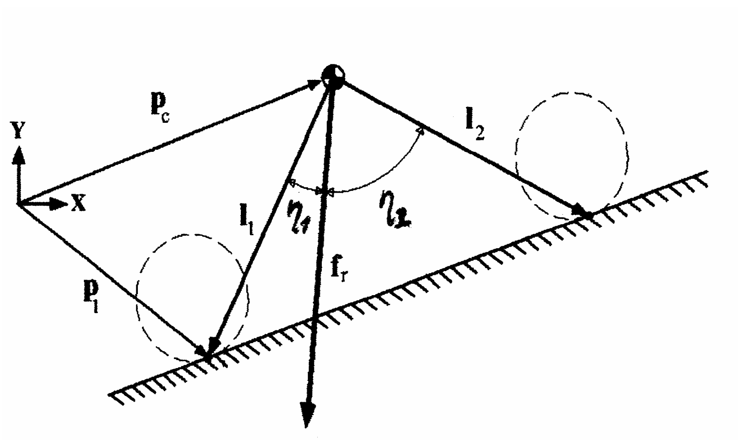

Figure (16): Planar Force- Angle stability measure. (Papadopoulos and Rey, 1996).

It can be seen obviously that critical tip over stability occurs when η goes to zero (i.e. when $\mathbf{f}_r$ coincides with $\mathbf{I}_1$ or $\mathbf{I}_2$) or, when the magnitude of $\mathbf{f}_r$ goes to zero and even the smallest disturbance may topple the vehicle. If $\mathbf{f}_r$ lies outside the cone described by $\mathbf{I}_1$ and $\mathbf{I}_2$, the angle becomes negative and tips over is in progress.

For a vehicle, which is capable of adjusting its center-of mass height, or for a vehicle, which carries a vehicle load, the tip over stability margin should be top-heavy sensitive. This is illustrated in Figure (17) for the Force-Angle stability measure where an increase in center of mass height results in a smaller minimum angle and a reduced measure of tip over stability margin.

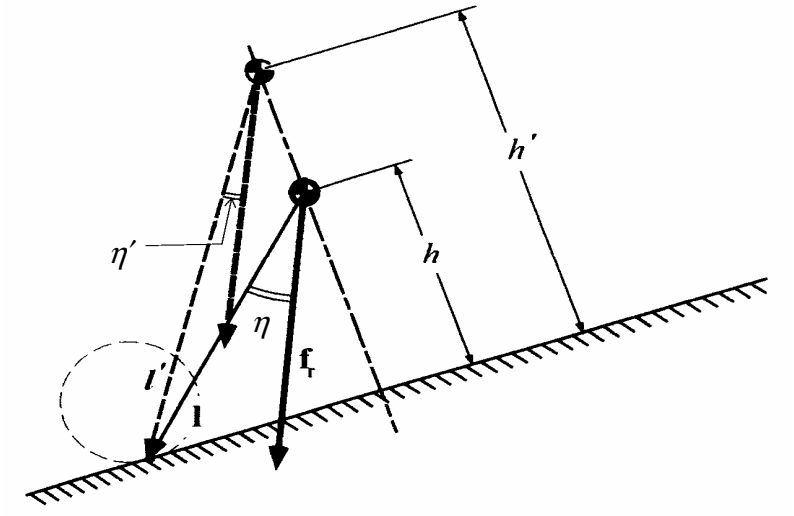

Figure (17): Effect of center- of- mass height. (Papadopoulos and Rey, 1996).

5.4 General Form

Consider outermost points of vehicle contact points with the ground, which form a convex support polygon when projected onto horizontal plane. These points will be defined to be the ground contact points. Let $\mathbf{p}_i$ represent the location of the i^{th} ground contact points.

$$\mathbf{p}_i = \begin{bmatrix} p_x & p_y & p_z \end{bmatrix}_i^T \qquad i = \{1,...,n\} \qquad \text{……..(25)}$$

And let $\mathbf{p}_c$ represent the location of the vehicle center-of-mass relative to reference frame in three dimensions. For generality all vectors are expressed in an inertial frame. For additional simplifications, it is easer to use of a reference frame located at vehicle center-of-mass, as $\mathbf{p}_c$ would be a zero vector. For a consistent formulation the $\mathbf{p}_i$ are numbered in ascending to right-hand rule convention where the thumb is directed down wards the gravity vector, i.e. points are numbered in clockwise order when viewed from above.

The lines that join the ground contact points are the tip over mode axes, $\mathbf{a}_i$, and the set of these lines will be referred to as the support pattern. The i^{th} tip over mode axis is given by (papadopoulas and Rey, 1996)

$$\mathbf{a}_i = \mathbf{p}_{i+1} - \mathbf{p}_i \qquad i = \{1,...,n-1\} \qquad \ldots\ldots\ldots\ldots\ldots \qquad (26)$$

$$\mathbf{a}_n = \mathbf{p}_1 - \mathbf{p}_n \qquad \ldots\ldots\ldots\ldots\ldots \qquad (27)$$

The ground contact point numbering convention is required in order to obtain aset of tip over axes whose direction all coincide with that of stabilizing moments. See Figure (18).

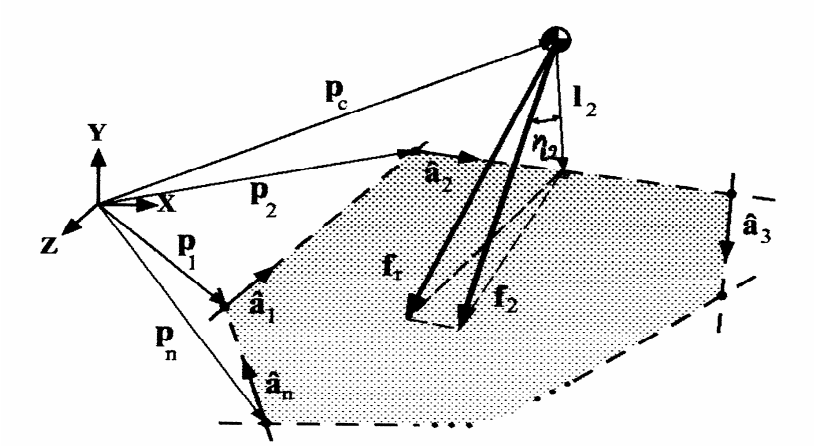

Figure (18): 3D Force-Angle stability measure. (Papadopoulos and Rey, 1996).

The natural tip over of the vehicle will always occur about a tip over mode axis $\mathbf{a}_i$. A tripped tip over of the vehicle occurs when one of the ground contact points encounters an obstacle or a sudden change in the ground conditions. In a tripped tip over the vehicle undergoes a rotation a bout an axis that is some linear combination of the tip over mode axes associated with the single remaining ground contact point. In a tripped instability the Force-Angle stability measure will go to zero and then become negative

for each contributing tip over mode axis so that it is not required to identify the exact tip over mode axis.

The tip over axis normals **I** which intersect the vehicle center- of- mass are given by subtracting from $(\mathbf{p}_{i+1} - \mathbf{p}_c)$ that portion which lies along $\hat{\mathbf{a}}_i$, that means

$$\mathbf{I}_i = (\mathbf{1} - \hat{\mathbf{a}}_i \hat{\mathbf{a}}_i^{\mathrm{T}})(\mathbf{p}_{i+1} - \mathbf{p}_c) \qquad \text{……..……(28)}$$

Where $\hat{\mathbf{a}} = \dfrac{\mathbf{a}}{\|\mathbf{a}\|}$

And $\|\mathbf{a}\| = \sqrt{\mathbf{a}_x^2 + \mathbf{a}_y^2 + \mathbf{a}_z^2}$

Note that **1** is the 3×3 identity matrix, i.e.

$$\mathbf{1} = \begin{bmatrix} 1 & 0 & 0 \\ 0 & 1 & 0 \\ 0 & 0 & 1 \end{bmatrix}$$

The tip over axis normal **1** for the last contact point could be identified as

$$\mathbf{I}_n = (\mathbf{1} - \hat{\mathbf{a}}_n \hat{\mathbf{a}}_n^{\mathrm{T}})(\mathbf{p}_1 - \mathbf{p}_c) \qquad \text{……..…(29)}$$

And from Newtonian Principles, one can obtain the following force equilibrium equation for the vehicle body

$$\sum \mathbf{f}_{\text{inertial}} = \sum (\mathbf{f}_{\text{grav}} + \mathbf{f}_{\text{manip}} + \mathbf{f}_{\text{support}} + \mathbf{f}_{\text{dist}}) \quad \text{.....(30)}$$

Where $\mathbf{f}_{\text{inertial}}$ are inertial forces, $\mathbf{f}_{\text{grav}}$ are the gravitational loads, $\mathbf{f}_{\text{manip}}$ are the loads transmitted by manipulator to the vehicle body (due to manipulator) dynamics, end-effecter loading, and end-effecter reaction forces), $\mathbf{f}_{\text{support}}$ are the reaction forces of the vehicle support system, and $\mathbf{f}_{\text{dist}}$ are any other external disturbance forces acting directly on the vehicle (forces due to a trailer implement). Note that in the absence of independent inertias between the vehicle body and the ground we have that the $\mathbf{f}_{\text{support}}$ are equal to the ground reaction forces.

The net force acting on the center of mass (c.m.) that would participate in a tip over instability, $\mathbf{f}_r$, is given by

$$\mathbf{f}_r = \sum (\mathbf{f}_{\text{grv}} + \mathbf{f}_{\text{manip}} + \mathbf{f}_{\text{dist}} - \mathbf{f}_{\text{inertial}}) \quad \text{.....(31)}$$

$$= -\sum \mathbf{f}_{\text{support}}$$

Similarly, there is a moment forces acting about the center of mass (c.m.). The net moment $\mathbf{n}_r$ can be defined as

$$\mathbf{n}_r = \sum \mathbf{n}_{\text{grav}} + \mathbf{n}_{\text{manip}} + \mathbf{n}_{\text{dist}} - \mathbf{n}_{\text{inertial}}) \qquad \text{.....(32)}$$

$$= -\sum \mathbf{n}_{\text{support}}$$

For a given tip over axis $\hat{\mathbf{a}}_i$, we are only concerned with those components of $\mathbf{f}_r$ and $\mathbf{n}_r$ which act about the tip over axis, so let

$$\mathbf{f}_i = (\mathbf{1} - \hat{\mathbf{a}}_i \hat{\mathbf{a}}_i^T)\mathbf{f}_r \qquad \text{.....(33)}$$

And

$$\mathbf{n}_i = (\hat{\mathbf{a}}_i \hat{\mathbf{a}}_i^T)\mathbf{n}_r \qquad \text{.....(34)}$$

Since the force-Angle stability measure is based on the computation of the angle between the net force vector and each of the tipover axis normal, it is necessary to replace the moment $\mathbf{n}_i$ with an equivalent force couple $\mathbf{f}_{n_i}$ for each tipover axis.

The equivalent force couple must lie in the plane normal to the moment $\mathbf{n}_i$. The most appropriate choice of the infinite possible force couple locations and direction in this plane, is that pair of minimum magnitude where one member of the couple passes through the center-of-mass and the other the line of the tipover axis (Papadopouls and Rey, 1996).

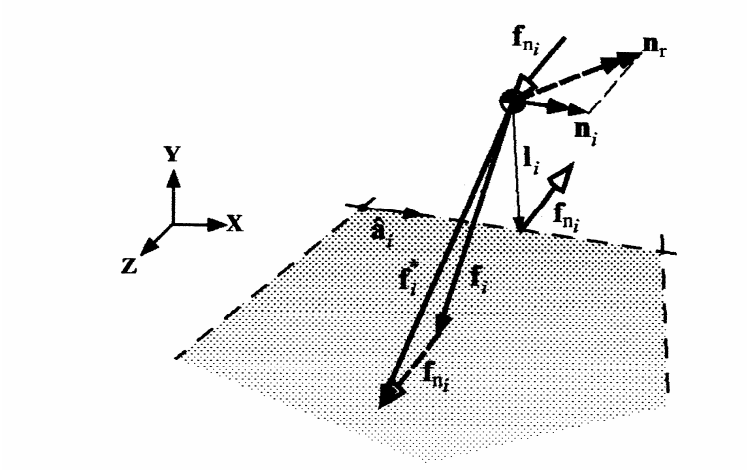

Figure (19): Use equivalent force couple to replace moment at c.m. (Papadopoulos and Rey, 1996).

By referring to Figure (19), the member of the force couple acting on the center-of-mass (c.m.) is given by

$$\mathbf{f}_{n_i} = \frac{\hat{\mathbf{I}}_i \times \mathbf{n}_i}{\|\mathbf{I}_i\|} \qquad \text{.....(35)}$$

Where

$$\hat{\mathbf{I}} = \frac{\mathbf{I}}{\|\mathbf{I}\|}$$

And

$$\|\mathbf{I}\| = \sqrt{\mathbf{I}_x^2 + \mathbf{I}_y^2 + \mathbf{I}_z^2}$$

The new net force vector $\mathbf{f}_i^*$ for the i^{th} tipover axis is thus

$$\mathbf{f}_i^* = \mathbf{f}_i + \frac{\hat{\mathbf{I}}_i \times \mathbf{n}_i}{\|\mathbf{I}_i\|} \qquad \text{..... (36)}$$

Now, Let $\hat{\mathbf{f}}^* = \frac{\mathbf{f}^*}{\|\mathbf{f}^*\|}$

Where $\|\mathbf{f}^*\| = \sqrt{\mathbf{f}_x^2 + \mathbf{f}_y^2 + \mathbf{f}_x^2}$

The angles for the Force-Angle stability measure are then given by

$$\eta_i = \sigma_i \cos^{-1}\left(\hat{\mathbf{f}}_i^* \cdot \hat{\mathbf{I}}_i\right) \qquad i = \{1,.....,n\} \qquad \text{..... (37)}$$

Where $-\pi \le \eta_i \le \pi$

The sign of η_i can be determined by σ_i as follows

$$\sigma_i = \begin{Bmatrix} +1 & \left(\hat{\mathbf{I}}_i \times \hat{\mathbf{f}}_i^*\right) \cdot \hat{\mathbf{a}}_i \le 0 \\ -1 & \text{otherwise} \end{Bmatrix} \qquad \text{..... (38)}$$

Where $i = \{1,.....,n\}$

The appropriate sign of the angle measure associated with each tipover axis is determined by establishing wither or not the net force vector lies inside the support pattern.

The overall force-Angle stability measure can be given by

$$\alpha = \min(\eta_i)\|\mathbf{f}_r\| \qquad i = \{1,.....,n\} \qquad \ldots\ldots\ldots\ldots\ldots\ldots \quad (39)$$

The previous scalar is an instantaneous measure of the tipover stability margin of the system (Papadopoulos and Rey, 1996).

Generally, one can note the following:

1- The magnitude of appositive α describes the magnitude of the tipover stability margin of a stable system.
2- Critical tipover stability occurs when $\alpha = 0$.
3- Negative values of α indicate that tipover instability is in progress.

One should note that the minimum angle is weighted by $\|\mathbf{f}_r\|$ in order to obtain heaviness sensitivity and not by $\|\mathbf{f}_i\|$ which would introduce discontinuities in α when ever the tipover axis index *i* associated with min (η_i) changes (Papadopoulas and Rey, 1996).

To compute the force-Angle stability measure, one must have the following information:

1- Knowledge of the location of the ground contact points of the vehicle relative to the vehicle center-of-mass location.
2- Knowledge of the external forces and moments acting on the vehicle.
3- Knowledge of the vehicle linear and angular acceleration.

These are necessary elements of any dynamic system simulation; also they are measurable quantities on a real system when it is equipped with an appropriate and suitable sensor.

There are many particular application of the force-Angle stability measure, the application for such stability measure are:

1- Tipover stability margin monitoring for a particular machine during operations or in simulation.
2- Tipover stability for comparing various machines in a given weight /size class on type of application such as (mobile robots, micro-rovers or forestry vehicles).
3- Tipover stability characterization for comparing various machines of different classes.

The previous application includes real-time monitoring (for tipover prediction and prevention purposes). And off-lines simulation (for path planning and optimization).
Determining when to make an automatic tipover prevention response, one must increase his knowledge of (Papadopoulos and Rey, 1997):

1- The systems present stability state, i.e. dynamic α and static α.
2- Determining the time rate of change (i.e. dynamic $\dot{\alpha}$ and static $\dot{\alpha}$).

To predict time-until-tipover, one must determine a single measure that combines from both stability margin information and stability margin gradient information. Tipover can be predicted when extrapolation of α yields a zero crossing, and then calculated time during tipover is given by (Papadopoulos and Rey, 1997):

$$\mathbf{t}_{\text{tip}} = -\frac{\hat{\alpha}}{\dot{\hat{\alpha}}} \qquad \text{.....(40)}$$

Two times until tipover predictions are computed, one for static $\hat{\alpha}$ and the other for the dynamic $\hat{\alpha}$. The previous two instantaneous measure would change at every time step with both $\hat{\alpha}$ and $\dot{\hat{\alpha}}$.

A voiding unnecessary execution of a tipover prevention response require ignoring prediction of impendent tipover which are of brief transient, i.e. it is not an effective indication for a danger to the system.

Initiating a response if the predicted time until tipover remains below some threshold for a given period of time, i.e. the tipover prediction is persistent can do this.
The proposed triggering algorithm (automatic tipover prevention response) consists of a running maximum over K points as follows (Papadopoulos and Rey, 1997):

If $\max(t_{tip_{n-k}}, t_{tip_{n-k+1}}, ..., t_{tip_{in}}) < t_{threshold}$

Then perform tipover prevention response, where $t_{\text{threshold}}$ is set much smaller than the system fundamental period.

As can be seen from Equation (39), the force-angle stability margin equation, one should note two possible elements of a tipover prevention action:

1- A geometric correction (where one attempts to increase $\min(\eta_i)$).

2- Loading correction (where one attempts to increase $\mathbf{f}_r$).

Equation (37) shows that $\min(\eta_i)$ can be increased by altering the direction of either $\mathbf{f}_i^*$ or $\hat{\mathbf{l}}_i$ in order to increase their angular separation. Many techniques can be used to achieve goal.

One geometric technique is to relocate the vehicle center-of-mass position $\mathbf{p}_c$, with respect to the tipover axis $\mathbf{a}_i$. For a legged system this can be done by changing the system footing. For wheeled or tracked system, this is not available option without special actuators.

For mobile robot applications, Robots with actively articulated suspensions, some times called “reconfigurable robots” can modify their suspension configuration and thus repositioning their center of mass in order to prevent tipover and achieve the required stability.

As an example of the articulated suspension robot is the Jet propulsions laboratory sample return rover (SSR) as shown in Figure (20 and 21). (Iagnemma et al, 2000).

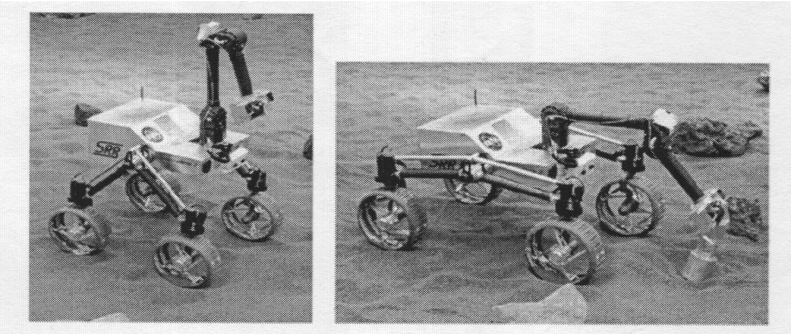

Figure (20): Jet Propulsion Laboratory Sample Return Rover (SRR), (Iagnemma et al, 2000).

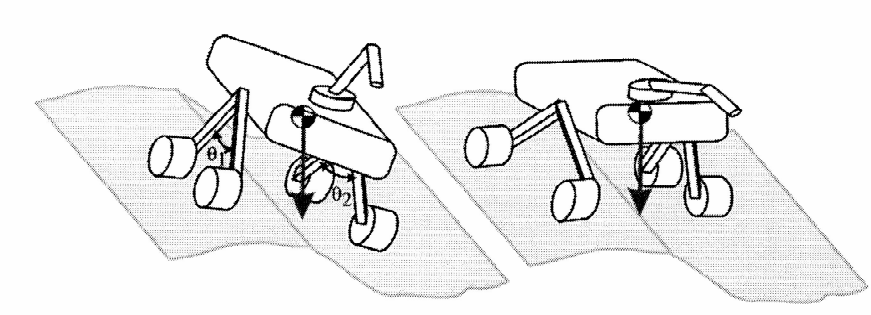

Figure (21): Articulated Suspension Robot Improving Stability by Adjusting Shoulder Joints, (Iagnemma et al, 2000).

The SRR can modify its two shoulder joints to change its center of mass location relative to the tipover axis $\mathbf{a}_i$ thus enhancing the rough terrain mobility. For example when traveling on an incline the SRR can adjust angles θ_1 and θ_2 to enhance stability. The mobile robot can also reposition its center of mass by moving its manipulator. See Figure (22).

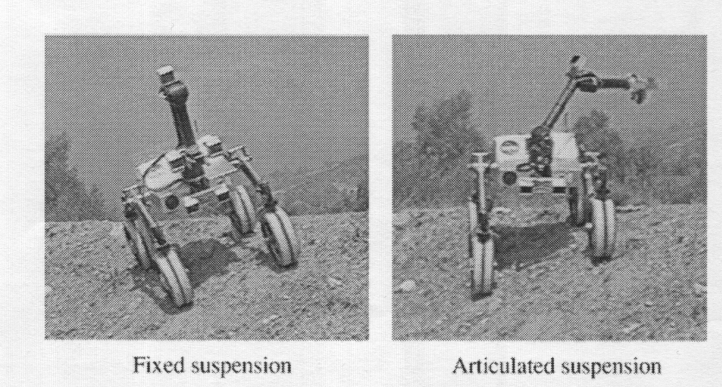

Figure (22): SRR during Rough-Terrain traverse, (Iagnemma et al, 2000, a).

The second technique consists of altering $\mathbf{f}_i^*$ by using the manipulator and / or the vehicle mobility actuators (i.e. wheels, tracks or legs). By using this technique, the effective response to a potential static stability ($\alpha|_{\text{stat}} \rightarrow 0$) had been determined to be the following combined use of both manipulator and the vehicle mobility actuators (Papadopoulos and Rey, 1997):

1- Return the manipulator to its inertial home configuration (where the inertial home configuration is assumed to be that stance for which the manipulator exerts a negligible moment on the vehicle base).
2- Use the vehicle mobility actuators to compensate for any temporarily destabilizing dynamic moments at manipulator base.

The first action redirects $\mathbf{f}_i^*$ away from the tipover axis and toward the interior of the support polygon. And the second action stabilizes the vehicle throughout the recovery motion.

The second action can be considered and implemented as a feedback law where the manipulator base joint destabilizing moment is computed and used to derive the vehicle mobility actuator commands.

The stability of this maneuver and during execution can be guaranteed if the vehicle wheels, tracks or legs are able to exert the required compensation loads in both direction and magnitude.

5.5 Wheel-Terrain Contact Angle Estimation

One of the important elements of a rover model that travel on a rough terrain is the wheel-terrain contact angle. As these angles greatly influence rover force application properties. Generally, these angles can be difficult to measure directly.

There is a method for estimating the wheel-ground contact angles of mobile robots using available on-board sensors (Iagnemma and Dubowsky, 2000,a).

Let consider a planar two-wheeled system on uneven terrain as shown on Figure (23). It was assumed two points

1- The terrain is rigid.

2- The wheels make point contacts with the terrain.

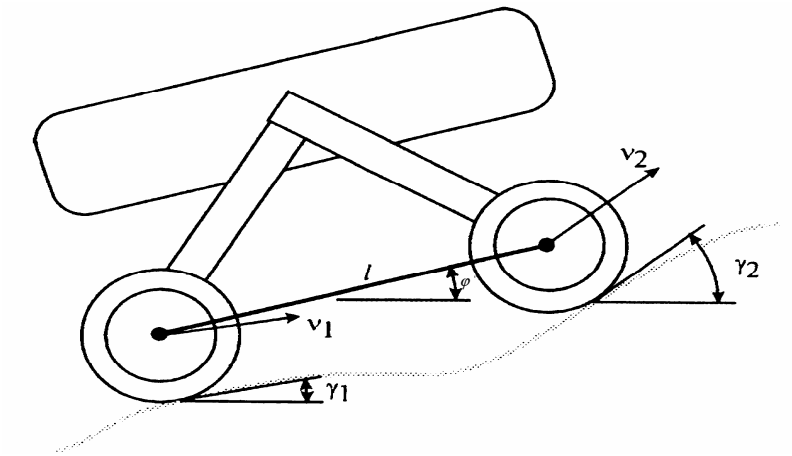

Figure (23): Planner system on un even terrain.(Iagnemma and Dubowsky, 2000,a).

The rear and front wheels make contact with the terrain at angles γ_1 and γ_2 from the horizontal. And the vehicle pitch, ϑ, is also defined with respect to the horizontal. The wheel centers have speeds v_1 and v_2. The distance between the wheel centers is defined as *l*.

For this system, the following kinematics equations can be written

$$v_1\cos(\gamma_1 - \vartheta) = v_2\cos(\gamma_2 - \vartheta) \quad \text{.....(41)}$$

$$v_2\sin(\gamma_2 - \vartheta) - v_1\sin(\gamma_1 - \vartheta) = l\dot{\vartheta} \quad \text{.....(42)}$$

Equation (41) represents kinematics constraint that the wheel center length *l* does not change. And Equation (42) is a rigid- body kinematics relation between the velocities of the wheel centers and the vehicle pitch rate $\dot{\vartheta}$

By substituting Equation (41) in Equation (42), it yields the following:

$$\sin(\gamma_2 - \vartheta - (\gamma_1 \vartheta)) = l\frac{\dot{\vartheta}}{v_1}\cos(\gamma_2 - \vartheta) \quad \text{.....(43)}$$

Note that,

$\theta = \gamma_2 - \vartheta$

$\beta = \vartheta - \gamma_1$

$a = l\frac{\dot{\vartheta}}{v_1}$

$b = \frac{v_2}{v_1}$

Equation (41) and (43) become:

$$(b\sin\theta + \sin\beta)\cos\theta = a\cos\theta \quad \text{.....(44)}$$

And

$$\cos\beta = b\cos\theta \quad \text{.....(45)}$$

By solving Equations (44) and (45) for the wheel-terrain contact angles γ_1 and γ_2 yields:

$$\gamma_1 = \vartheta - \cos^{-1}(h) \quad \text{.....(46)}$$

$$\gamma_2 = \cos^{-1}(\frac{h}{b}) + \vartheta \quad \text{.....(47)}$$

Where:

$$h = \left(\frac{1}{2a}\right)\sqrt{2a^2 + 2b^2 + 2a^2b^2 - a^4 - b^4 - 1}$$

The previous solution is for vehicle with a rigid-connected wheel pair. This method can be extended to vehicles with greater than two wheels.

There are two special cases that must be considered:

- Case1:

Occurs when the rover is stationary. So Equations (44) and (45) do not yield a solution, since if $\dot{\vartheta} = \nu_1 = \nu_2 = 0$, this lead that both a and b are undefined. From a physical point of view, the lack of solution results from the fact that a stationary rover can have an infinite set of possible contact angles at each wheel. (Iagnemma and Dubowsky, 2000, b).

- Case2:

It occurs when $\cos(\theta)$ equals zero. In this case $\gamma_2 = \pm\frac{\pi}{2} + \vartheta$ from the definition of θ, Equation (47) produces the solution $\gamma_1 = \pm\frac{\pi}{2} + \vartheta$.

And physically this is due to two possible cases (Iagnemma and et al, 2003):

a) The rover is undergoing to pure translation.

b) The rover is undergoing to pure rotation. Refer to Figure (24)

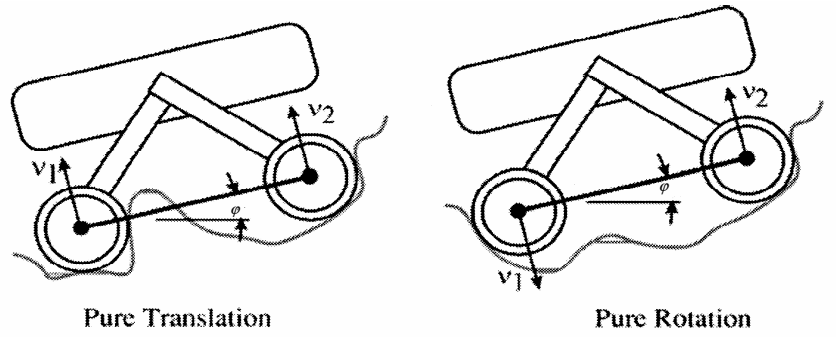

Figure (24): Physical interpretations of cos(θ) = 0. (Iagnemma and et al., 2003).

These cases are unlikely to occur in practice, and they are easily detectable. For the case of pure rotation, $v_1 = -v_2$, the solution for $\gamma_1 = \gamma_2$ can be written as:

$$\gamma_1 = \vartheta + \frac{\pi}{2}\operatorname{sgn}(\dot{\vartheta}) \quad \text{.....(48)}$$

And

$$\gamma_2 = \vartheta - \frac{\pi}{2}\operatorname{sgn}(\dot{\vartheta}) \quad \text{.....(49)}$$

For the case of pure translation, $\dot{\vartheta} = 0$ and $v_2 = v_1$. Thus, h is undefined and the system of Equations (44) and (45) has no solution. For low-speed rovers, the terrain profile varies slowly with respect to the data-sampling rate. And it is reasonable to assume that wheel-terrain contact angles computed at a given time step will be similar to wheel-terrain contact angles computed at the previous time step. Thus, previously estimated contact angles can be used when a solution to the estimation equations does not exist.

Rate gyroscope or simple in clinometers are used to measure the pitch and pitch rate. While the wheel center speeds can be estimated from the wheel angular rate and can be

measured by using $\dot{\vartheta}$ tachometer. And it is important to note that the wheels do not have substantial slip.

Thus, wheel-terrain contact angles can be estimated with common and low-cost on board sensors. But the sensor noise and wheel slip will degrade these measurements.

6 Comparisons with Literatures

Messuri and Klein (1985) proposed the use of the minimum work required to tipover the vehicle. Their energy-based approach was extended by (Ghasempoor Sephri, 1995). I adopted and used a previous method for making the simulation program. This method was developed by (Papadopoulos and Ray, 1996), it has a simple graphical interpretation and easily computed than the measure of Ghasempoor Sephri since it does not require any integration.

Iagnemma et al. (2000) used a reference frame located at the mobile robot center of mass as p_c would be a zero vector; i.e. the reference frame moves with the robot traveling. In this research, the reference frame is fixed, and the mobile robot moves with respect to this fixed-reference frame. Accordingly, A method had been developed in order determine the location of the center-of-mass exactly with respect to robot wheels and reference frame.

Papadopoulos and Rey (1996) studied in their paper the kinematic-stability of a mobile manipulator by using a planar simulation.

Their simulation program was designed for studying the mobile manipulator stability while it is being at a fixed position. In this research, the stability is studied when the mobile robot traverse the rough-terrain through a continuous movement. So multiple shapes and types of grounds were generated in three-

dimensions through a simulation program in order to represent, to somewhat, the real surfaces.

Iagnema et al. (2000) developed sample return rover (SRR) that has the ability to modify the kinematic configuration to enhance the stability on the rough terrains. For example, when the robot (SRR) moving on an incline, it can lower one side of its suspension in order to increase its stability margin. In this thesis, the kinematic instability is improved by using invert pendulum that is installed at the center of mobile robot body. This pendulum has a movable mass at the end of the pendulum bar. And when the robot looses its stability when moving on a slope, the movable mass at the end of the pendulum bar is transferred to a position where the tipover is prevented.

Problem Solving Methodology

1 Introduction and objectives

During traveling, the mobile robot is exposed to be unstable that may be enough to turn over due to moving on steep inclinations or climbing on stones and rocks. So, we need to study many factors and variables that affect stability in order to form enough knowledge about the probability of turning over from a kinematics point of view. A force-angle stability measure of a mobile robot had been implemented from a previous work (Papadopoulos and Rey, 1996) and simulated in this research. A method was introduced in order to achieve the stability when the mobile robot reaches instability margins on the ground.

The proposed mobile robot in the following discussion is a robot with variable number of wheels supported and connected to the mobile robot body by shoulders and legs. It is required to move on various types of terrains and surfaces that can be regular and flat, or in the other extreme irregular and rough.

Three types of mobile robots will be discussed according to its number of wheels:

1. Four-wheel mobile robot with equal distance between the wheels supposed here to be two distance units. Wheels on each side are connected with one angulated shoulder as shown in Figure (25).

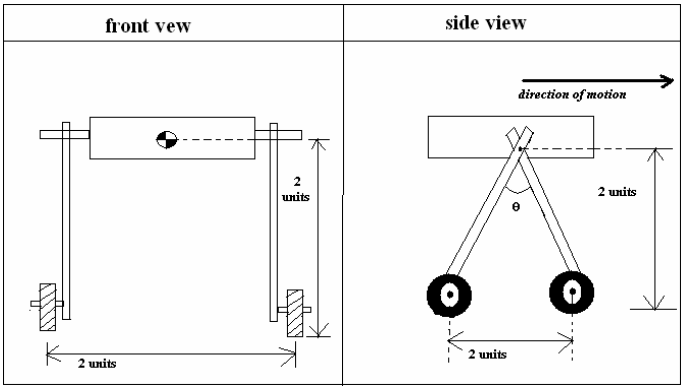

Figure (25): A four-wheel mobile robot (front and side views)

2. Three-wheel mobile robot with two wheels on the front side and one wheel in the rear side as shown in Figure (26).

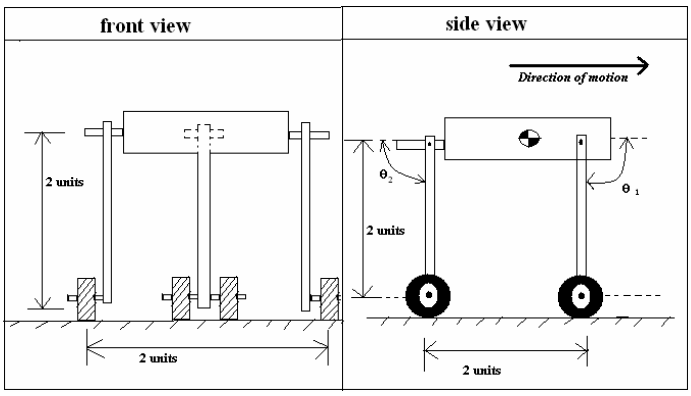

Figure (26): Three-wheel mobile robot (two wheels in front side and one wheel in rear side)

3. Three-wheel mobile robot with one wheel on the front side and two wheels on the backside as shown in Figure (27).

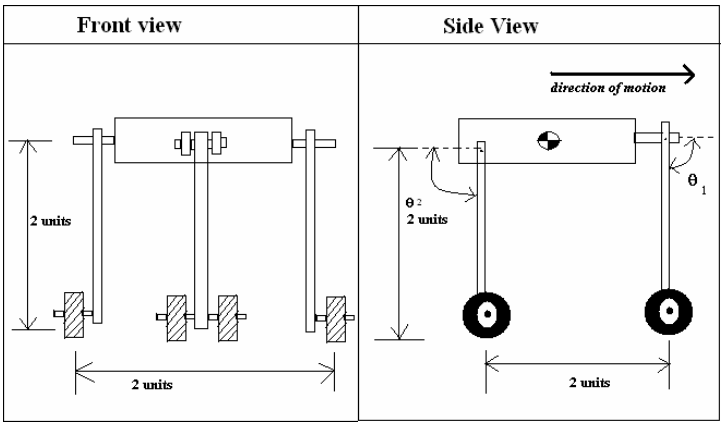

Figure (27): Three-wheel mobile robot (one wheel in front side and two wheels in rear side)

With respect to the surfaces and terrains, multiple shapes and types of these grounds were generated such as flat, inclined and rough surfaces with hills and valleys and they may simulate to somewhat real surfaces using MATLAB as a programming tool. See Figure (28) as an example.

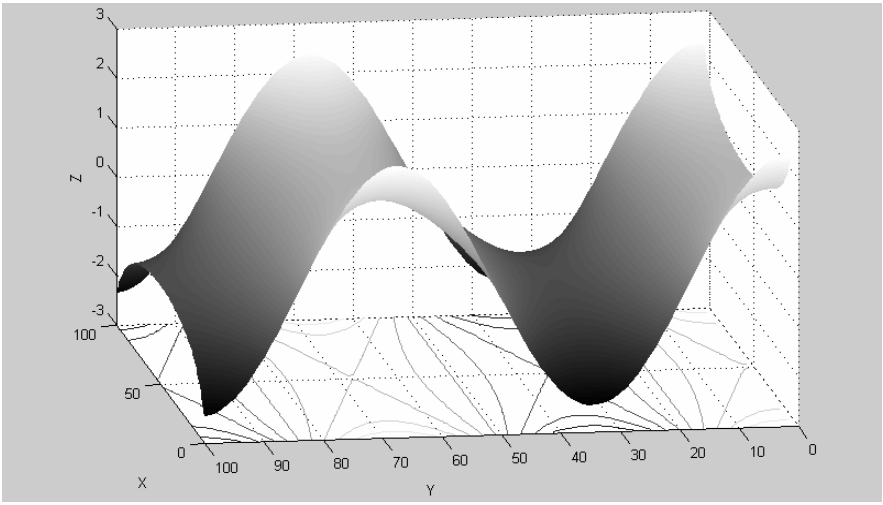

Figure (28): Example of simulated rough terrain.

The model of this thesis is simulated using a powerful user-friend programming tool, MATLAB.

MATLAB is a high-performance language for technical computing. It integrates computation, visualization, and programming in an easy-to-use environment. MATLAB is an interactive system whose basic data element is an array that does not require dimensioning. This allows solving many technical computing problems, especially those with matrix and vector formulations (such as in our study), in a fraction of the time it would take to write a program in a scalar noninteractive language such as C or Fortran. The name MATLAB stands for matrix laboratory.

To compute the force-angle stability measure one must have knowledge of the location of the ground contact points of the rover relative to the rover center-of-mass location, knowledge of the external forces and moments acting on the rover, and knowledge of the rover linear and angular accelerations. These are necessary elements of dynamic system simulation. And they are quantities that can be measured on a real system. But for the sake of this research, many assumptions should be taken into consideration in order to suit cases as in mobile robots moving on a rough terrain:

1. It is better for traveling mobile robots not to move in a high speed, because these robots are designed for investigational purposes such as planetary exploration, military rescue and scientific discoveries, so accuracy is needed in

such cases rather than speed. For example, SRR mobile robot speed was 6 cm/sec (Iagnemma et al., 2000). Accordingly, dynamic forces do not have a large effect on system behavior, and thus quasi-static movement is more appropriate.

2. Traveling speed of mobile robots is better to be constant, since acceleration causes dynamic forces such as inertial moments and forces that is better to be neglected for simplicity leaving the only force that affects the rover is the gravity force.
3. The wheels of the robot are assumed to have a point-contact with the terrain.
4. The body of the mobile robot is assumed to have a symmetrical solid object with homogenous mass distribution, the location of the center of mass is at the middle of the robot body. So simple stability calculations can be obtained (because the objectives of this research are to study the effect of some variables on the stability of mobile robot and not to design a physically-hardware robot).
5. There are many variables affecting the robot stability like number of wheels, surface inclination, height of the center of the mass, friction forces, reaction forces, slipping…etc., but in this study, we will focus on the first three variables and will thoroughly study them with ignoring other variables since the robot is very low and the motion is nearly quasi-static.
6. Let p_c represents the location of the vehicle center-of-mass; generally all vectors are expressed in an inertial frame. This means that all contact points and center of mass of a mobile robot must refer to reference frame. Here, it is important to find method for determining the location of center of mass with respect to identified reference or inertial frame.

7. The body of the mobile robot will be assumed to be a symmetrical solid object with homogenous mass distribution, and the location of the center of mass will be at the middle of the robot body. This procedure and assumption are taken into consideration because our attention is to determine the mobile robot stability as a first step. And after checking that the stability mathematical equations are working properly, then one can search for finding the exact mass distribution in order to make a physical robot design and this will not be included in this thesis.

2 Determining the Location of the Center of Mass

Let p_1, p_2, p_3 and p_4 are contact points between the mobile robot wheels and ground, and assume that they lie at three-dimensions on an arbitrary square plane relative to initial coordinate frame. The center of mass for this robot is assumed to be above the middle of that plane, and the line connecting between the center of mass and plane center must be perpendicular to this plane as shown in Figure (29).

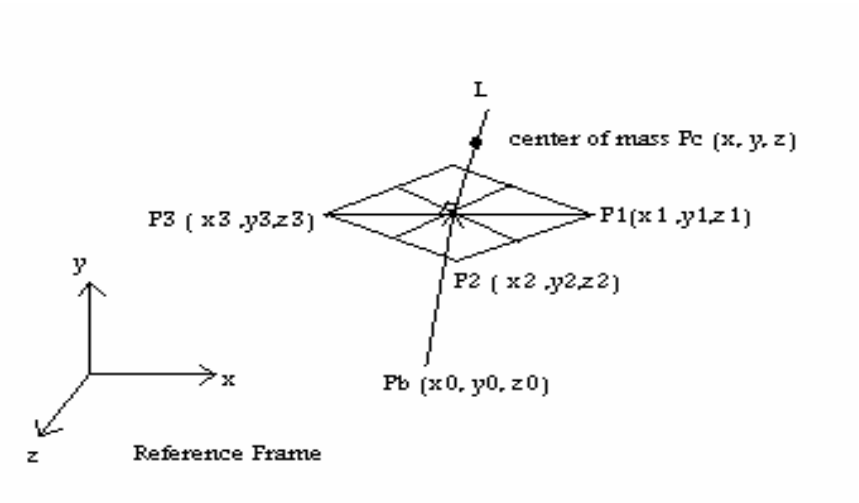

Figure (29): The center of mass location with respect to square plane in three-dimensions

Since the points p_1, p_2 and p_3 lie in the plane, the vector $\overrightarrow{p_1p_2} = \langle x_2 - x_1, y_2 - y_1, z_2 - z_1 \rangle$ and $\overrightarrow{p_1p_3} = \langle x_3 - x_1, y_3 - y_1, z_3 - z_1 \rangle$ are parallel to the plane. Therefore:

$$\mathbf{v} = \overrightarrow{p_1p_2} \times \overrightarrow{p_1p_3} = \begin{vmatrix} \mathbf{i} & \mathbf{j} & \mathbf{k} \\ (x_2 - x_1) & (y_2 - y_1) & (z_2 - z_1) \\ (x_3 - x_1) & (y_3 - y_1) & (z_3 - z_1) \end{vmatrix} = \mathbf{Qi} + \mathbf{Rj} + \mathbf{Sk}$$

Where Q, R and S are constants and the resultant vector **v** is perpendicular on the plane (Kreyszig, 1993). Any line in 3-space can be determined uniquely by specifying a point on the line and a non-zero vector parallel to the line as shown in Figure (30).

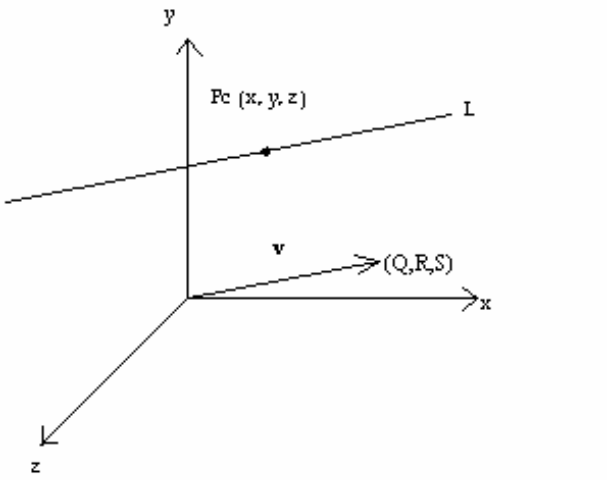

Figure (30): A unique line L passes through p_0 and is parallel to **v**.

The following theorem gives parametric equations of the line through a point p_c and parallel to a non-zero vector **v** (Anton, 1999).

Theorem:

The line in 3-space that passes through the point p_c (x, y, z) and is parallel to the non-zero vector $\mathbf{v} = \langle Q, R, S \rangle = Q\mathbf{i} + R\mathbf{j} + S\mathbf{k}$ has parametric equations

$$x = x_0 + Qt, \qquad y = y_0 + Rt, \qquad z = z_0 + St \qquad \text{where} \qquad -\infty < t < +\infty$$

It is required to consider the followings:

1. The perpendicular vector **v** is parallel to the line L (i.e. **v**//L), where L is the line passes through center of mass p_c and center of plane point p_b.
2. Center of plane p_b belongs to the line L (i.e. $p_b \in$ L). The center of plane point p_b can be calculated from the following relation: $p_b = \left(\frac{x_1 + x_3}{2}, \frac{y_1 + y_3}{2}, \frac{z_1 + z_3}{2} \right)$ = (x_0, y_0, z_0).

3. Considering that the center of mass point (p_c (x, y, z)) and the center of plane point (p_b) are both on the line L. The distance between them equals a length that represents the height of the center of mass from the ground (d), i.e. d (p_c,p_b) = d.

Accordingly, one must have the following equations:

$$x - \left(\frac{x_1 + x_3}{2}\right) = \mathrm{Qt} \qquad \text{.....(50)}$$

$$y - \left(\frac{y_1 + y_3}{2}\right) = \mathrm{Rt} \qquad \text{.....(51)}$$

$$z - \left(\frac{z_1 + z_3}{2}\right) = \mathrm{St} \qquad \text{.....(52)}$$

and the equation of distance between two points,

$$\left(x_0 - \left(\frac{x_1 + x_3}{2}\right)\right)^2 + \left(y_0 - \left(\frac{y_1 + y_3}{2}\right)\right)^2 + \left(z_0 - \left(\frac{y_1 + y_3}{2}\right)\right)^2 = \mathrm{d}^2 \text{ .....(53)}$$

By substituting Equations (50), (51) and (52) in Equation (53) we get the following relation:

$$t = \sqrt{\frac{\mathrm{d}^2}{\mathrm{Q}^2 + \mathrm{R}^2 + \mathrm{S}^2}} \qquad \text{.....(54)}$$

The result is positive and negative magnitude of *t*, return back and substitute again in Equations (50) through (52). We will get two points of p_c; you should select the point that has higher magnitude of *z*.

3 Enhancing the Stability of Mobile Robot

When mobile robots move on a rough-terrain with difficult topography, the robots are exposed to reach instability margins, and some times they may tip over. These manners occur when η goes to zero (i.e. when the resultant force f_r Coincide with any of the tip over axis normal **I**) or, when the magnitude of f_r lies out side the cone described by the tip over axis normal **I**; so the angle becomes negative and tip over is in progress.

To avoid tip over, it is required to modify the center of mass location for the mobile robot. One way for repositioning the center of mass of the robot is by introducing the invert pendulum with a certain mass to its body. The pendulum has the ability to move (in three direction) a mass existing at the end of its bar to a position opposite to the tip over mode axis where turning over occurs around it.

Accordingly, a new center of mass will be established at new location. This mean that the net forces f_r will pass through a region that is far enough from the toppling axis.

The center of mass is a balance point. And it is known from experience that there is a point associated with any mass distribution, the coordinates of the center of mass are calculated from (Crummett and Western, 1994):

$$x_{c.m} = \frac{\sum_{i=1}^{n} m_i x_i}{\sum_{i=1}^{n} m_i} \qquad \text{.....(55)}$$

$$y_{c.m} = \frac{\sum_{i=1}^{n} m_i y_i}{\sum_{i=1}^{n} m_i} \qquad \text{.....(56)}$$

Where mass m_i is located at coordinates (x_i, y_i). If the mass- points are spread out in three dimensions, a similar equation must be written for $z_{c.m}$. From previous equations; one can note that the center of mass is just a weighted average of the positions of all the masses.

A suggested design of the invert pendulum hardware and its photograph is shown in Figure (31 – a and b), This pendulum can move in three directions. The motor in the center rotates the bar with the actual pendulum attached to one end and the counter weight at the other (Kissel and Sutherland, 1997).

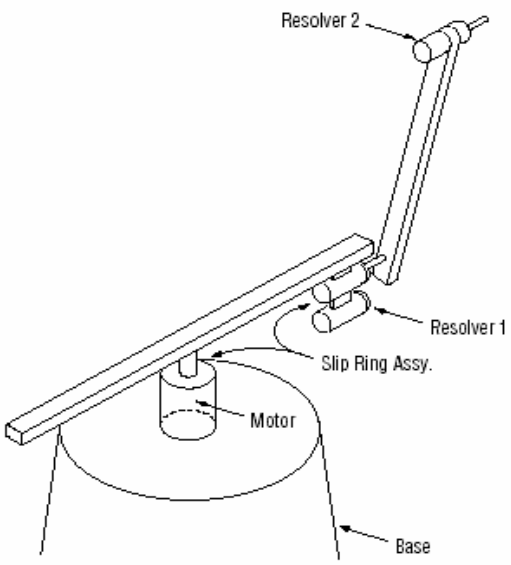

Figure (31 - a): Line drawing of the pendulum hardware (Kissel and Sutherland, 1997).

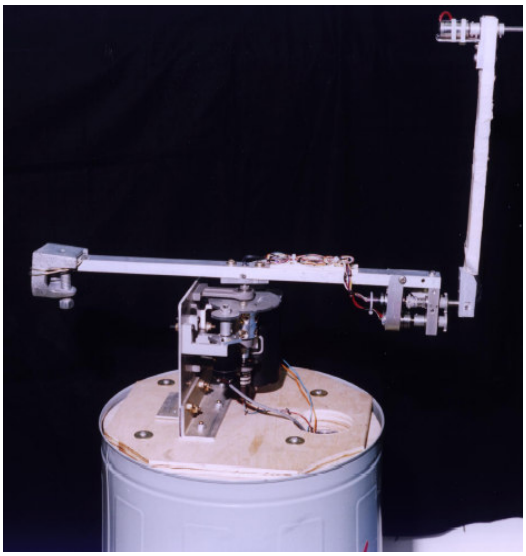

Figure (31 - b): Photograph of the single pendulum hardware (Kissel and Sutherland, 1997).

A tachometer is geared to the motor for one of the three inputs. A resolver is geared to the pendulum to measure the position of the pendulum as the second input. The

command goes to the motor for the systems only output. The motor position measurement would be desirable (Kissel and Sutherland, 1997).

Let assume that the mobile robot has a mass equals to 1 kg. And the mass of the invert pendulum is 0.5 kg (notice that this is mainly the movable mass which is installed at the end of the pendulum bar (arm)). Also it is assumed that the length of bar is 0.5 unit. It is assumed to install the pendulum at the center of the four- wheel mobile robot body. The dimensions of the four- wheel mobile robot as the following:

1) Equal distance between each two wheels to be (2 units).
2) The height of the center of mass with respect to the ground is (2 units).

When doing the simulation, the bar (arm) of the invert pendulum will extend in two dimensions x and y when the mobile robot becomes kinematically unstable. As an example, when the mobile robot moves in the y direction (by using the simulation program), and when the magnitude of the stability angle of wheel number 1 becomes equal to zero or negative amount (the case of instability), then the new location of the center of mass will be (x_1, y_1, z_1) after reconfiguration the position of the invert pendulum. Where x_1 and z_1 are the same component as the old location of the center of mass (before reconfigurability) and y_1 is a component equal to:

$$y_1 = \frac{y_o + 0.5(y_o + 0.5)}{1.5} \qquad \text{.....(57)}$$

The following table (Table (1)) illustrates the modifications on the center of mass when instability occurs.

Table (1): The modifications on the center of mass when instability occurs.

The unstable wheel (tipover mode axis $\mathbf{a}_i$)	The center of mass modification
Wheel no. 1	$y_1 = \frac{y_o + 0.5(y_o + 0.5)}{1.5}$
Wheel no. 2	$x_1 = \frac{x_o + 0.5(x_o + 0.5)}{1.5}$
Wheel no. 3	$y_1 = \frac{y_o + 0.5(y_o - 0.5)}{1.5}$
Wheel no. 4	$x_1 = \frac{x_o + 0.5(x_o - 0.5)}{1.5}$

The results of simulation for the mobile robot after repositioning its center of mass will be viewed at the end of discussion and results. The flow chart shown at the next pages represents the complete simulated steps that are used in determining the stability margin of a four-wheel mobile robot. The flow chart on Figure (32) illustrates the procedures that are taken into consideration when the robot reaches the instability margins and the decisions taken in order to prevent tipover.

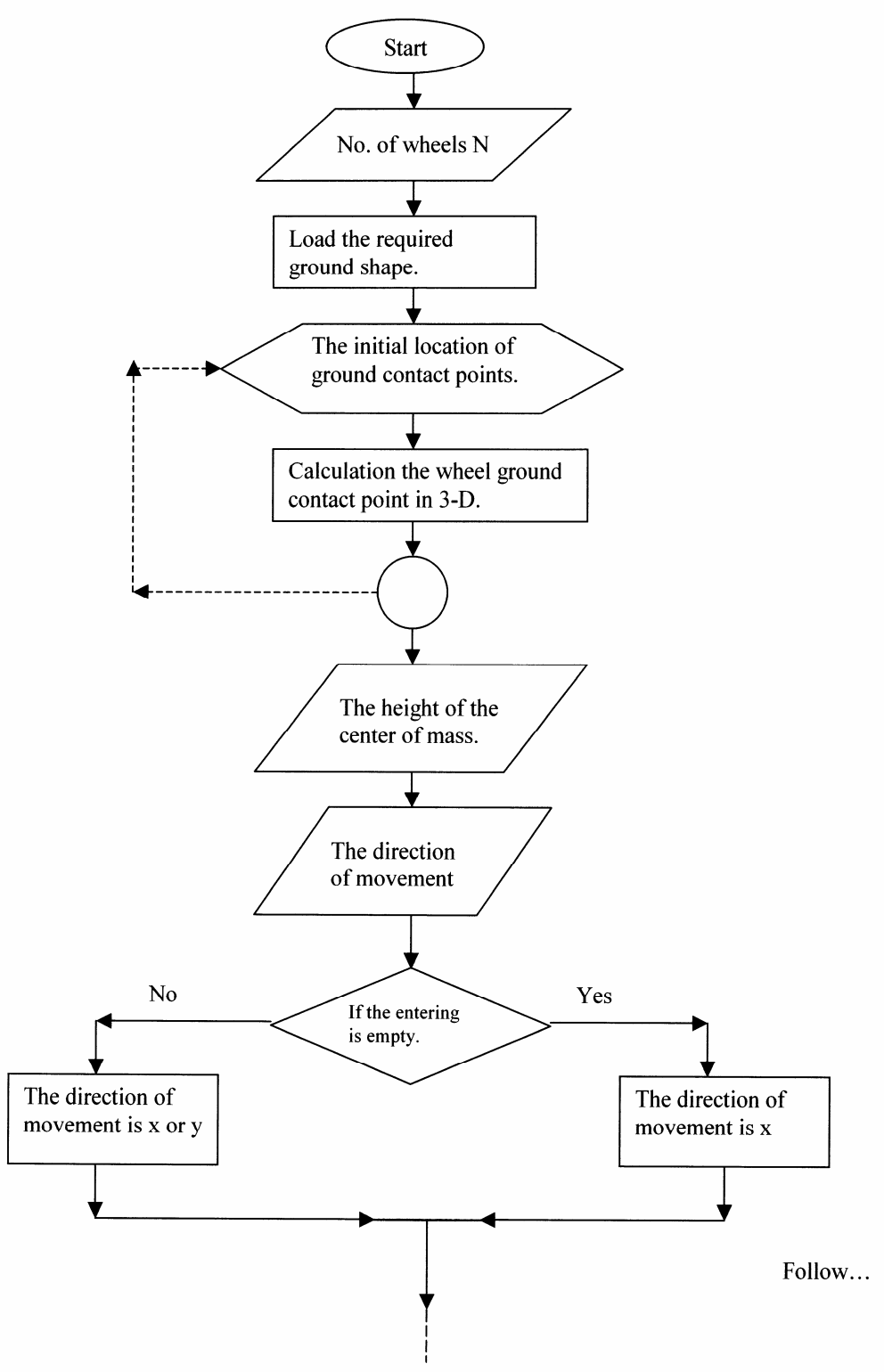

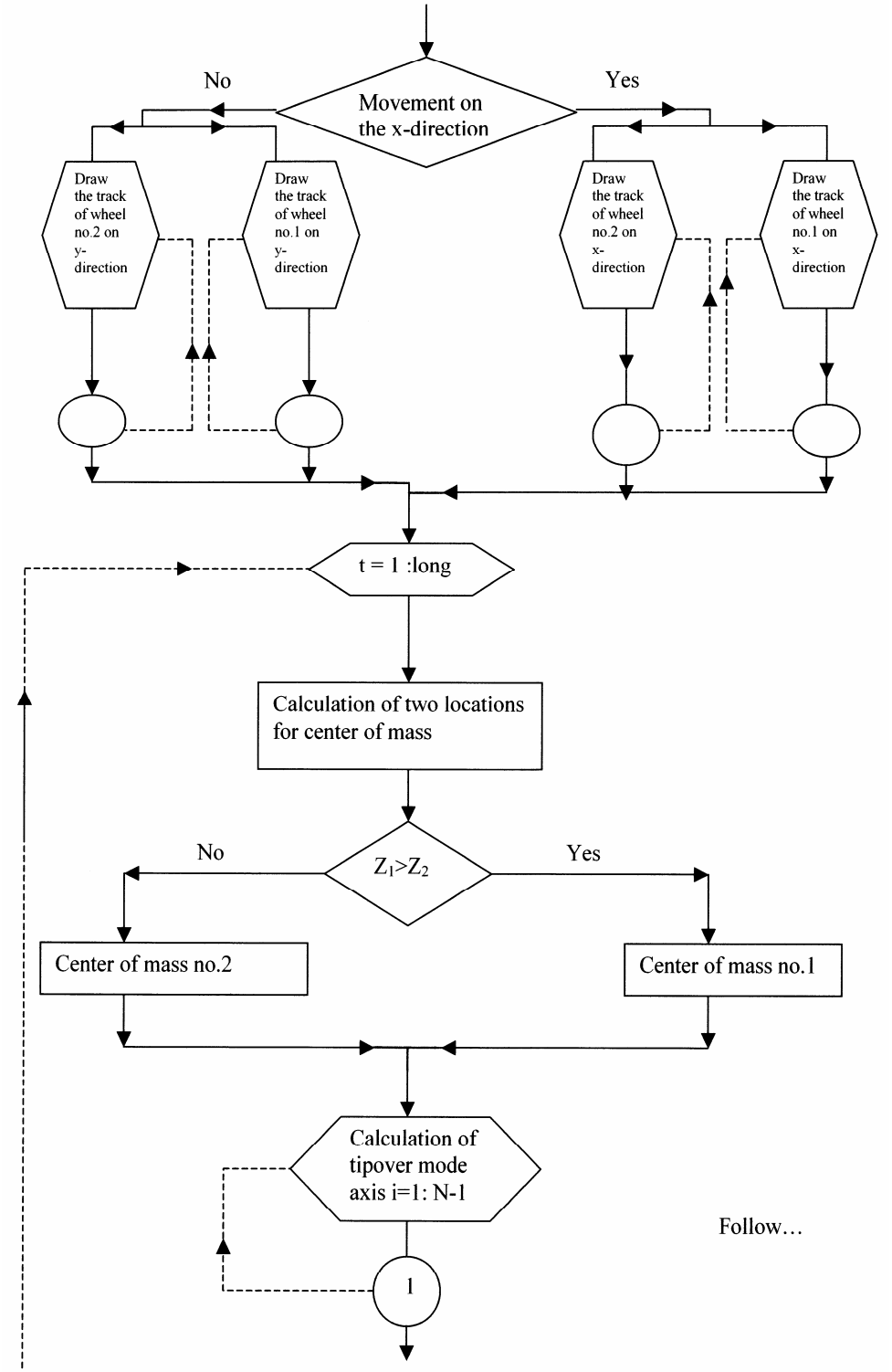

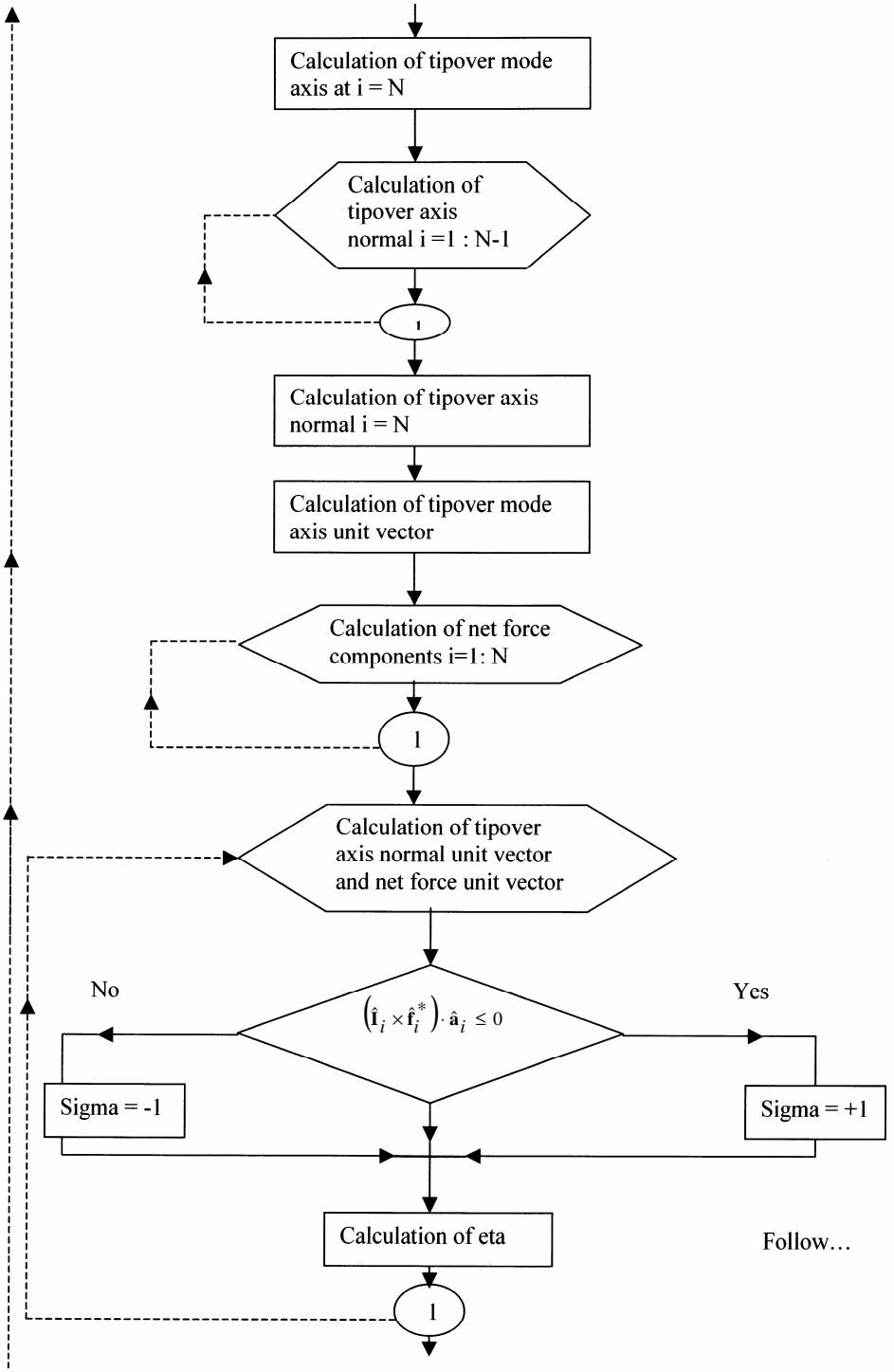

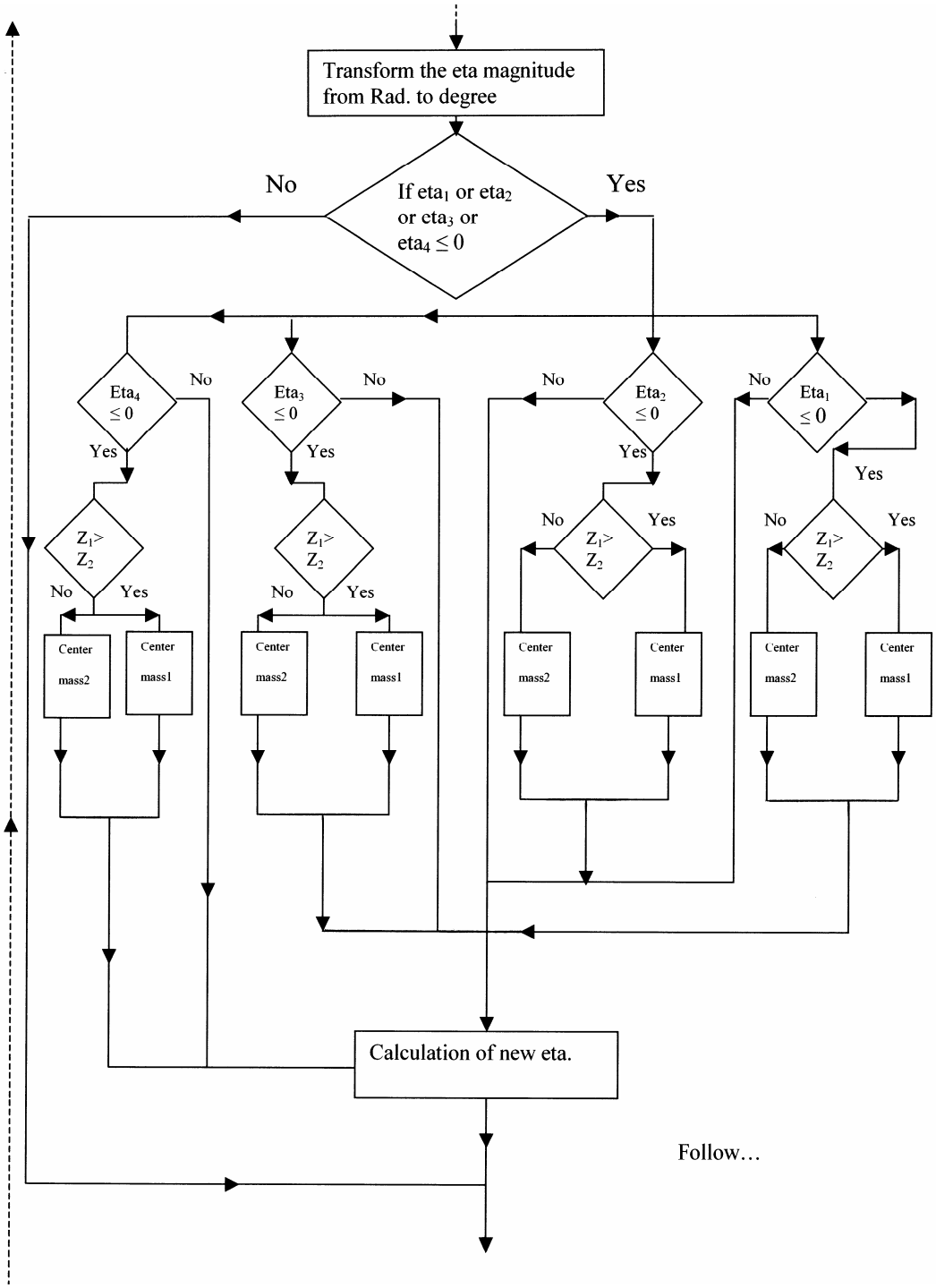

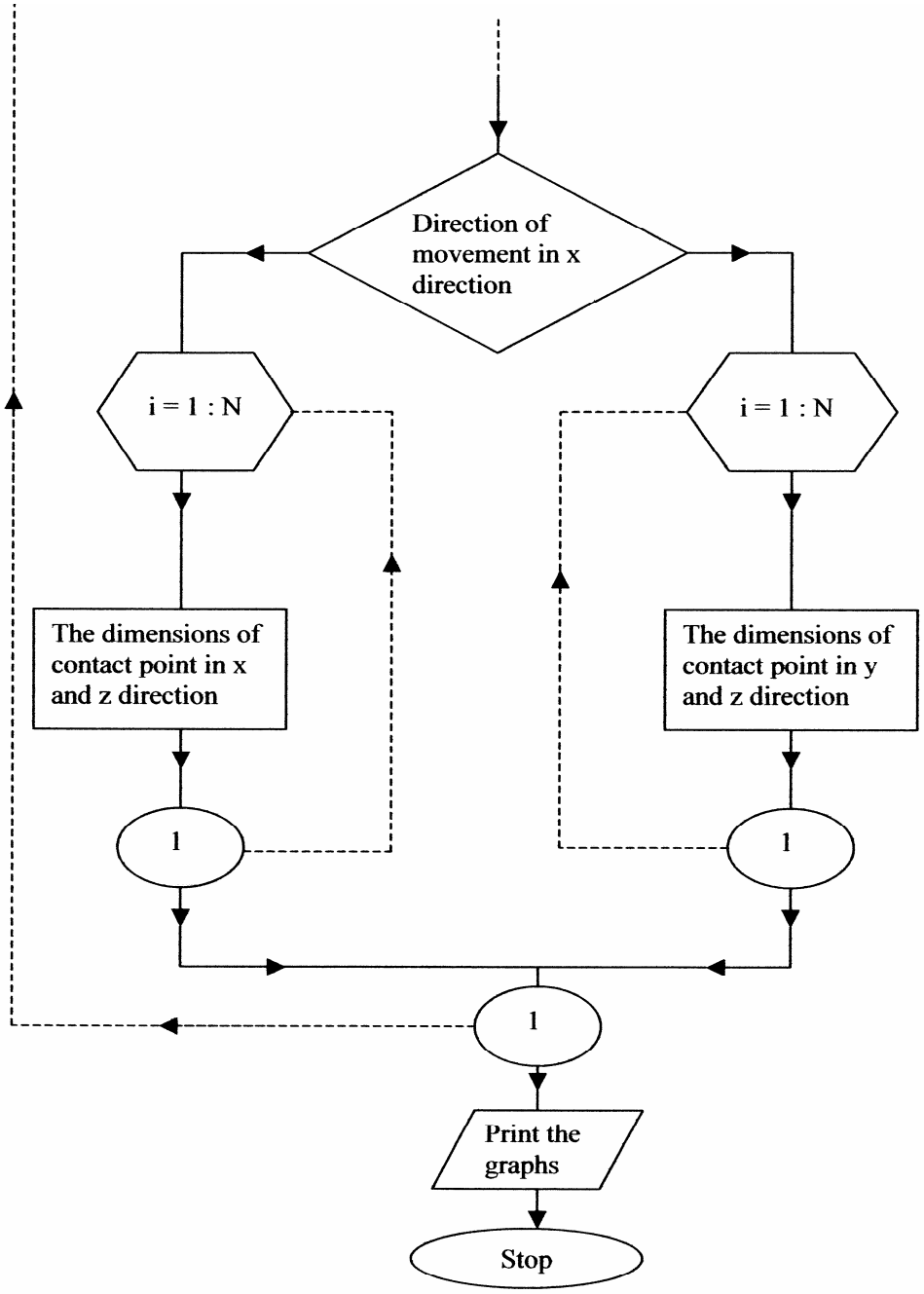

Figure (32): Flow chart diagram showing the steps of simulation program of four-wheel mobile robot.

Discussion and Results

1 Four-Wheel Mobile Robot Simulation

Three types of mobile robots will be studied in this research (according to geometrical wheels distribution). This section will describe the four-wheel mobile robots and their stability while moving on a three-dimensional (3-D) rough terrain by the use of simulation program.

Let the four-wheel mobile robot traverse through the simulated rough surface in y-direction (notice that the four-wheel mobile robot can move in two dimensions, x and y directions). The start point of movement will be shown in Figure (33).

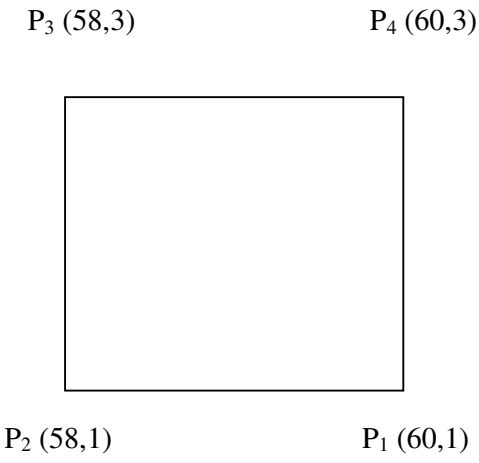

Figure (33): The start of four-wheel mobile robot moving in y-direction.

Of all the mobile robot contact points with the ground, only consider the outermost points as been assumed by Papadopoulos model in chapter 2, which form a square when projected onto the horizontal plane. These outermost contact points (wheels) are designated by P_1(60,1), P_2 (58,1), P_3 (58,3) and P_4 (60,3). Notice that these points are arranged in a clockwise (c.c) pattern as was assumed by the model.

This described mobile robot will traverse through a random surface (rough terrain), as shown in Figure (34).

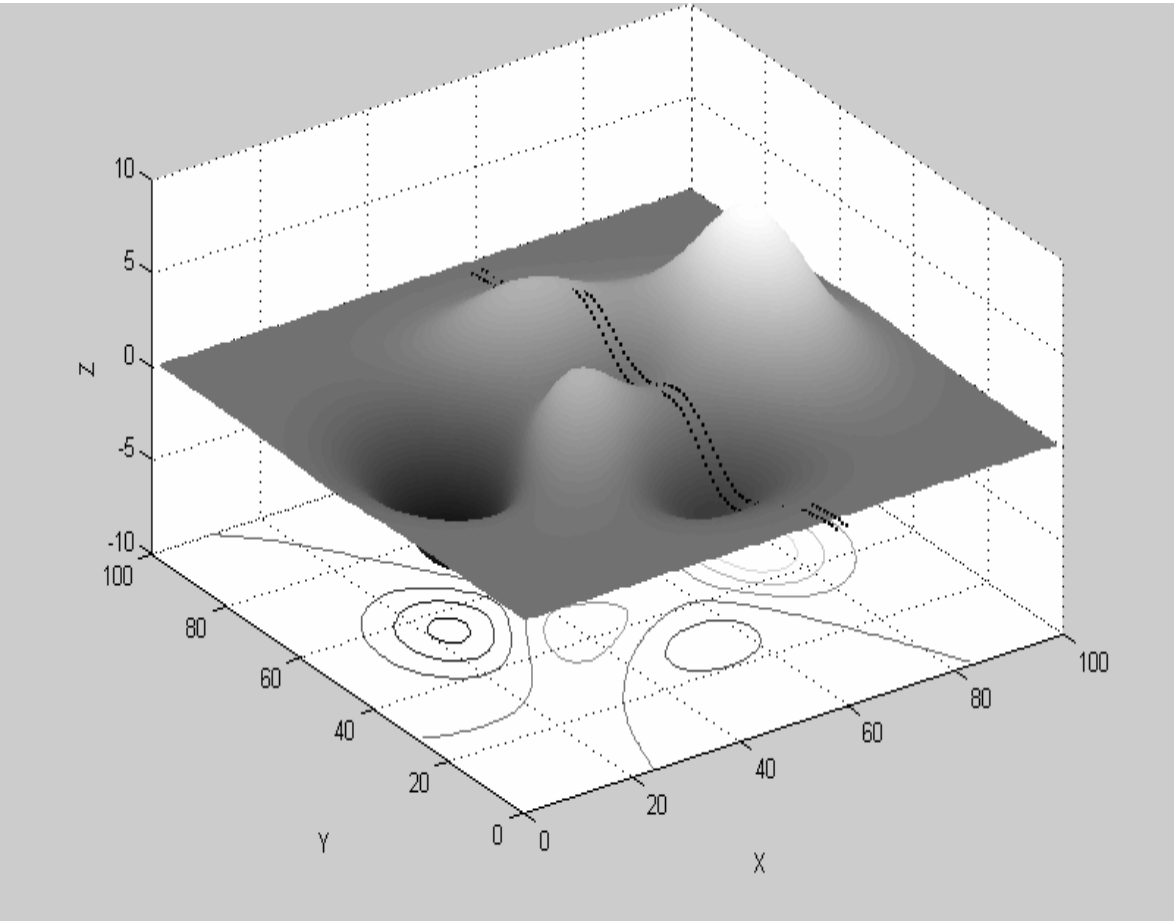

Figure (34): A rough terrain with a shown track of mobile robot

This rough terrain is simulated in three dimensions so including many elevations and depressions that can be considered as a hills and valleys. Figures (35 a and b) represent some side views of this surface to take a better look in different projections.

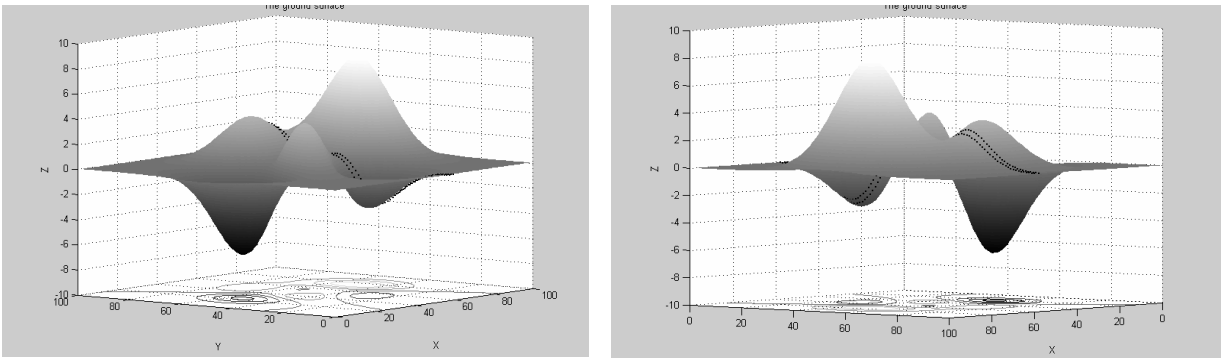

Figure (35): A and B are different views of Figure (34)

Back to Figure (34), the dashed-line track represents the four-wheel mobile robot path. As shown, the mobile robots passed through an excavation or let us say a valley then through many highs or hills.

To study the stability margin of the mobile robot, one should firstly insist on the idea of stability again. As discussed previously, two main axes were obtained: the tip over axis normal (**I**) and the net force (gravity force) axis. The angle between them that is called the force-angle stability measure (η) can help us in the assessment of stability margin. If the angle is positive, the net force vector will lie inside our assumed plane (i.e. between the four wheels) and the mobile robot is stable. If the angle is zero or negative, this means that the net force vector lies at the edge (so even smallest disturbance may

topple the vehicle) or outside the assumed plane (so tip over is in progress), respectively.

So we have three possibilities for the angle (η):

1. Negative: means that tip over is in progress.
2. Zero: means whatever the obstacle is small, the vehicle may topple (critical tip over stability).
3. Positive: means that the mobile robot is stable.

The simulation program studies all the previous possibilities of stability; for example, Figures (36, 37, 38 and 39) are plots of distance (units) against η (degrees) for every wheel through a track drawn on rough terrain (Figure (34)). For wheel 1 (Figure (36)), the stability margin increases till reaching the maximum at distance 20 units (i.e. 20 units in y-direction) then start decreasing from distance 20 units to about distance 37 units which is the lowest stable point for wheel 1. This indicates that the robot is now crossing a steep portion of the valley.

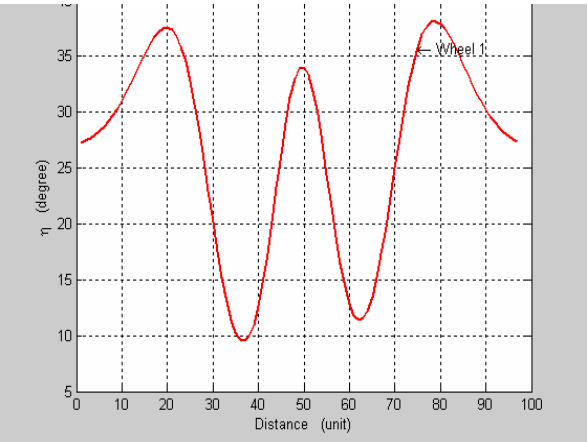

Figure (36): Four-wheel mobile robot stability margin according to wheel 1.

From the last Figure, a concentration should be made on two main ideas:

First, stability margin increases and decreases according to the location on the rough terrain. And, in general, stability margin is maximum when the four-wheel mobile robot getting a horizontal or semi-horizontal position and minimum as the position is very steep.

Second, wheel 1 is not exposed to tipover all through its track, as the angle is always positive, this is applied only for forces studied in this research with neglecting others.

The previous discussion is applicable to the other wheels P_2, P_3 and P_4 (Figures 37, 38 and 39, respectively) with the same principles.

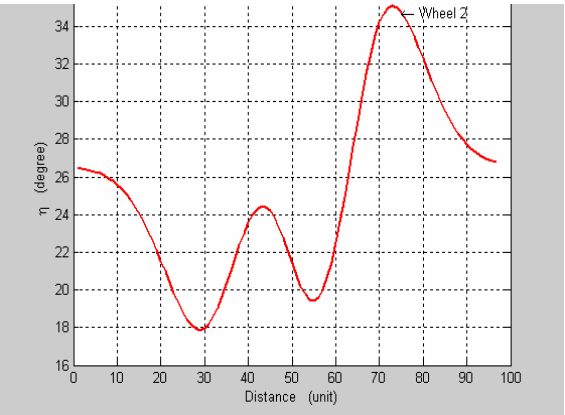

Figure (37): four-wheel mobile robot stability margin according to wheel 2.

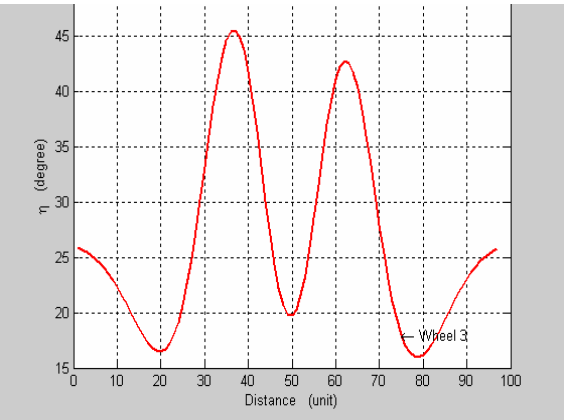

Figure (38): four-wheel mobile robot stability margin according to wheel 3.

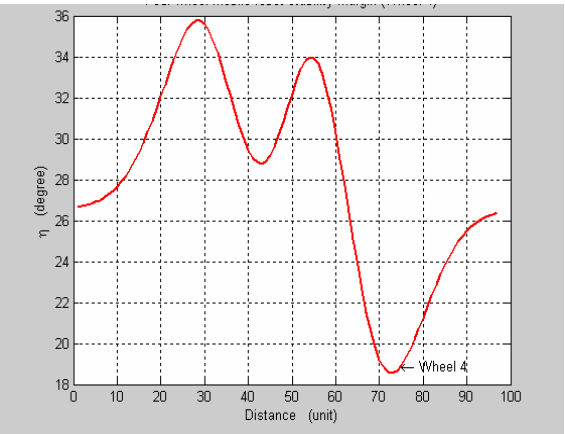

Figure (39): four-wheel mobile robot stability margin according to wheel 4.

It is worthwhile to compare the stability margin of two wheels at the same time. So Figures (40 through 43) are plots represent a comparison of the stability margin of two wheels at the same graph.

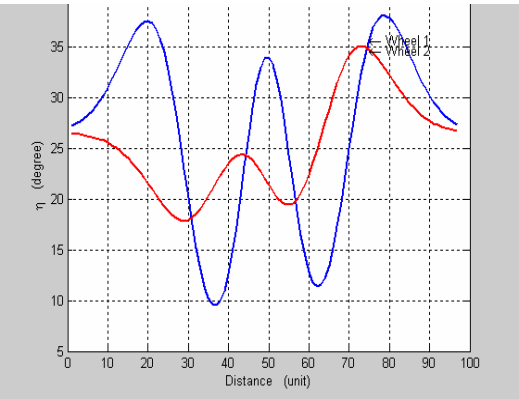

Figure (40): A combined graph of four-wheel robot stability margin at wheels 1 and 2.

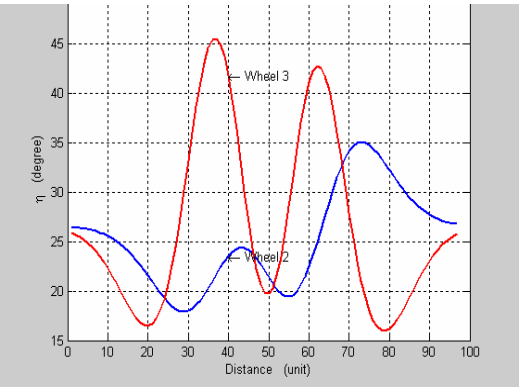

Figure (41): A combined graph of four-wheel robot stability margin at wheels 2 and 3.

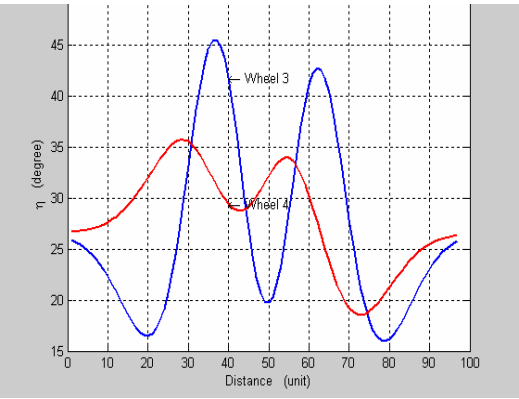

Figure (42): A combined graph of four-wheel robot stability margin at wheels 3 and 4.

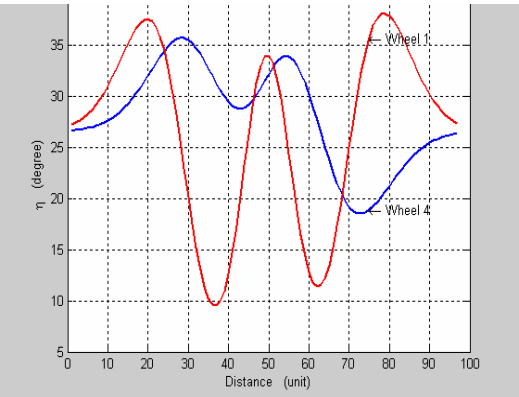

Figure (43): A combined graph of four-wheel robot stability margin at wheels 4 and 1.

Three possibilities at every passed distance were obtained:

1. The angles of stability at both wheels are both positives: this means that the mobile robot is stable at both wheels.
2. One is positive and the other is negative: here, tipover is in progress around line connecting that wheel and the next one (i.e. around tipover mode axis, $\mathbf{a}_i$).
3. The two angles are negative: so tipover is in progress around the second unstable wheel and the other three wheels will loose their contact with the surface.

As the latter illustration, it is beneficial to compare two wheels stability at the same time and by returning back to Figures (40, 41, 42 and 43), it can be deduced that all comparisons are positive and the mobile robot is stable all through its track. For example, Figure (44) represents a comparison between four-wheel mobile robot stability margin at both wheels 1 and 2. One can note that the lowest point of stability of the two wheels all through the track is on wheel 1 at about distance of 37 units and η equals 9 degrees. This is the lowest point, but it is still positive and the robot is still stable at that location. Figure (44) shows stability margin at the four wheels on the same plot.

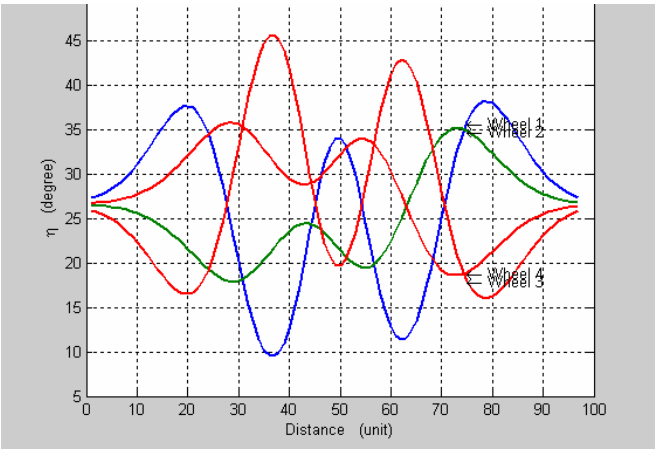

Figure (44): A combined graph of four-wheel robot stability margin at the four wheels.

Another way to assess stability margin of four-wheel mobile robot is by concentrating on the minimum stability angle for a selected group of wheels. It is used when we need to comment on the stability of the rover and where tipover will occur, with no importance to know at what wheel or at what mode axis tipover will occur (i.e. the mere judgment if it is stable, critical tipover or tipover in progress).

For example, Figure (45) shows minimum stability margin of the four wheels.

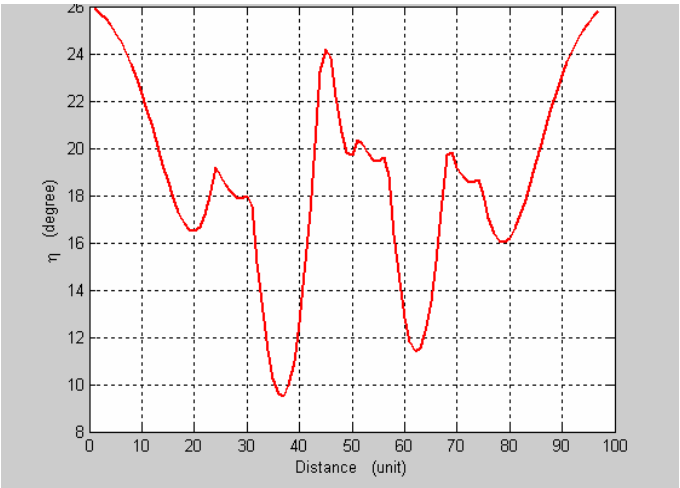

Figure (45): The minimum stability margin for the all four wheels.

From this Figure, it can be concluded that the rover is stable from the beginning to the end of its path, because the minimum stability margin is always positive. Also, one can conclude that any point in the graph represents the lowest stable point of every wheel apart, for example, at distance 78 units; the angle is about 16 degrees, which corresponds to the lowest stability margin of all the four wheels, wheel 3 (see Figure (45)). Figures (46 through 49) represent the minimum stability margin of every two wheels apart.

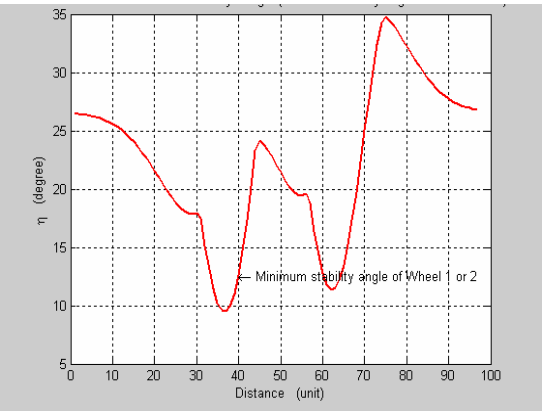

Figure (46): The minimum stability margin for the wheels 1 and 2.

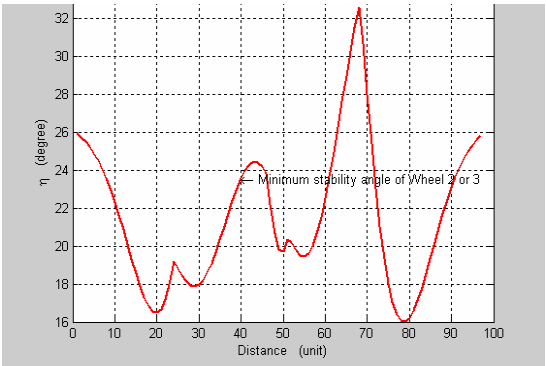

Figure (47): The minimum stability margin for the wheels 2 and 3.

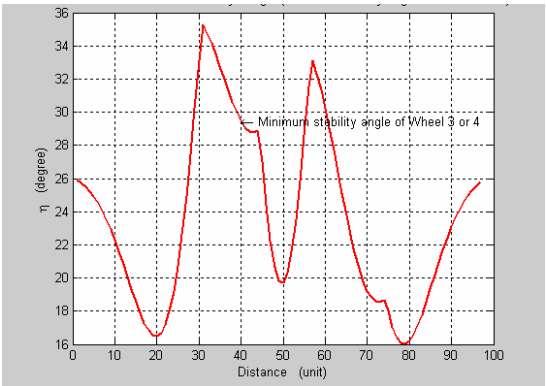

Figure (48): The minimum stability margin for the wheels 3 and 4.

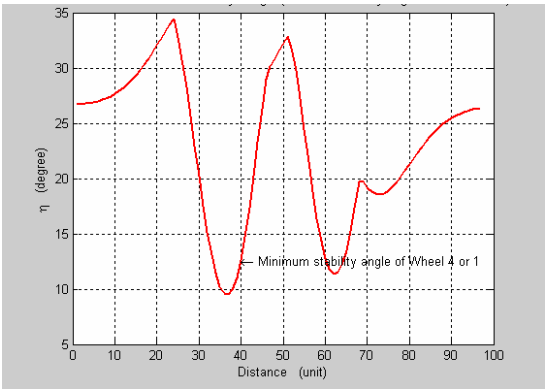

Figure (49): The minimum stability margin for the wheels 4 and 1.

The simulation program can also plot the center of mass distance in different axes relative to the reference frame (units) against distance (units).

Figure (50) shows the center of mass distance in Y-direction relative to the reference frame.

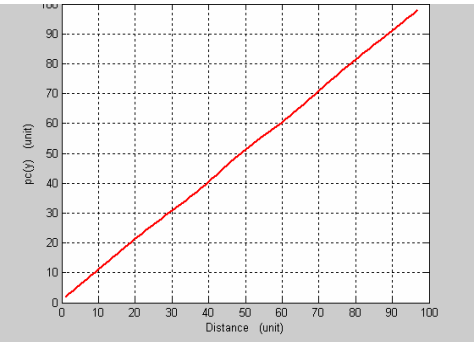

Figure (50): Center of mass in y-direction relative to the reference frame.

This graph is somewhat linear because it was assumed in this sample that the robot path is straightforward in the Y-direction. In Figure (51), which represents the center of mass distance in X-direction relative to the reference frame.

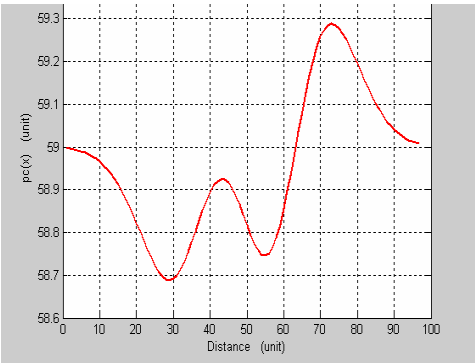

Figure (51): Center of mass in x-direction relative to the reference frame.

It is obviously a magnitude ranging from 58.7 units and 59.3 units. From this one can deduce that the four-wheel mobile robot turns slightly clockwise and counterclockwise around the Y-axis and as a result, slight change in the position of the center of the mass causing this range of measurement. Also, it can be expected that if the rover walks on a long flat surface, there will be no range in the center of the mass distance in X-direction.

Figure (52) shows center of mass distance in Z-direction relative to the reference frame. This graph is a simple side view of the four- wheel mobile robot track.

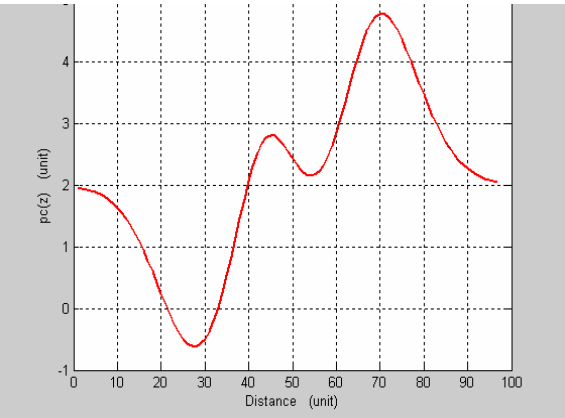

Figure (52): Center of mass in z-direction relative to the reference frame.

Figure (53) represents the center of mass distance magnitude of a rover moving on a rough surface relative to the reference frame. This is calculated as $\sqrt{x^2 + y^2 + z^2}$, so it is logical to have a non-linear relationship.

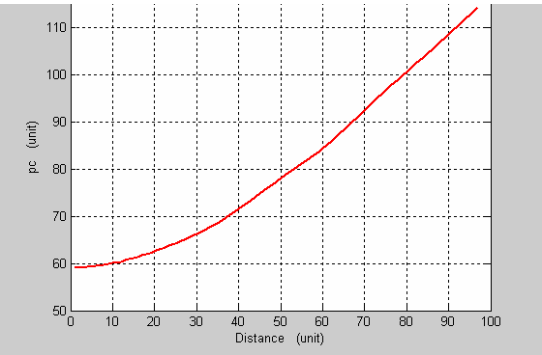

Figure (53): Center of mass distance magnitude relative to the reference frame.

Remark: refer to appendix B in order to see the remaining graphs of the three-wheel mobile robots (the previous two types that were mentioned).

2 Mobile Robot Stability on Flat Surface

The proposed algorithm and the MATLAB implementation has been implemented and applied to several examples in order to study its efficiency and performance. All of the examples correspond to the three-dimensional motion of the mobile robot.

The following example or case is one of the cases that were used to study the problem of robot stability. All the simulated samples were quoted directly from MatLab simulator. The first sample is the simplest one; when the four-wheel mobile robot moving on a flat surface as shown from Figure (54).

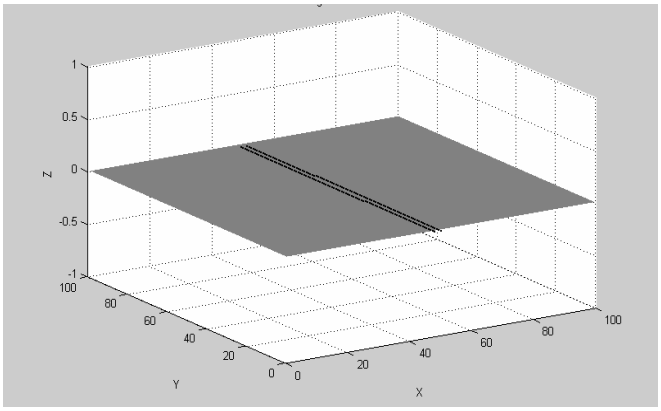

Figure (54): Flat surface.

All wheels are subjected to the same degree of inclination; it's a flat surface and the inclination equals zero. Consequently the force-angle stability measure that is the angle between tip-over axis normal (**I**) and net force (gravity force) for all tipover mode axis is the same. The force-angle stability measure is 26.57^{o} for all the wheels of mobile robot that has height of two units between the center of mass and ground, refer to Figure (55).

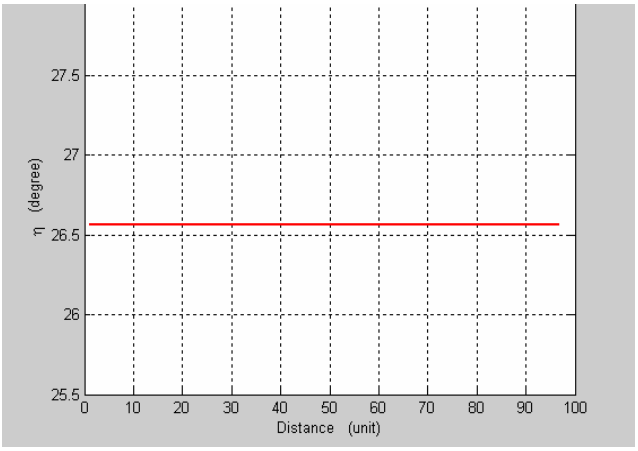

Figure (55): Four-wheel mobile robot stability margin on flat surface.

The graph is a straight line, so the stability margin is constant all through the crossed distance. Tipover may not occur since the angle is positive all the time, and the net force vector lies inside the assumed plane between the four wheels (four constants points). If the stability angles of any point reach zero or negative magnitude (not in this sample), the rover will be in progress to tipover.

3 Mobile Robot Stability on Inclined Flat Surface

The following simulated sample shows in detail the stability measure on every wheel for four-wheel mobile robot when moving on the following surfaces:

1) Case 1: inclined flat surface turned clock wisely around an imaginary axis in y-direction (figure 56).

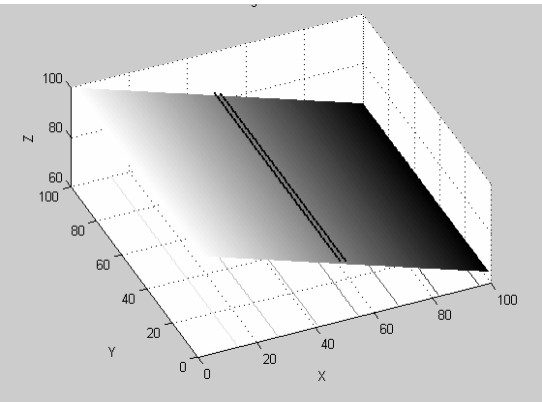

Figure (56): Inclined flat surface turned clock wisely around an imaginary axis in y-direction.

2) Case 2: inclined flat surface turned counter clock wisely around an imaginary axis in x-direction (Figure 57).

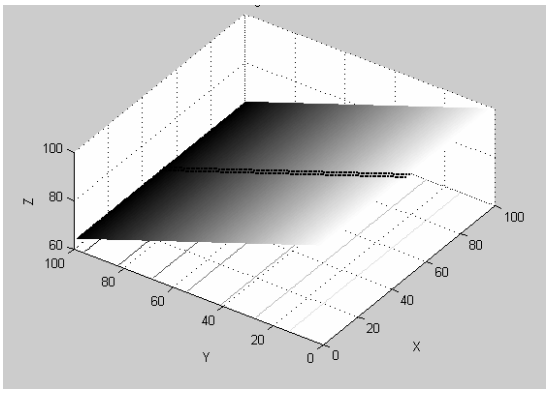

Figure (57): Inclined flat surface turned counter clock wisely around an imaginary axis in x-direction.

3) Case 3: inclined flat surface turned counter clock wisely around an imaginary axis in y-direction (Figure 58).

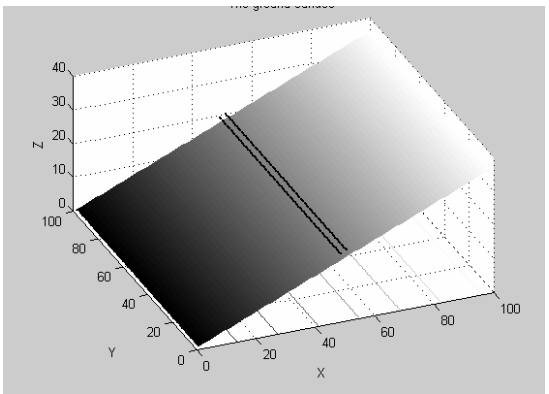

Figure (58): Inclined flat surface turned counter clock wisely around an imaginary axis in y-direction.

4) Case 4: inclined flat surface turned clock wisely around an imaginary axis in x-direction (Figure 59).

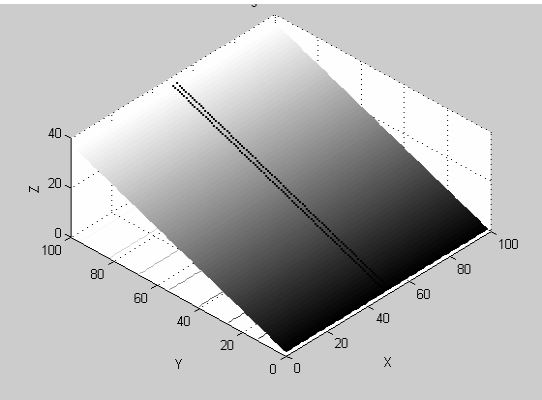

Figure (59): Inclined flat surface turned clock wisely around an imaginary axis in x-direction.

Through the four cases, the mobile robot moves on a track in y-direction. The magnitude of inclination angle is constant for all cases and it equals 20°.

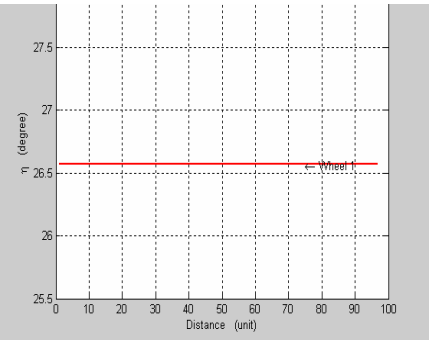

Figure (60): Stability margin at wheel 1 for mobile robot moving on an inclined surface of case 1.

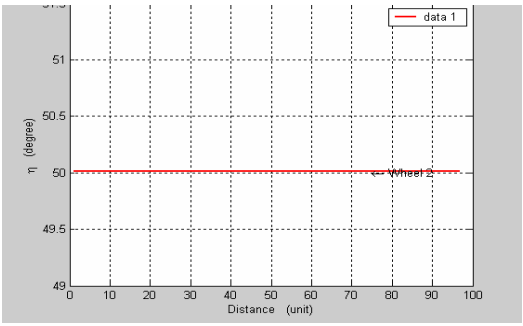

Figure (61): Stability margin at wheel 2 for mobile robot moving on an inclined surface of case 1.

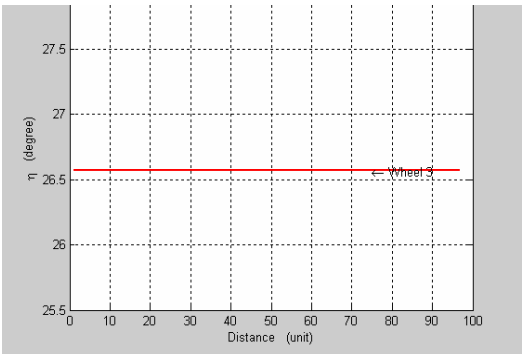

Figure (62): Stability margin at wheel 3 for mobile robot moving on an inclined surface of case 1.

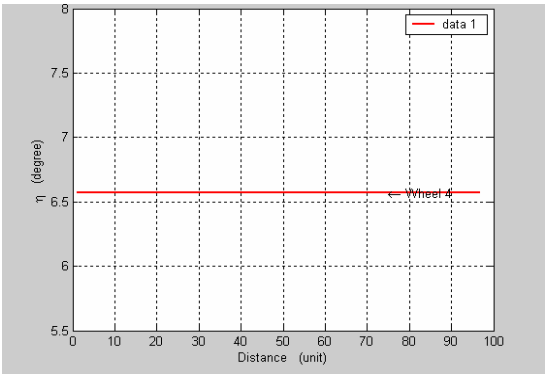

Figure (63): Stability margin at wheel 4 for mobile robot moving on an inclined surface of case 1.

By referring to Figures (60 through 63) of case 1, one can note that the minimum force angle stability measure occurs on wheel number 4 and it equals 6.57° while the angle measure for wheel 1 and 3 is 26.57° and for wheel number 2 is 50.01°. If the angle of stability for wheel 4 is negative (i.e. the net force vector lies out side the polygon from the connecting between the wheels 4 and 1 "$\mathbf{a}_4$"), the tipover will be in progress and the rover will turn over around the mode axis $\mathbf{a}_4$ (the connecting line between wheel 4 and 1). This mean that the rover will stand on two wheels; wheel 1 and 4, and the other wheels will loose contact with surface. Refer to Figure (64).

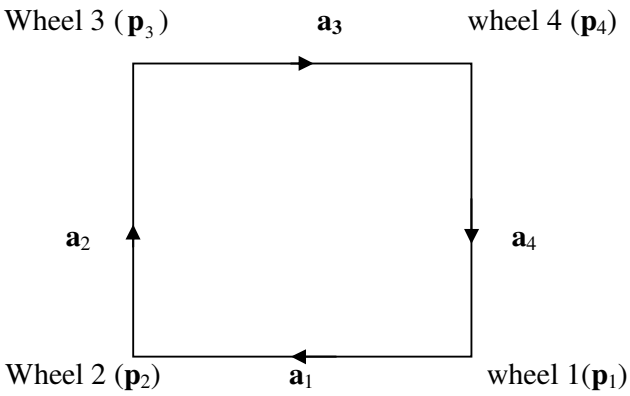

Figure (64): Four-wheel contact point polygon and their mode axes.

The lowest angle stability in case 2 occurs on wheel number 3 and equals 6.57° while it is 26.57° for wheel 2 and 4. The highest stability is at wheel 1 (50.01°). In this case, the probability of turning over will occur (if stability angle is negative) around the mode axis $\mathbf{a}_3$ which is the line connecting between wheels 3 and 4 and the rover will stand on the previous two wheels. On the other side, wheels 1 and 2 will loose their contact with surface. See Figures (65through 68).

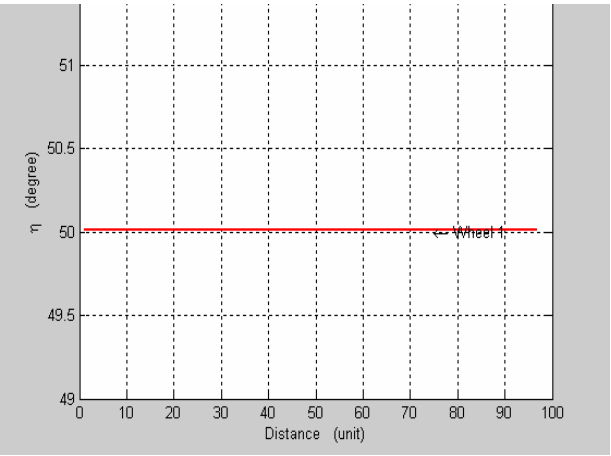

Figure (65): Stability margin at wheel 1 for mobile robot moving on an inclined surface of case 2.

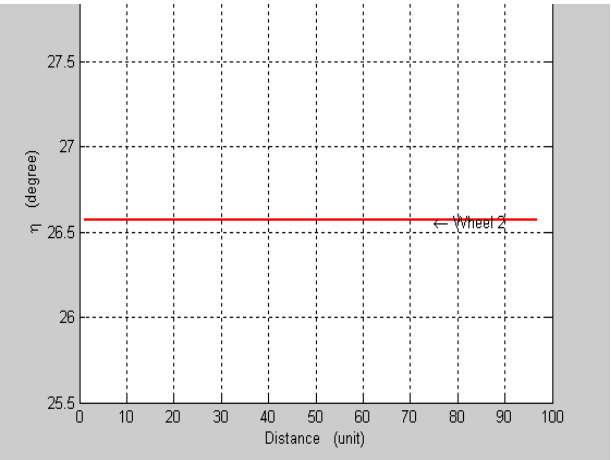

Figure (66): Stability margin at wheel 2 for mobile robot moving on an inclined surface of case 2.

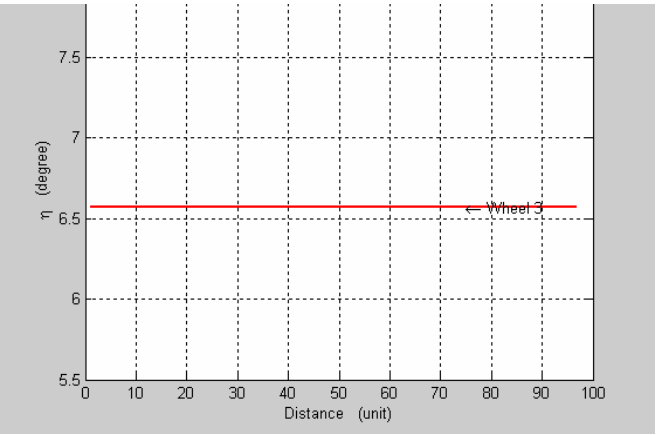

Figure (67): Stability margin at wheel 3 for mobile robot moving on an inclined surface of case 2.

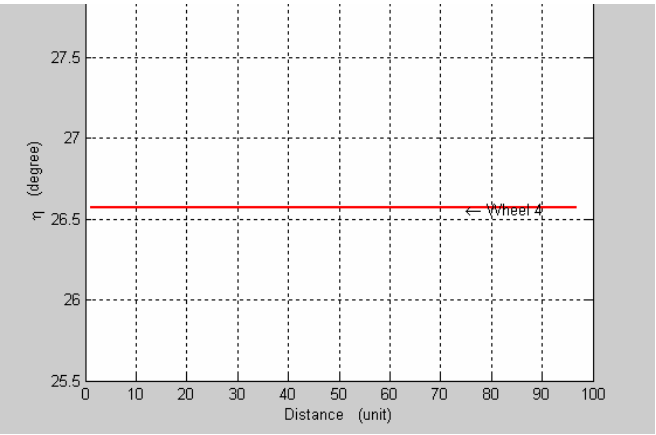

Figure (68): Stability margin at wheel 4 for mobile robot moving on an inclined surface of case 2.

In case 3, the highest angle stability occurs on wheel 4 which equals 50.01° and it is 26.57° for wheel 1 and 3. The lowest stability occurs on wheel 2 with 6.57° look to Figures (69 through 72).

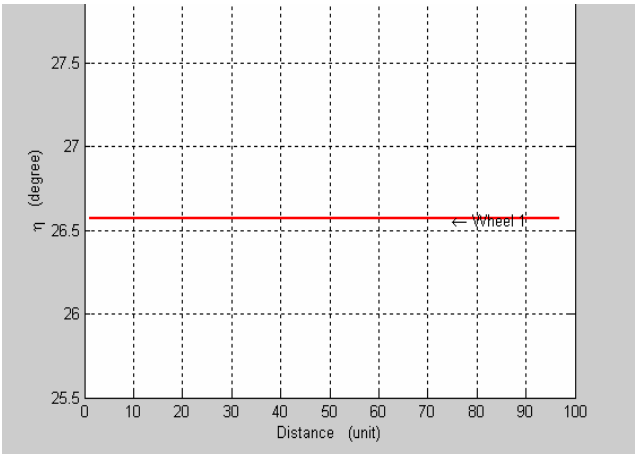

Figure (69): Stability margin at wheel 1 for mobile robot moving on an inclined surface of case 3.

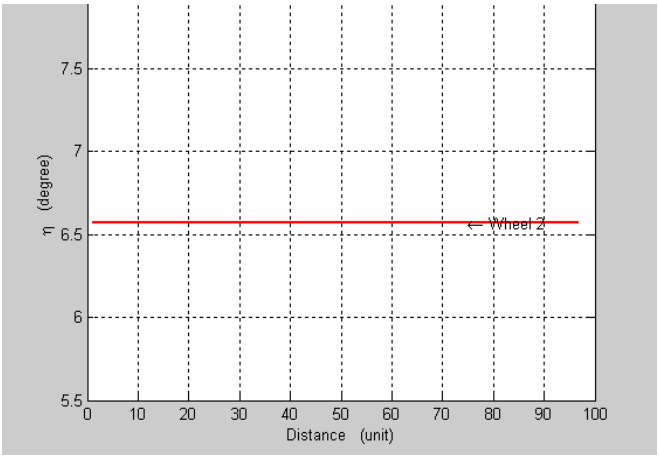

Figure (70): Stability margin at wheel 2 for mobile robot moving on an inclined surface of case 3.

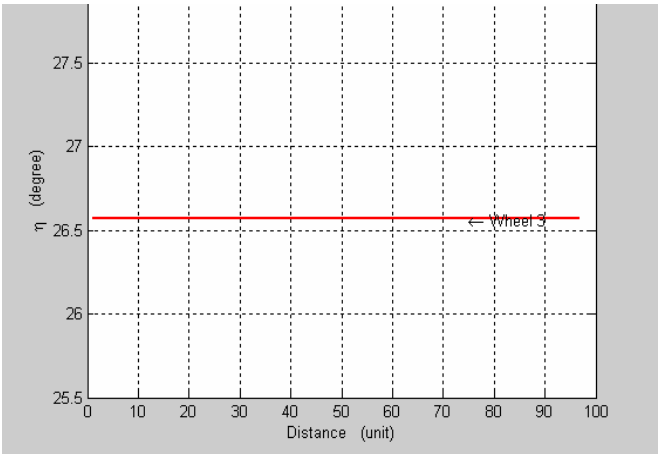

Figure (71): Stability margin at wheel 3 for mobile robot moving on an inclined surface of case 3.

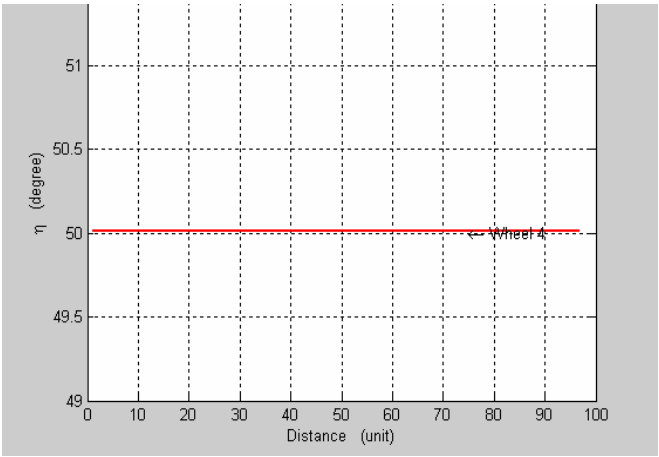

Figure (72): Stability margin at wheel 4 for mobile robot moving on an inclined surface of case 3.

The same is applied on case 4, but with the least stability on wheel 1 which equals 6.57° and the highest stability on wheel 3 with 50.01°. Wheels 2 and 4 are equal in stability. See Figures (73 through76).

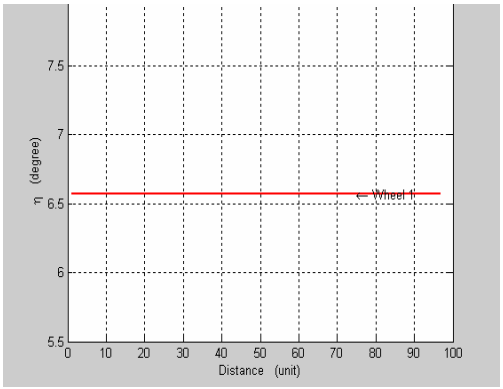

Figure (73): Stability margin at wheel 1 for mobile robot moving on an inclined surface of case 4.

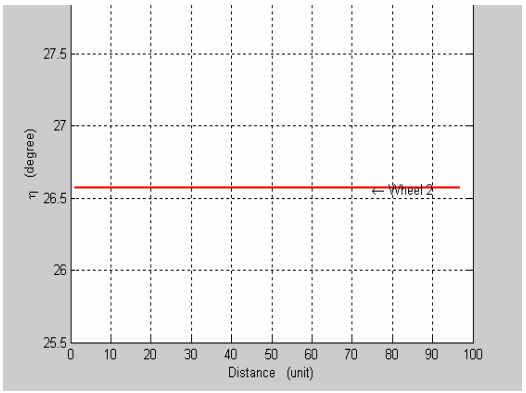

Figure (74): Stability margin at wheel 2 for mobile robot moving on an inclined surface of case 4.

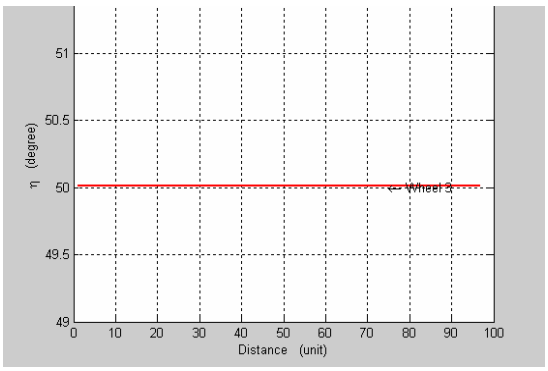

Figure (75): Stability margin at wheel 3 for mobile robot moving on an inclined surface of case 4.

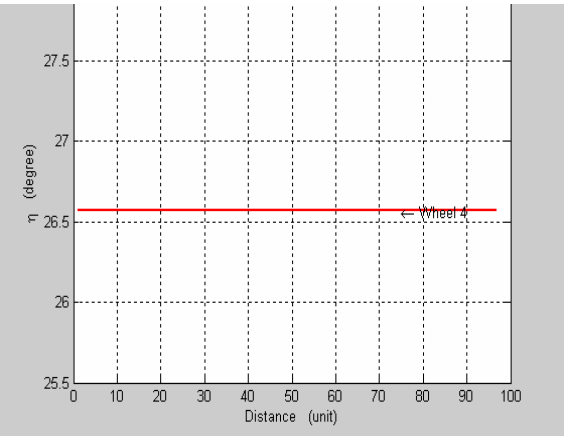

Figure (76): Stability margin at wheel 4 for mobile robot moving on an inclined surface of case 4.

4 The Stability Margin for Different Number of Wheels

As was discussed previously, there are three main factors affecting the stability of a mobile robot moving on a surface. These are:

1. Number of wheels of the mobile robot (for a specific wheel distribution).
2. Height of the center of mass.
3. The angle of the inclined surface.

So, to study every factor apart, one should consider the other two factors to be constant. Here in this section, The effect of the number of wheels on the stability of a mobile robot for one surface and fixed height of the center of mass will be studied.

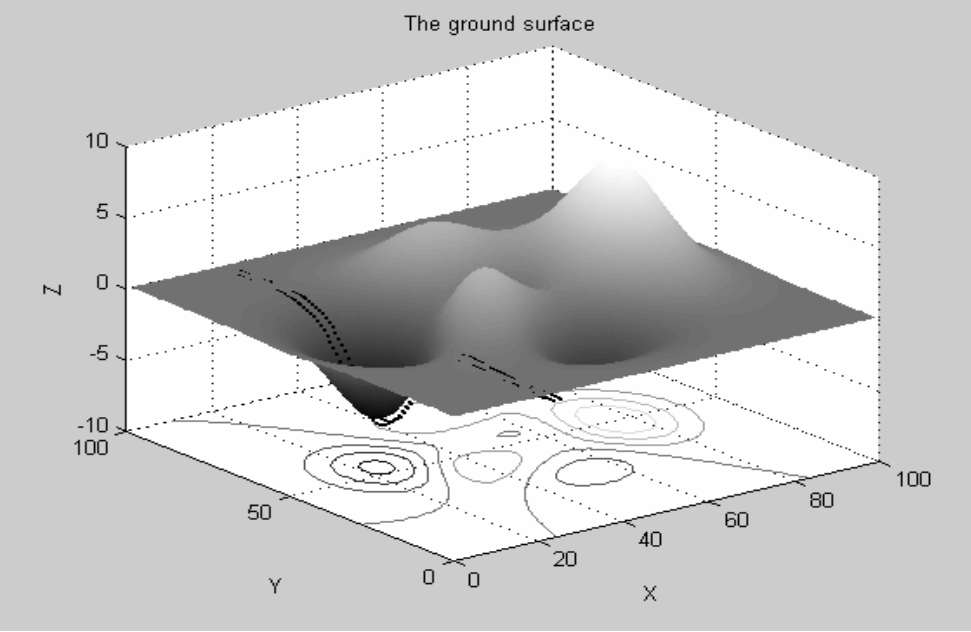

Figure (77): Rough terrain with a track of mobile robot passing through a valley.

Figure (77) shows rough terrain with a track of mobile robot passing through a valley. As the mobile robot goes down through the valley, its stability decreases till the lowest at distance 43 units as shown in Figure (78).

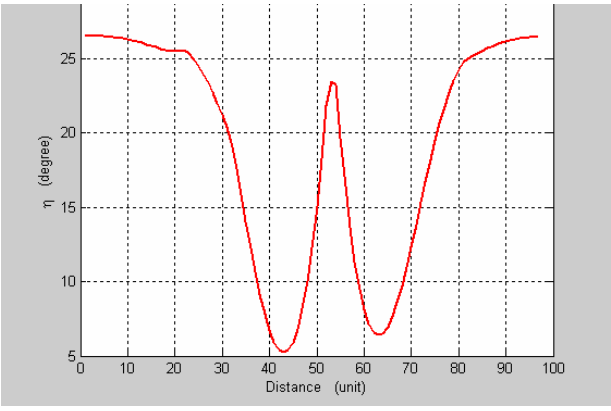

Figure (78): Four-wheel mobile robot stability margin on moving on a rough terrain.

This lowest stability coincides with the steepest portion of the valley. At distance 53 units, the stability of mobile robot is the highest and equals 24° and this coincides with the bottom of the valley where the mobile robot gets a semi-horizontal position. As the mobile robot start ascending, the stability decreases again.

This discussion was applied on a four-wheel mobile robot. But we have three types of mobile robots assumed in this research: four-wheel mobile robot, three-wheel mobile robot with one wheel on the front side and three-wheel mobile robot with one wheel on the rear side. Figure (79) shows a comparison between the stability of these three types of mobile robots.

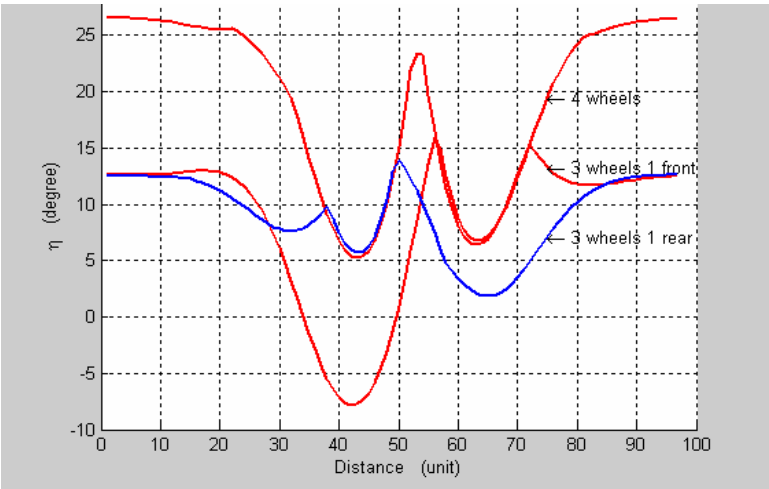

Figure (79): Comparison between the stability of three types of mobile robots.

From this Figure note that:

- Four-wheel mobile robot is the most stable one all through the assumed track except in two positions:
    1. Distance from 37 to 47 units that coincide with the steepest portion of the valley during descending. Here, the three-wheel mobile robot with one wheel in rear is more stable.
    2. Distance from 57 to 67 that coincide with the steepest portion of the valley during ascending. Here, the three-wheel mobile robot with one wheel in front is more stable.
- The four-wheel mobile robot and the three-wheel mobile robot with one wheel on the rear side are stable all through their track because their angles of stability are always positive.

On the other hand, the three-wheel mobile robot with one wheel on the front side has negative angle of stability, which means that during distance 35 units to 49 units, (i.e. during descending down through the valley), tipover will be in progress and we can not use this model to investigate such track in this terrain.

As a general conclusion, the stability increases with the increase in number of wheels, so less reliable to have tipovers.

5 The Stability Margin for Different Inclined Surfaces

In this section, the height of center of mass is constant (H=2), and the number of wheels is also constant, because a four-wheel mobile robot is used.

Here, four surfaces are obtained; all have inclinations around the x-axis with variable angles $(10^{\circ},20^{\circ},30^{\circ}\text{and}\,40^{\circ})$.

Figure (80) represents an inclined surface (the angle equals 10°) with a shown track of a four-wheel mobile robot.

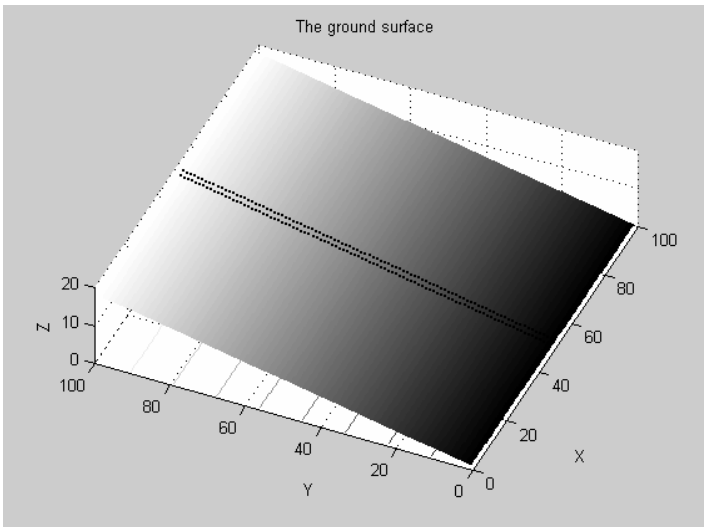

Figure (80): Inclined surface (the angle equals 10°) with a shown track of a four-wheel mobile robot.

By studying stability on the mobile robot, one can found that it is stable all through its track and this is obvious in Figure (81), were the stability angle is always positive (i.e. no tipover) and equals 16.57°.

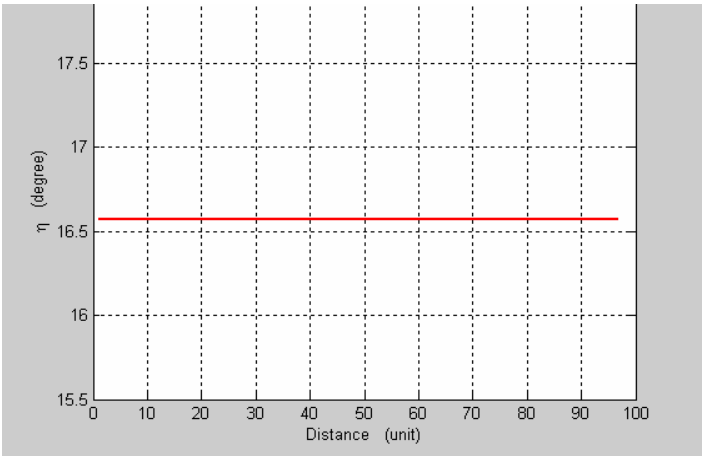

Figure (81): Four-wheel mobile robot stability margin when moving on an inclined surface (angle= 10°).

As the inclination angle is increased (angle= 20°, see Figure (82)), the stability decreases and the angle of stability becomes 6.57°. But it is still positive all through its track, as a result no tipover in this case (Figure (83)).

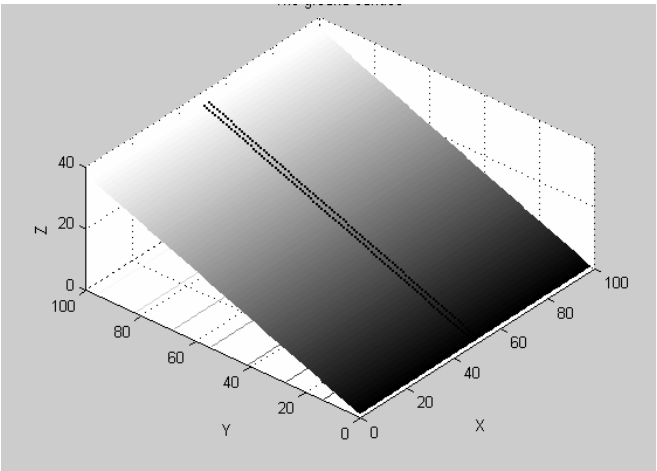

Figure (82): Inclined surface (the angle equals 20°) with a shown track of a four-wheel mobile robot.

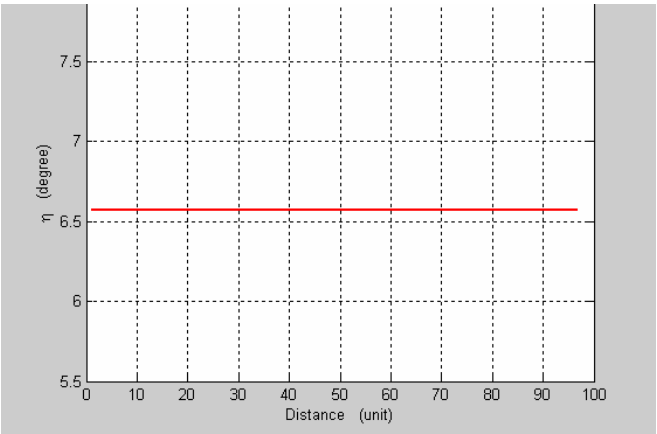

Figure (83): Four-wheel mobile robot stability margin when moving on an inclined surface (angle= 20°).

Increasing the angle of inclination to 30° (Figure (84)), the stability margin decreases and the angle of stability equals -3.43°. This means that the mobile robot is unstable and he is in his way to tipover. And many procedures should be taken into consideration in order to prevent turning over. See Figure (85).

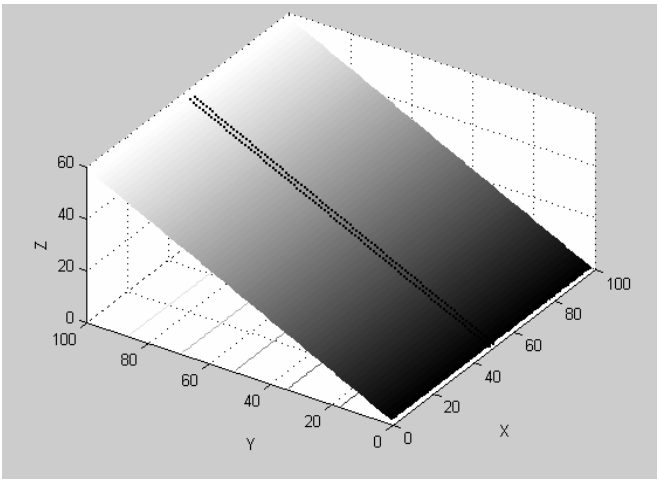

Figure (84): Inclined surface (the angle equals 30°) with a shown track of a four-wheel mobile robot.

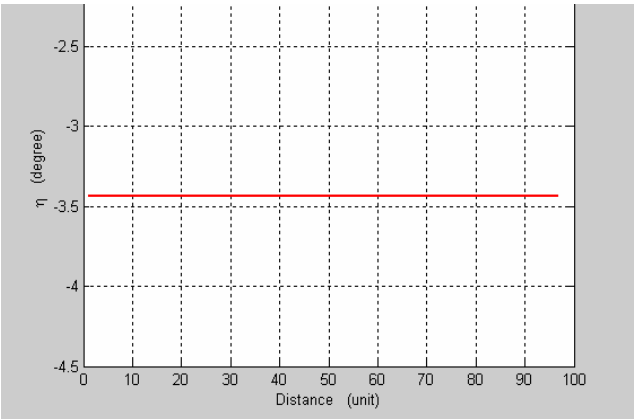

Figure (85): Four-wheel mobile robot stability margin when moving on an inclined surface (angle=30°).

In a higher angle (40°) as in Figure (86), the mobile robot is unstable and tipover is in progress because the angle of stability is always negative ($\eta = -13.43^{\circ}$) as shown in Figure (87). This means that we cannot use such a mobile robot in such surface because it is exposed to turning over through its track.

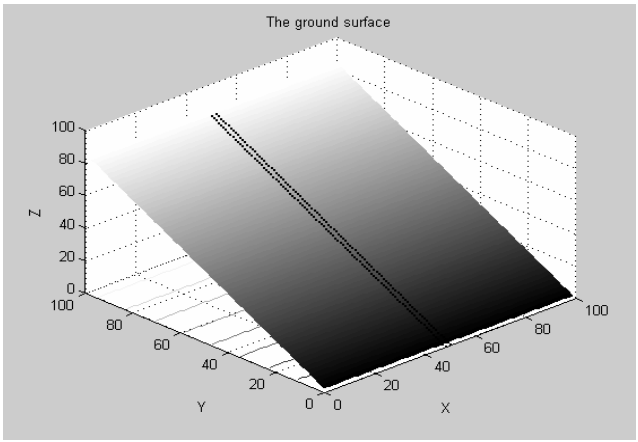

Figure (86): Inclined surface (the angle equals 40°) with a shown track of a four-wheel mobile robot.

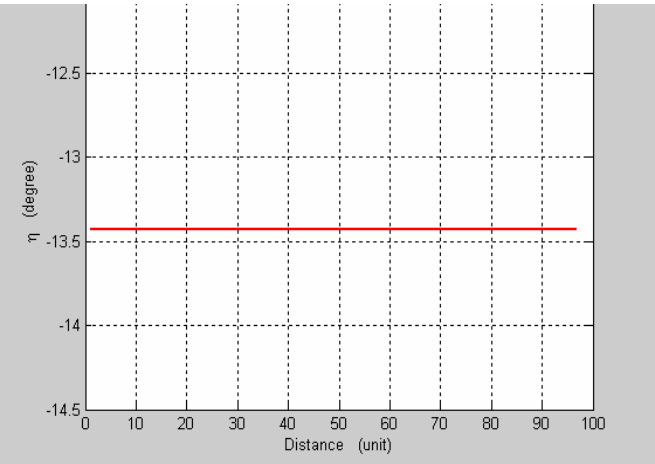

Figure (87): Four-wheel mobile robot stability margin when moving on an inclined surface (angle= 40°).

As a conclusion, increasing the angle of inclination surface, leads to a decrease in the angle of stability (η) and as a result, the mobile robot becomes less stable and more prone to tipover.

6 The Stability Margin with Different Heights of Center of Mass

We studied in the last two sections the effect of number of wheels and the effect of the angle of inclination surface. Here in this section, the number of wheels is constant (four wheels) and we will study the stability of the vehicle with variable heights of the center of mass and variable degrees of inclined surfaces.

Figure (88) is a graph represents inclined surface slope in x-axis against stability magnitude in y-axis. Four graphs were obtained; each one is taken on different height of the center of mass (H).

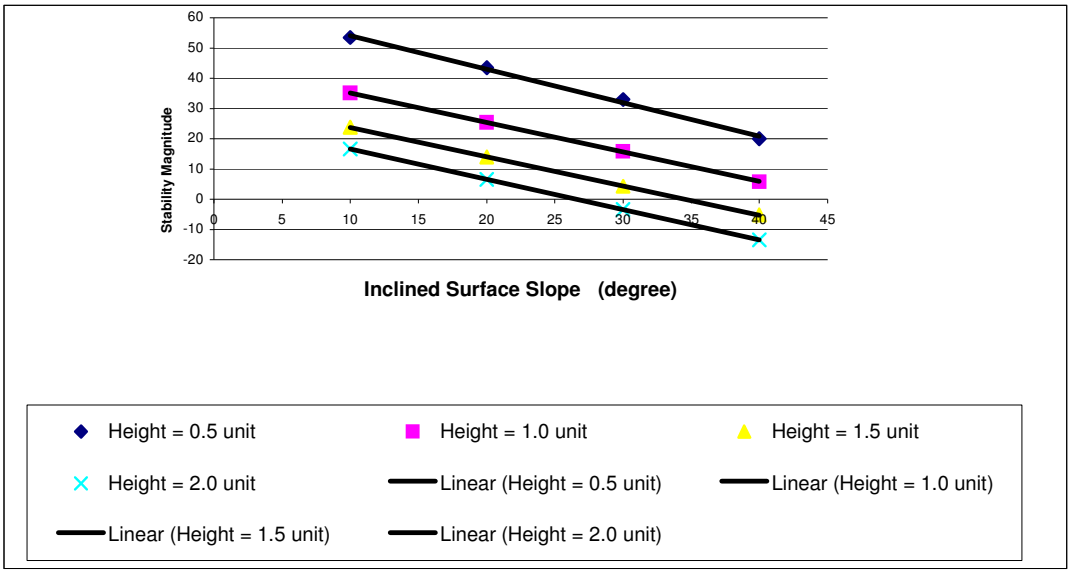

Figure (88): Inclined surface slope in x-axis against stability magnitude in y-axis with variable heights of center of mass.

Taking a constant angle of inclination, for example 10°, one can note that the mobile robot is most stable at H =0.5 and the stability magnitude equals 53.44°. At H = 1.0, the stability magnitude is also positive and equals 35.10°. At H = 1.5, the stability magnitude decreases but still positive and equals 23.75°. At H = 2.0, the stability magnitude equals 16.57°. This means that the less the height of the center of mass, the more stable is the robot at constant angle of inclination and constant number of wheels.

Graphs (when H = 0.5 and H=1.0) at any inclination surface angle, is always positive. This means that these are safe heights for the mobile robot at any inclination from 10° to 40°. For graphs (at H = 1.5 unit), the stability magnitude is positive at inclined surface when the inclined surface angle ranging from $10^{\circ} - 29^{\circ}$, but at 40° degrees it equals -5.22°, this is unstable region and at this angle the tipover is in progress. When the height of the mobile robot equals 2.0 units, the stability magnitude is positive at inclined

surface angles ranging from $10^{\circ} - 19^{\circ}$. The instability region will start from the inclination angle (20°) and above. See Table (2) for summary of the results in Figure (88).

Table (2): The stability magnitude at different inclined surface slopes and different heights of the center of mass.

Inclined surface slope (degree)	H=0.5	H=1.0	H=1.5	H=2.0
10	53.44	35.1	23.75	16.57
20	43.44	25.39	13.95	6.57
30	32.91	15.84	4.3	-3.43
40	19.98	5.78	-5.22	-13.43

As a result, the increase in height of the center of mass leads to decrease in stability magnitude and the vehicle becomes more exposed to tipover.

7 The Stability Margin with Different Tracks on a Rough Terrain

In this simulation, several tracks that the mobile robot can move on it were assumed, and Figures (89 and 90) show some of them.

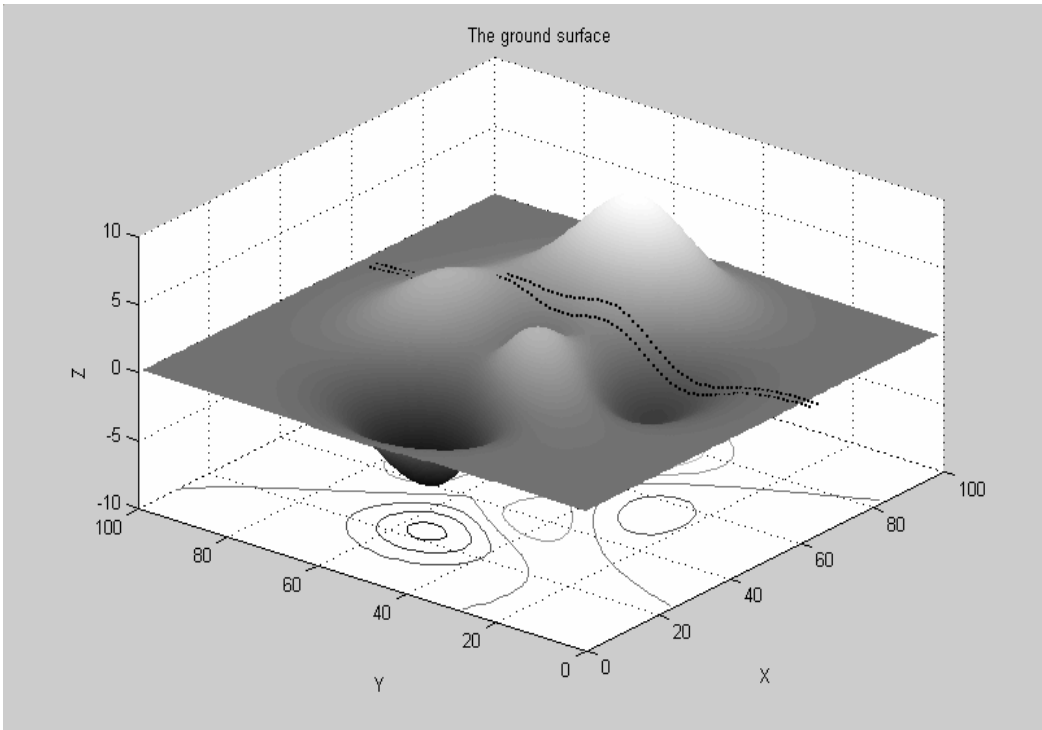

Figure (89): Rough terrain with a shown track of four-wheel mobile robot (track 1).

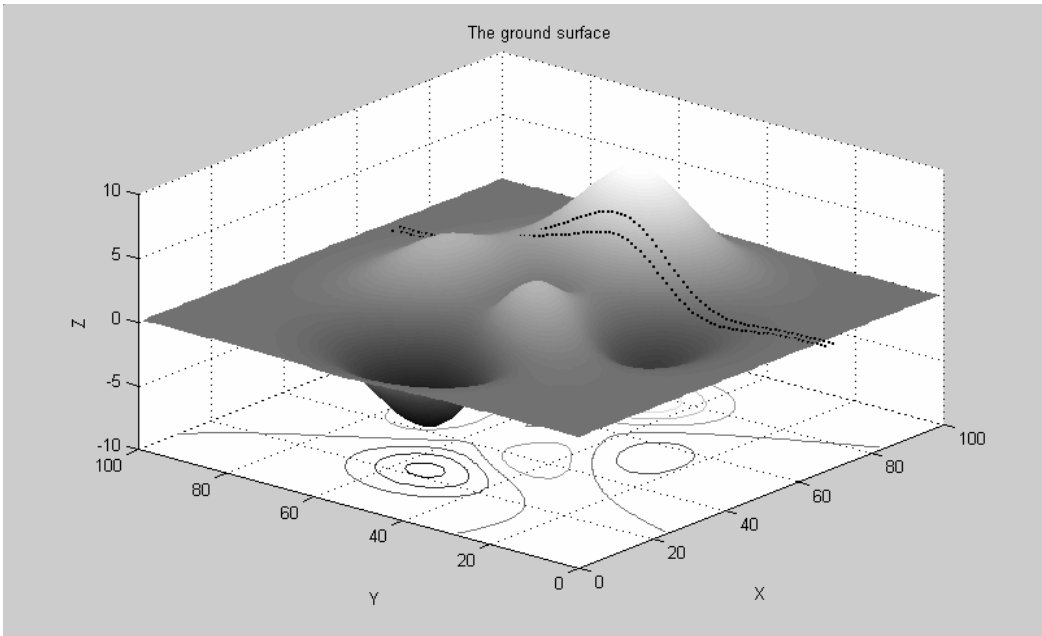

Figure (90): Rough terrain with a shown track of four-wheel mobile robot (track 2).

Let the mobile robot walk on different tracks; track1 and 2 (Figures 89 and 90; respectively), the resultant stability margin are shown in Figures (91 and 92).

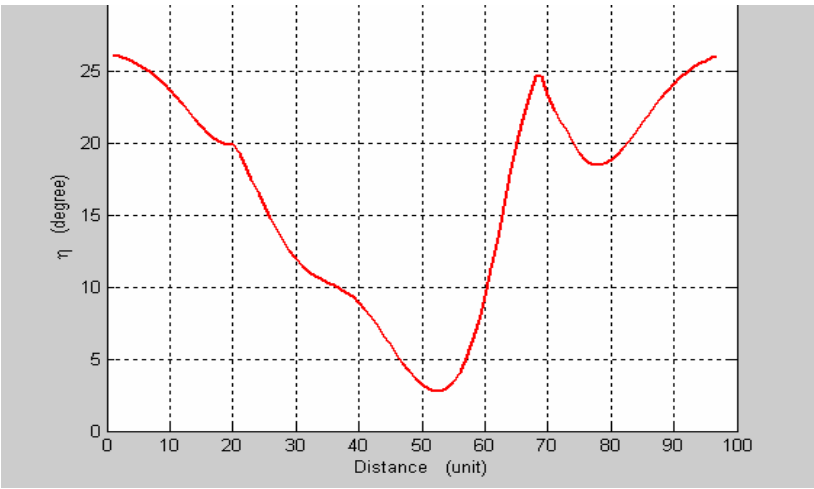

Figure (91): Four-wheel mobile robot stability margin through moving on track (1).

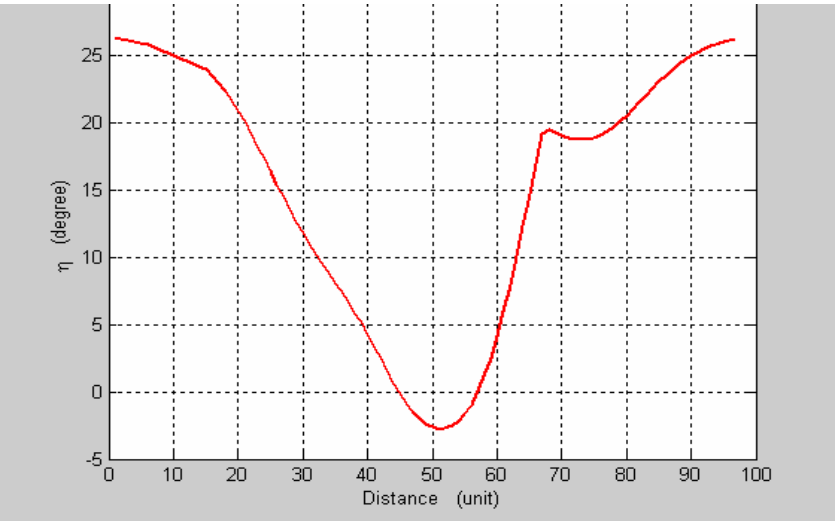

Figure (92): Four-wheel mobile robot stability margin through moving on track (2).

Notice that:

Track (1) passes through multiple elevations and depressions; however, the stability margin is always positive which means that the four-wheel mobile robot is stable through track (1). (See Figure (91)).

In track (2), the mobile robot also passes through elevations and depressions, but somewhat steeper than track (1), this is shown in Figure (92) with rapid decrease in the stability margin. At distance 45 units, the stability margin reaches zero, which is the critical tipover stability and any movement after that leads to tipover as the stability angle (η) becomes negative.

8 Trigonometric Calculations of Force-Angle Stability Measure

First: four-wheel mobile robot moving on flat surface

One can easily find the force-angle stability measure of four-wheel mobile robot by doing simple trigonometric calculations. By referring to figure (55), it was found that the measure of the angle between the gravity force vector and tipover axis normal ($\mathbf{I}_1$) for wheel 1 equals 26.57^0.

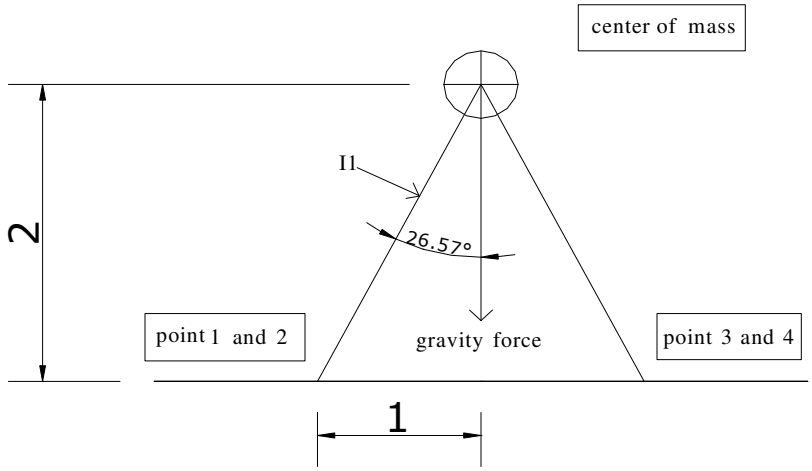

Figure (93): Planar force-angle stability measure for a mobile robot moving on flat surface.

A simple drawing is plotted (see Figure (93)) and the stability angle is $\eta = \tan^{-1}\frac{1}{2} = 26.57^0$.

The result is the same as the simulated model answer and this verify that the model and the simulation are both correct.

Second: four-wheel mobile robot moving on inclined flat surface

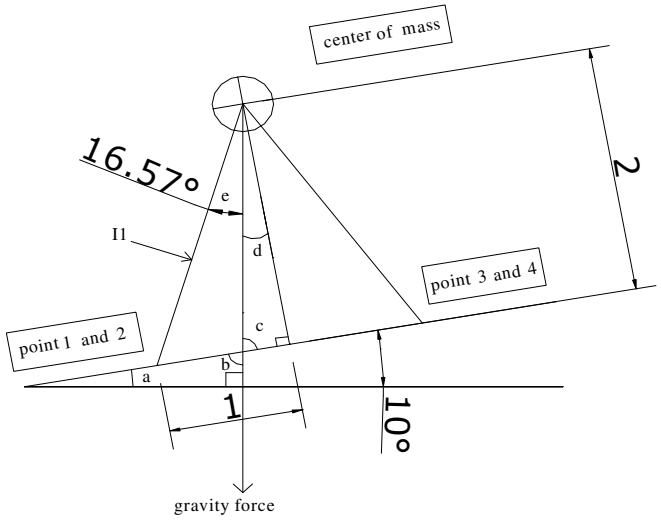

Figure (94): Planar force-angle stability measure for a mobile robot moving on 10^0-inclined flat surface.

Be referring to Figure (94), one can calculate force-angle stability measure of a four-wheel mobile robot moving on 10^0-inclined flat surface (wheel 1) as follows:

Angle b= 180^0-90^0-10^0=80^0

Angle b =angle c = 80^0

Angle d = 180^0-90^0-80^0 = 10^0

Angle (e + d) = $\tan^{-1}\frac{1}{2} = 26.57^0$

e= 26.57^0-10^0 =16.57^0

The result is the same as the simulated model answer on Figure (81). From the two previous cases, one can note that the used model and programmed simulations are correct. Refer to Figures (95-97) to see the effect of surface inclination on the stability margin.

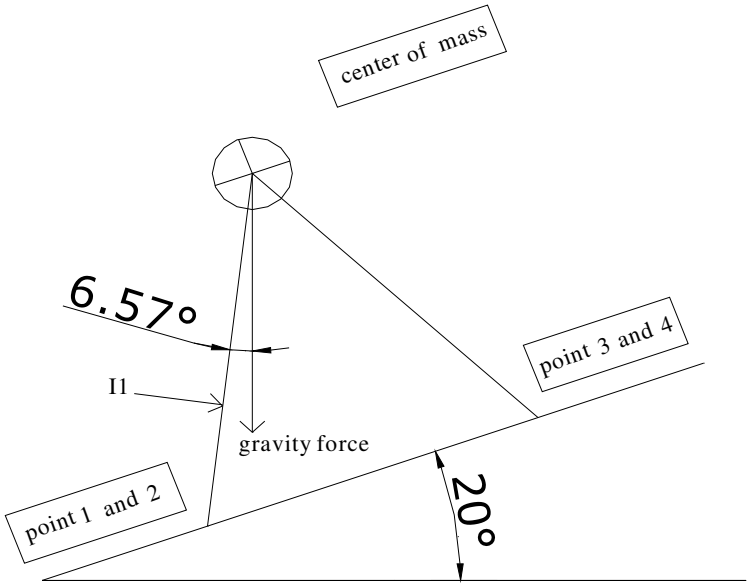

Figure (95): Planar force-angle stability measure for a mobile robot moving on 20^0-inclined flat surface.

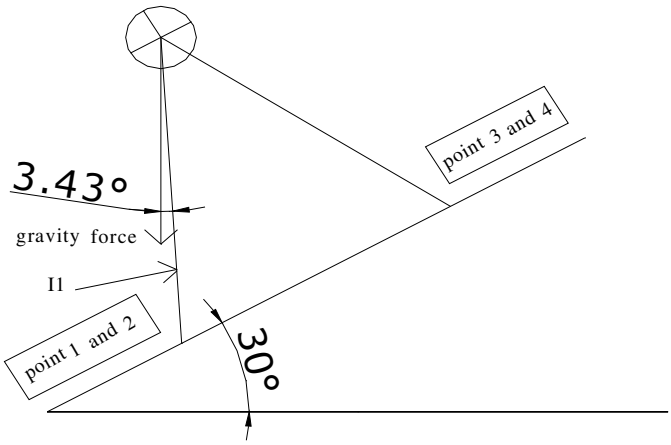

Figure (96): Planar force-angle stability measure for a mobile robot moving on 30^0-inclined flat surface.

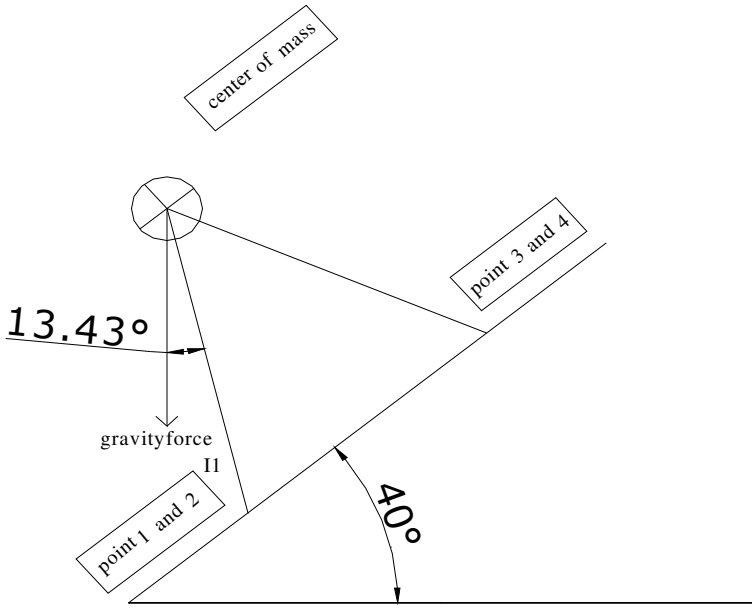

Figure (97): Planar force-angle stability measure for a mobile robot moving on 40^0-inclined flat surface.

9 The Stability Margin After Repositioning of the Center of Mass for A Mobile Robot

Let a four-wheel mobile robot with height (2 units) and distance equals to (2 units) between each two wheels moves on a rough terrain as shown in Figure (98). When running the simulation program, the initial starting point for wheel no. 1 is p(70, 1), p(68, 1) for wheel no. 2, p(68, 3) for wheel no. 3 and p(70, 3) for wheel no. 4 and the direction of movement is forward at y-direction. The track of the movement here is the same as track no. 2 on Figure (90) and the dimensions for the mobile robot here are also identical to the robot that moves in Figure (90).

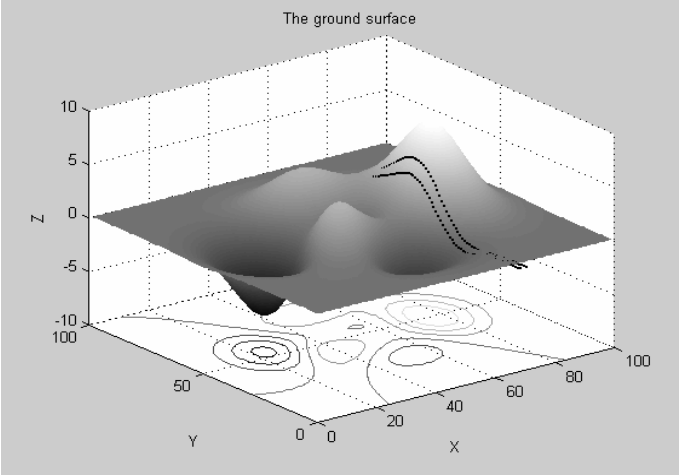

Figure (98): Four-wheel mobile robot moving on a rough terrain with initial start point for wheel no. 1 by p (70, 1). The direction of movement is forward at y-direction.

Let us study the procedures that are applied on the mobile robot when reach instability margin at specific distance. As an example, the mobile robot will be unstable at distance equal to 52 (when the robot moves at y- direction). The magnitude of center of mass for this robot at that moment is $p_{c.m}$ (67.8878, 52.1341, 6.584); refer to Figure (99), which

represents a 3-D geometrical sketch of four- wheel mobile robot. This Figure is showing stability before and after reconfiguration the center of mass.

By looking to that figure, one can note that the stability angle (η_2) between the component of the net force vector $\mathbf{f}_2$ and tip over axis normal $\mathbf{I}_2$ of wheel number 2 before the reconfiguration equal (-2.755°), the negative sign of the angle means that the component of net force vector $\mathbf{f}_2$ lies outside the wheels boundary, i.e. beyond the tip over mode axis ($\mathbf{a}_2$) that connect between wheel number 2 and wheel number 3, and the mobile robot is in his way for tipping over.

The mobile robot must take action in order to prevent tipping over, this mean; it is required to modify the location of center of mass, the invert pendulum will now extend his arm which carry a certain specific mass to a position which is opposite to the tip over mode axis ($\mathbf{a}_2$) where turning over occurs around it. It is assumed in this work that:

(1) The position of the mass the invert pendulum before the reconfiguration is located at the mobile robot center of mass.

(2) The magnitude of mass of the mobile robot is 1.0 kg.

(3) The magnitude of mass of invert pendulum is 0.5 kg.

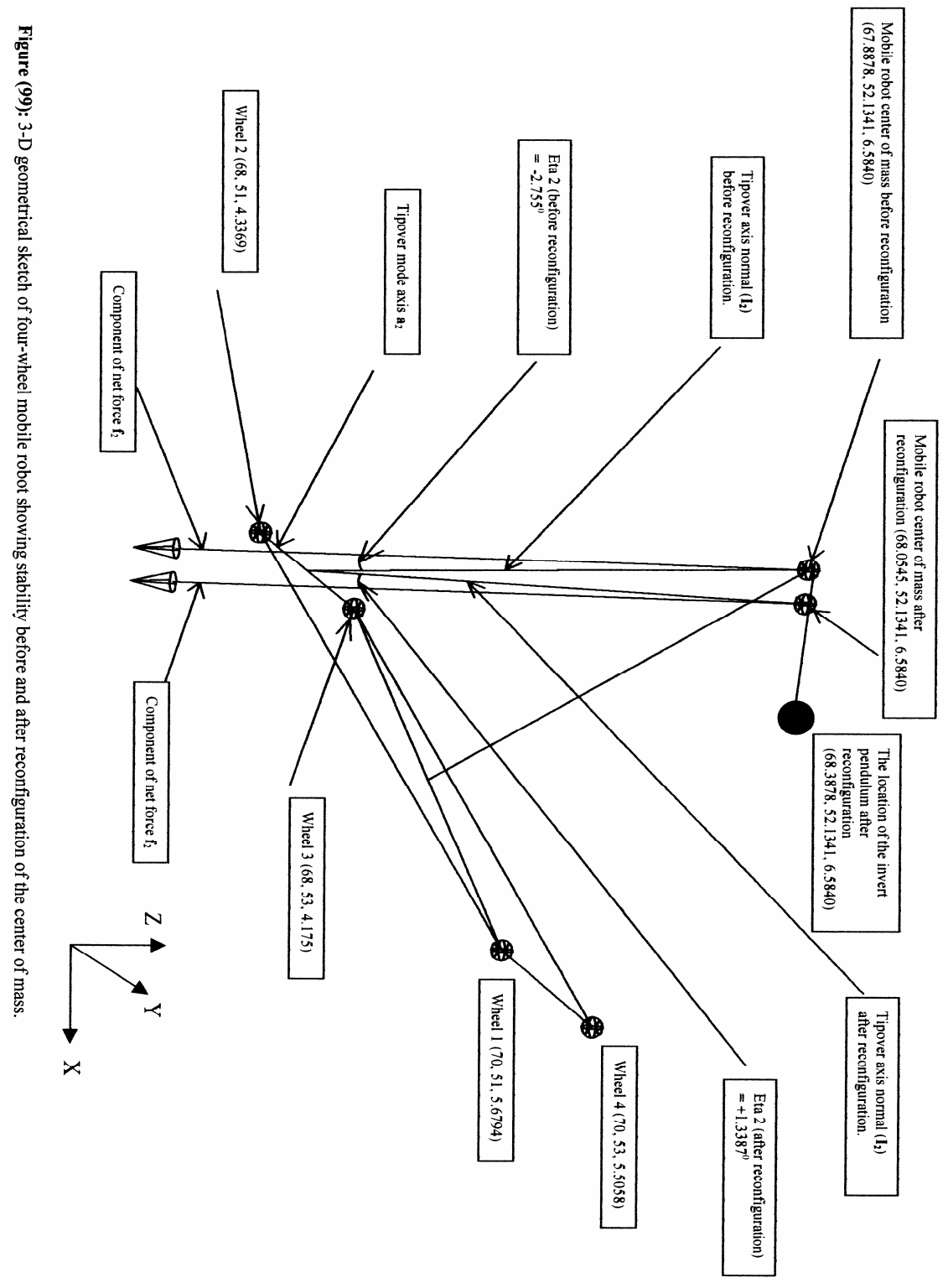

Figure (99): 3-D geometrical sketch of four-wheel mobile robot showing stability before and after reconfiguration of the center of mass.

The mass location of the invert pendulum after reconfiguration at x-direction would be as in the following relation

$$x = x_{c.m} + 0.5 = 67.8878 + 0.5 = 68.3878$$

So, the new position of the invert pendulum mass is (68.3878, 52.1341, 6.5840). The coordinate of center of mass for the mobile robot after reconfiguration on x-direction can be computed as in the following formula:

$$x = \frac{x_0 + 0.5(x_0 + 0.5)}{1.5} = \frac{67.8878 + 0.5(67.8878 + 0.5)}{1.5} = 68.0545$$

The coordinates of center of mass of the mobile robot after reconfiguration will be (68.0545,52.134,6.5840). It can be seen from Figure (99) that the stability angle after reconfiguration becomes $+1.3387^{\circ}$, *i.e.* the component of net force $\mathbf{f}_2$ for the mobile robot that passes through the new center of mass (after reconfiguration) lies inside the wheels polygon. So the stability has been achieved.

By looking to the simulation results on Figure (100), one can note that the robot will loose his stability between the distance (45-56) and the minimum magnitude of the stability angle on the instability region is -2.76°. The robot will topple around the tip over mode axis $\mathbf{a}_2$ that connect between wheels no. 2 and 3. Figure (101) shows the overall stability margin of the four-wheels.

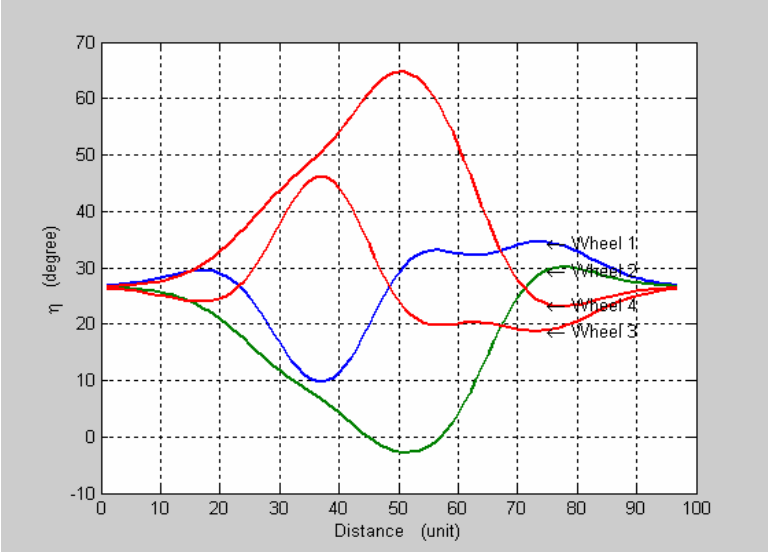

Figure (100): The stability margin for all the mobile robot wheels.

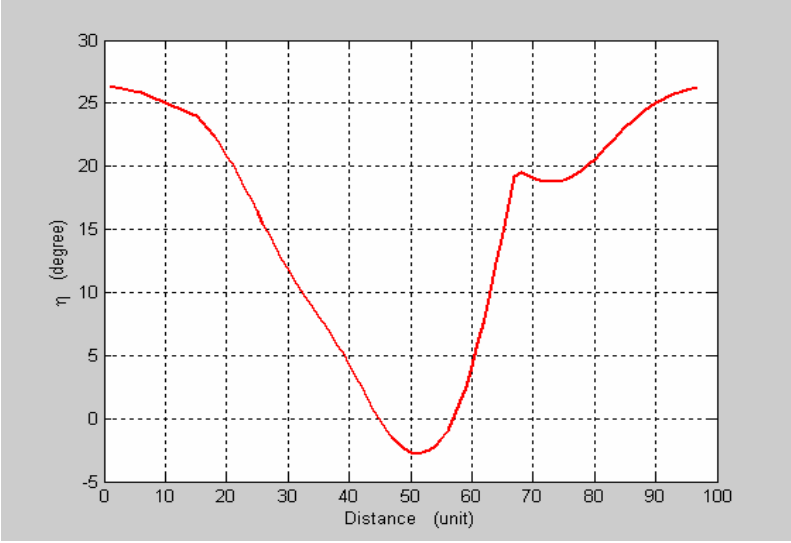

Figure (101): The overall minimum stability margin.

Now and after installing the invert pendulum and when the repositioning of the mass takes its place during the movement, the robot will reach stability margin through all crossed distance and the minimum stability angle will be $+0.02^{\circ}$. Refer to Figures (102-103).

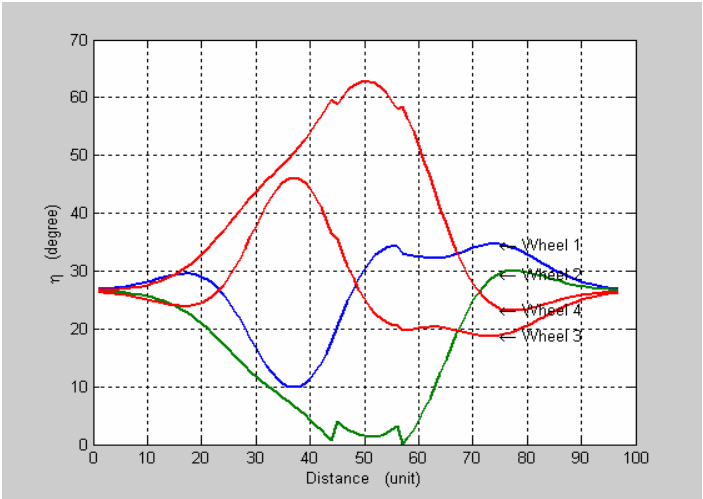

Figure (102): The stability margin for the mobile robot wheels after (c.m) reconfiguration.

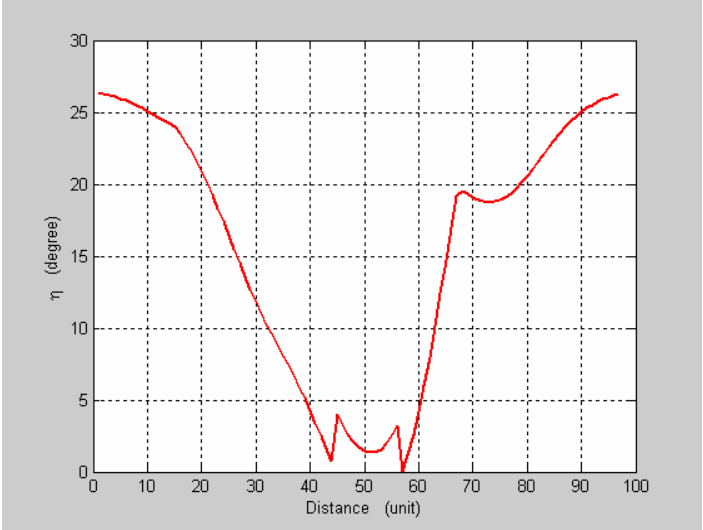

Figure (103): The overall minimum stability margin after (c. m) reconfiguration.

10 The Stability of a mobile robot when climbing a stone

The stability behavior is studied when a mobile robot is moving on a flat surface and the climbing at small stone on his way. A simulation program had been built for a surface contains a flat terrain with a stone located at the middle of it. The height of the stone is equal 0.56 unit as shown in Figure (104). The location of the stone center is p(50, 50).

A four-wheel mobile robot with height (5 units) and distance equals to (5 units) between each two wheels. When running the simulation program; the initial start point for wheel no. 1 is p(55, 1), p(50, 1) for wheel no. 2, p(50, 6) for wheel no. 3 and p(55, 6) for wheel no. 4. The direction of movement is straightforward at the y-direction.

When the robot starts moving; it will cross a flat surface at the beginning. The stability angle would be constant for all the wheels and it is equal 26.05^0 . Wheel no. 3 would firstly pass through the stone as shown in Figure (105), and the stability angle of mode axis $\mathbf{a}_3$ (that connect between wheel 3 and wheel 4) will increase to reach of 36^0 . After crossing the stone (i.e. the stone become between wheel no. 2 and 3), the overall stability angle will return to become 26.05^0 for all wheels.

The mobile robot will then cross the same stone through wheel no. 2. The magnitude of stability angle would now decrease on mode axis $\mathbf{a}_3$ to reach about 17^0 . When the robot completely gets over the stone; the stability angle would be constant again and reach 26.05^0 .

Refer to Figure (106) to see the stability angle of wheel no. (mode axis $\mathbf{a}_2$) and refer to Figure (107) to view the total overall stability of the mobile robot.

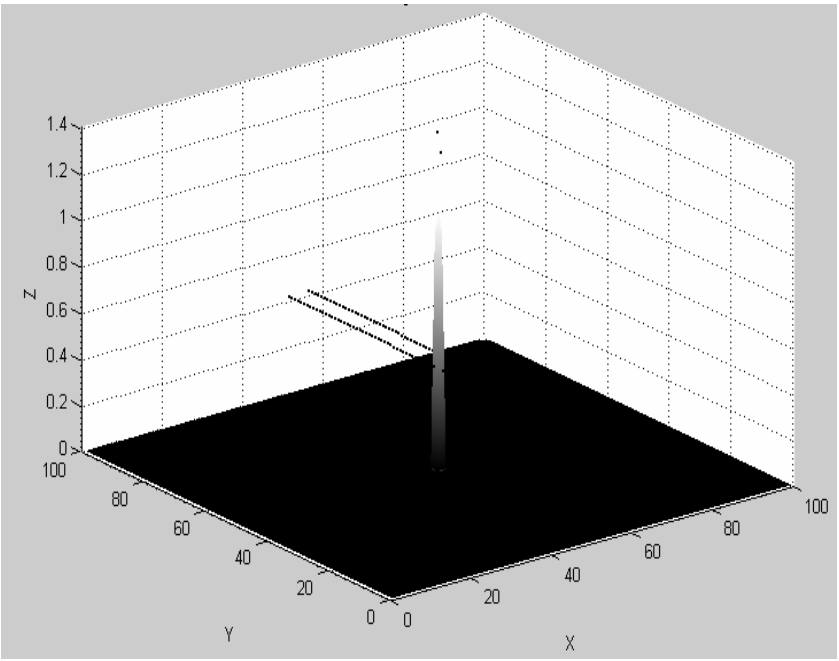

Figure (104): Flat surface with stone at the middle.

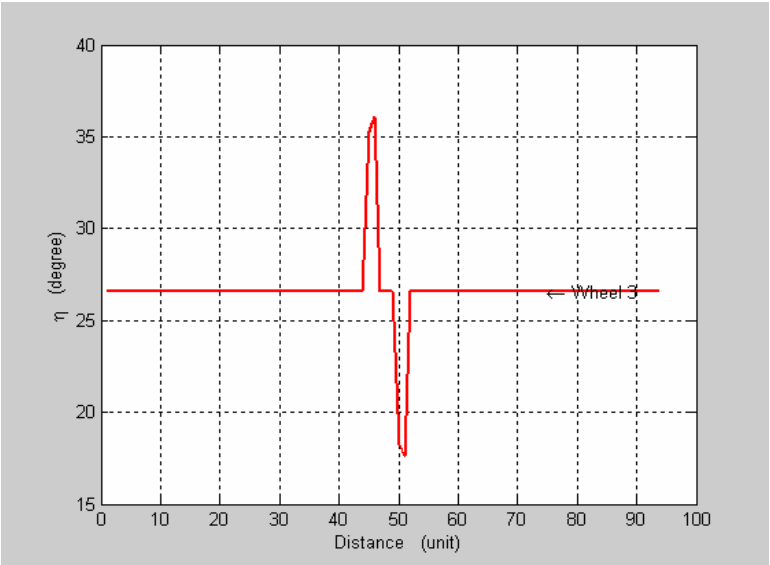

Figure (105): Stability angle of wheel no. 3 ($\mathbf{a}_3$).

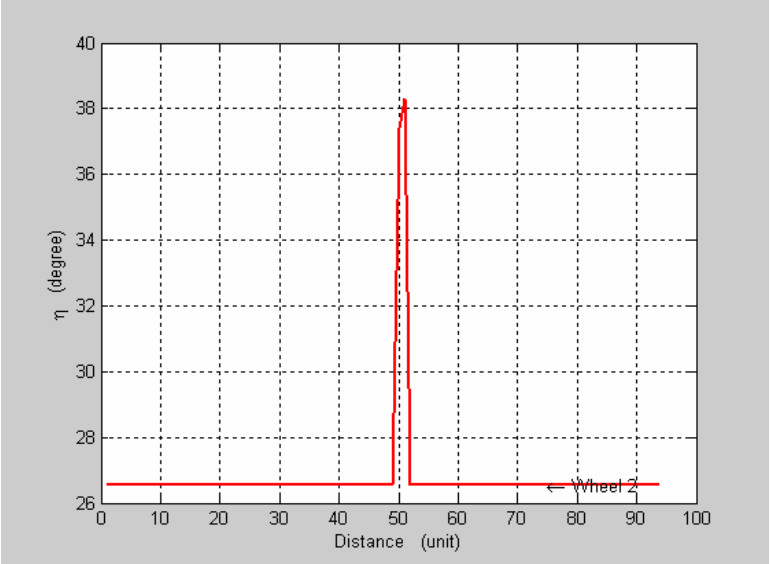

Figure (106): Stability angle of wheel no. 2 ($\mathbf{a}_2$).

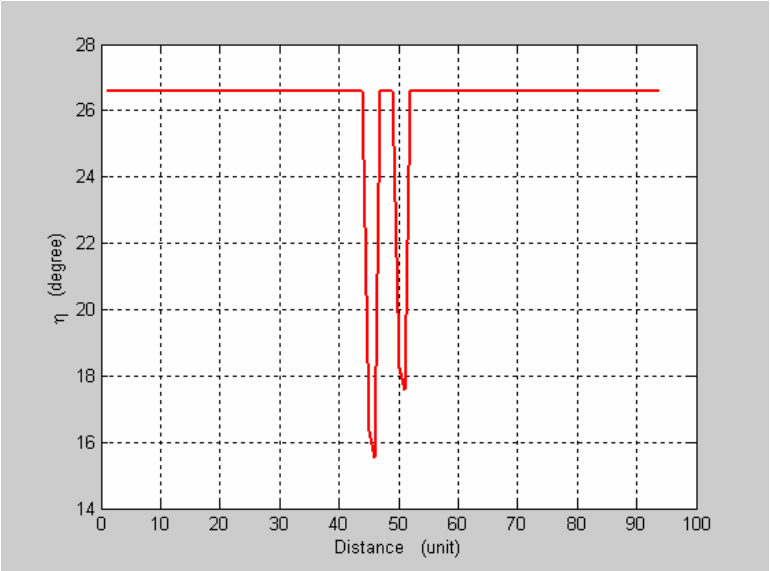

Figure (107): Overall stability angle.

Summary, Conclusions and Recommendations

1 Summary

The problem of finding kinematic-stability angle measure for a mobile robot has been presented in this research. A force-angle stability measure has been adopted and implemented to perform robot's stability checks and tip over

The proposed mobile robot in this research was assumed to be a rover with variable number of wheels supported and connected to the mobile robot body by shoulders and legs. It had been required to move on various types of terrains and surfaces that can be regular and flat, or in the other extreme, irregular and rough.

It had been noted that during traveling, the mobile robot was exposed to be unstable with the possibility of tip over due to moving on steep inclinations or climbing on stones and rocks. Accordingly, many factors and variables were studied that affect stability in order to form enough knowledge about the probability of turnover from a kinematic point of view. With respect to the surfaces and terrains, multiple shapes and types of the ground was generated in three-dimensions.

To prevent the robot's tip over, an inverted pendulum was used to enhance the stability by changing the robots center of gravity. An automatic controller may be used to provide the pendulum with a proper control law based on sensor data and the stability adapted criterion.

2 Conclusions

The force-angle stability measure of a mobile robot had been implemented and simulated in this research. The kinematic stability measure was applied on four-wheel and three-wheel mobile robots. Several types of surfaces and terrains were introduced to the program in order to investigate the mobile robot kinematic-stability. And finally stability of mobile robot was enhanced when introducing the invert pendulum to the robot body.

Generally, the way to assess stability margin of four-wheel mobile robot is by concentrating on the minimum stability angle for a selected group of wheels. The minimum stability angle is used when we need to comment on the stability of the rover and where tipover will occur, with no importance to know at what wheel or at what mode axis tipover will occur (i.e. the mere judgment is basically if it is stable, critical tipover or tipover in progress).

Three types of mobile robots were assumed in this research: four-wheel mobile robot, three-wheel mobile robot with one wheel in front side and three-wheel mobile robot with one wheel in the rear side. Through the previous analysis; the four-wheel mobile robot is the most stable one all through the assumed tracks. And as a general conclusion, the stability increases with the increase in number of wheels for a specific wheels layout.

When a flat surface with zero-degree inclination was introduced to study its effect on stability, the force-angle stability measure was noticed to be the same for all wheels. The stability margin is constant all through the crossed distance. Tipover may not occur since the angle is positive all the time, and the net force vector lies inside the assumed polygon between the four wheels.

Increasing the angle of inclined flat surface, lead to a decrease in the angle of kinematic stability (η), and as a result, the mobile robot became less stable and more prone to tipover.

As a result, the increase in height of the center of mass lead to decrease in stability magnitude and the mobile robot became more exposed to tipover. This is geometrically due to that any increase in center of mass height clearly results in a smaller minimal angle and a reduced measure of tipover stability margin.

3 Recommendations for Future Extensions

The results of the ongoing researches have shown that a number of further research activities are possible:

1. It is important to develop robots that can reposition their center of mass to improve stability in rough terrain (Re-configurable robots). In this thesis, the concept of invert pendulum was introduced in order to enhance the robot stability and preventing tipping over, but it still needs more research so as to apply this method on a physical system.

2. Some applications require designing mobile robots that move, somewhat, at higher speed. So, it is required, at this speed, to take into consideration the effect of the external forces and moments that acting on the mobile robot due to differences in speed, and determining the mobile robot linear and angular acceleration. All of these are necessary elements of any dynamic system simulation.

3. This work can be directly applied on a real mobile robot equipped with appropriate suite of sensors. Different stability setups maybe tested and verified

4. Finally, it is vital to introduce and study some important parameters on this system such as friction forces, reaction forces, slipping, which were relaxed in this work. This makes the problem more comprehensive but more complex.

REFERENCES

Anton, H., (1999). **Calculus**, (6th ed). New York: JohnWiley and Sons, Inc.

Borenstein, J., (1995). **Control and Kinematic Design of Multi-Degree-of-Freedom Mobile Robots with Complaint Linkage**, IEEE Transaction on Robotics and Automation, February 1995, Vol.11, No.1,pp 21-35.

Crummett, W. P. and Western, A. B. (1994). **University Physics Models and Applications**, (1st ed.). Kerper Boulevard: Wm. C. Brown Publishers.

Davidson, J., Schweitzer, G., (1990). **A Mechanics- Based Computer Algorithm for Displaying the Margin of Static Stability in Four- Legged Vehicles**, Transactions of the ASME.

Ghasempoor, A., Sepehri, N., (1995). **A Measure of Machine Stability for Moving Base Manipulators**, IEEE International Conference on Robotics and Automation.

Gwo, Y., Shiller, Z., (1991). **Dynamic Motion Planning of Autonomous Vehicles, IEEE Transactions on Robotics and Automation**, VOL. 7, NO. 2.

Iagnemma, K., Dubowsky, S., Huntsberger, T, Pirjanian, P , Rzepniewski, A and Schenker, P, (2000). **Mobile Robot Kinematics Reconfigurability for Rough-Terrain**, SPIE Proceeding Vol. 4196.

Iagnemma, K., Dubowsky, S., (2000). **Mobile Robot Rough-Terrain Control (RTC) for Planetary Exploration**, Proceeding of 2000 ASME IDETC/ CIE: 26th Biennial Mechanisms and Robotics Conference September 10-13,2000, Baltimore, Maryland.

Iagnemma, K., Dubowsky, S., (2000). **Vehicle Wheel-Ground Contact Angle Estimation: with Application to Mobile Robot Traction Control**, Proceeding of the 7th International Symposium on Advances in Robot Kinematics, ARK '00.

Iagnemma, K., Dubowsky, S., Rzepniewski, A and Schenker, P, (2003). **Control of Robotic Vehicles with Actively Articulated Suspensions in Rough Terrain**, Autonomous Robots 14, 5- 16.

Kissel, R. R. and Sutherland, W. T. (1997, May). **Inverting the Pendulum Using Fuzzy Control**. NASA Technical Memorandum 108535. Retrieved from http://trs.nis.nasa.gov/archive/00000390/01/tm108535.pdf#search='inverting%20the%20pendulum

Klein, C. ,Messupi, D., (1985). **Automatic Body Regulation for Maintaining Stability of a Legged Vehicle During Rough-Terrain Locomotion**, IEEE Journal Of Robotics and Automation, VOL. RA-1, NO. 3.

Kreyszig,E., (1993). **Advanced Engineering Mathematics**, (7th ed). New York Chichester Brisbane Toronto Singapore:JohnWiley and Sons, Inc.

Papadopoulos, E., Rey, D., (1996). **A New Measure of Tipover Stability Margin for Mobile Manipulators**, Proc. IEEE Int. Conf. On Robotic and Automation Minneapolies, MN.

Papadopoulos, E., Rey, D., (1997). **On-Line Automatic Tipover Prevention for Mobile Manipulators**, Submitted to IEEE/RSJ Int. Conf. On Intelligent Robots and Systems.

Sreenivasan, S., Waldron, K., (1994). **Displacement Analysis of an Actively Articulated Wheeled Vehicle Configuration With Extensions to Motion Planning on Uneven Terrain**, Transactions of the ASME.

Sreenivasan, S., Wilcox, B., (1994). **Stability and Traction Control of an Actively Actuated Micro-Rover**, Journal of Robotic systems 11(6), 487-502.

Appendices

A: Graphs of three-wheel mobile robot (one wheel on the rear side and two wheels on the front side).

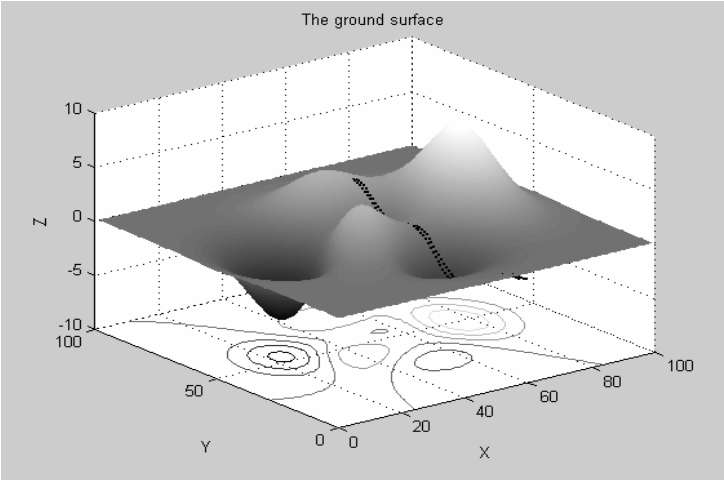

Figure (A-1): A rough terrain with a shown track of three-wheel mobile robot.

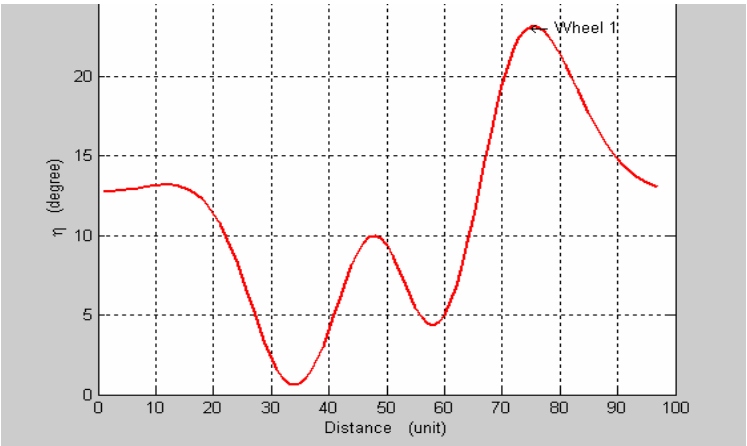

Figure (A-2): Three-wheel mobile robot stability margin according to wheel 1.

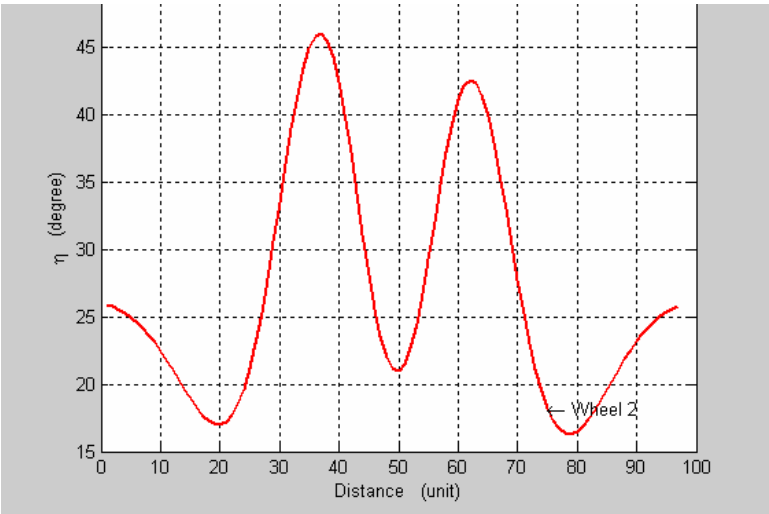

Figure (A-3): Three-wheel mobile robot stability margin according to wheel 2.

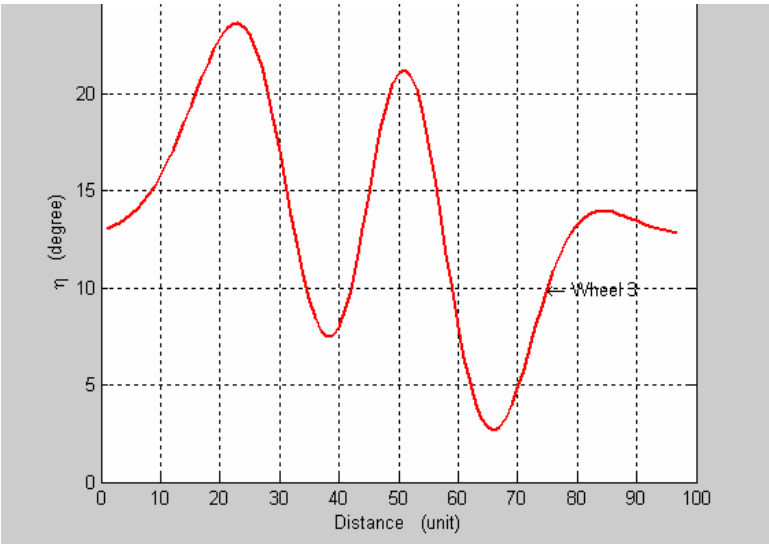

Figure (A-4): Three-wheel mobile robot stability margin according to wheel 3.

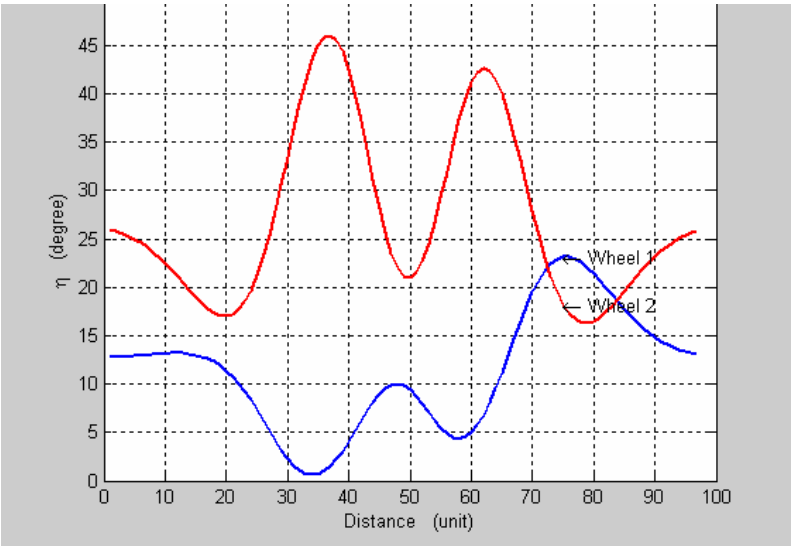

Figure (A-5): A combined graph of three-wheel robot stability margin at wheels 1 and 2.

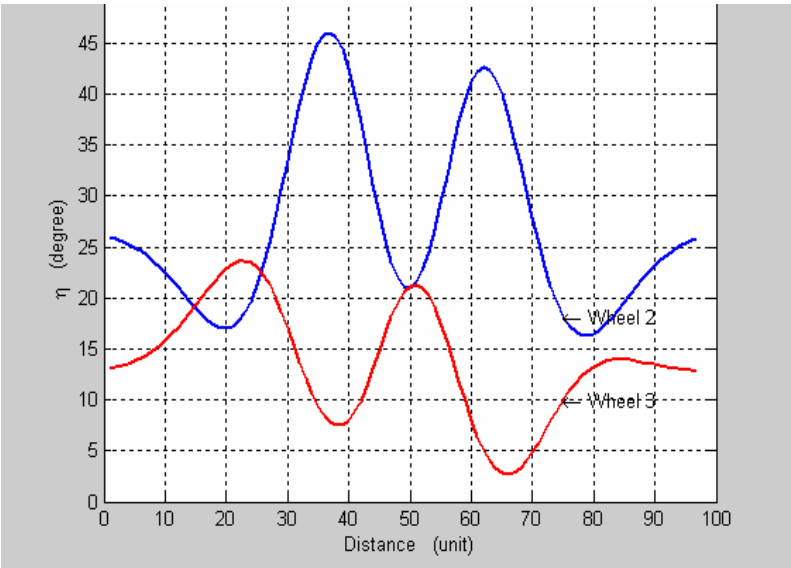

Figure (A-6): A combined graph of three-wheel robot stability margin at wheels 2 and 3.

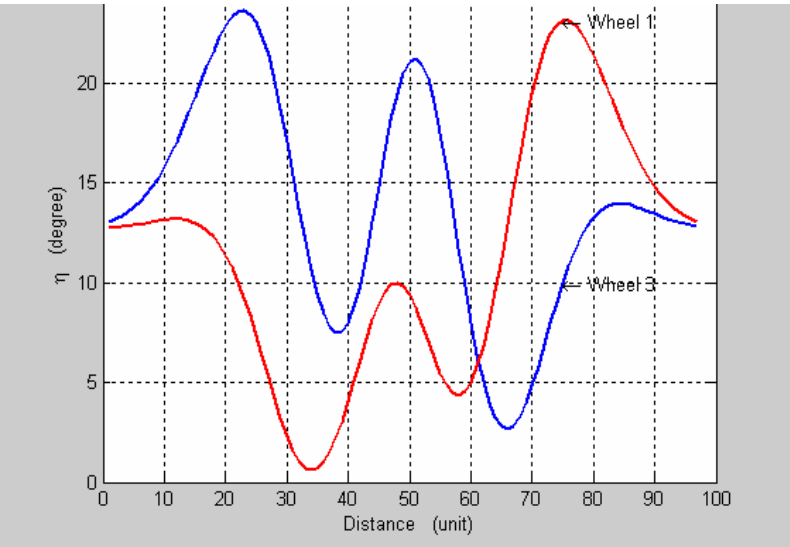

Figure (A-7): A combined graph of three-wheel robot stability margin at wheels 3 and 1.

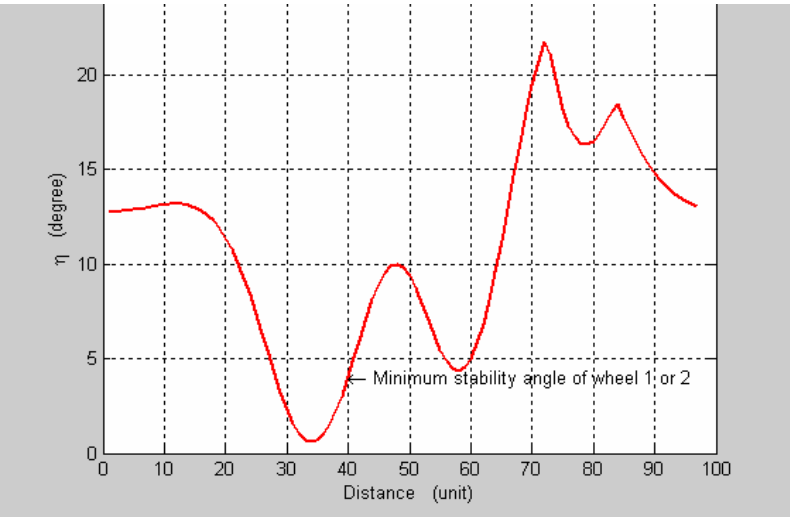

Figure (A-8): The minimum stability margin for the wheels 1 and 2.

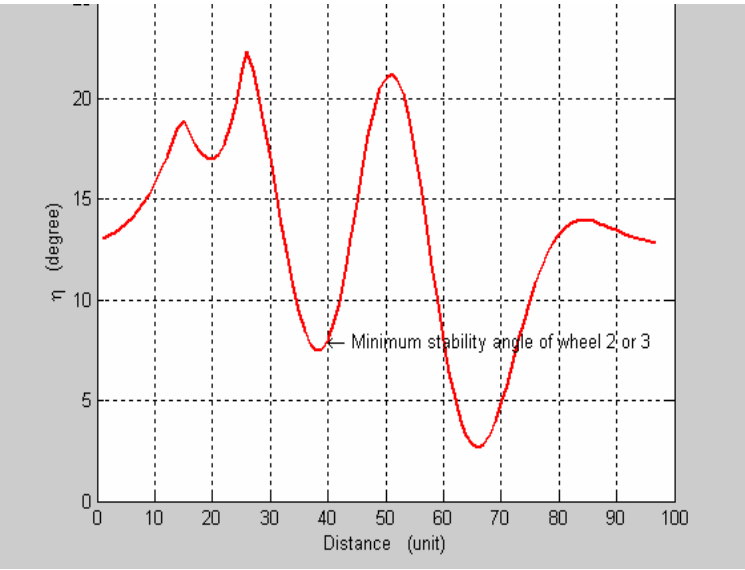

Figure (A-9): The minimum stability margin for the wheels 2 and 3.

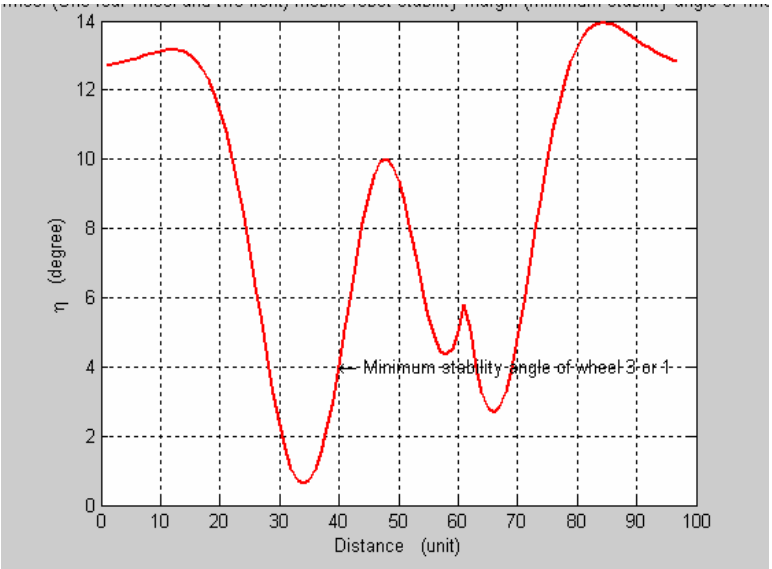

Figure (A-10): The minimum stability margin for the wheels 3 and 1.

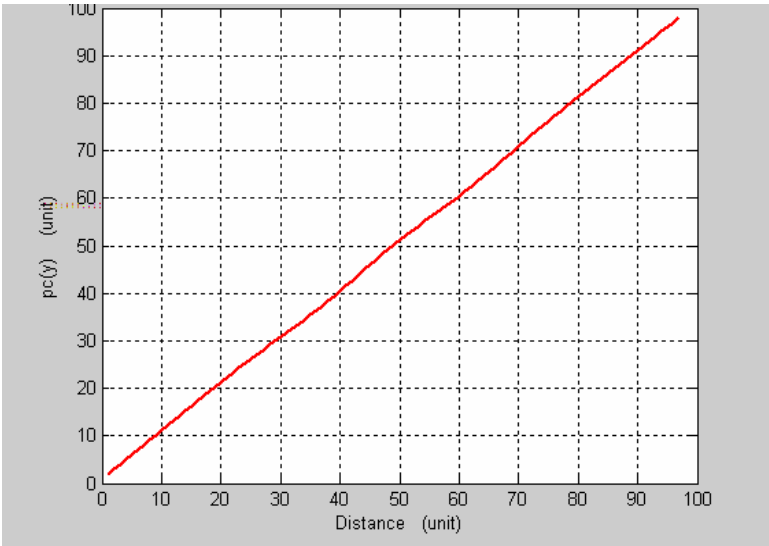

Figure (A-11): Center of mass in y-direction relative to the reference frame.

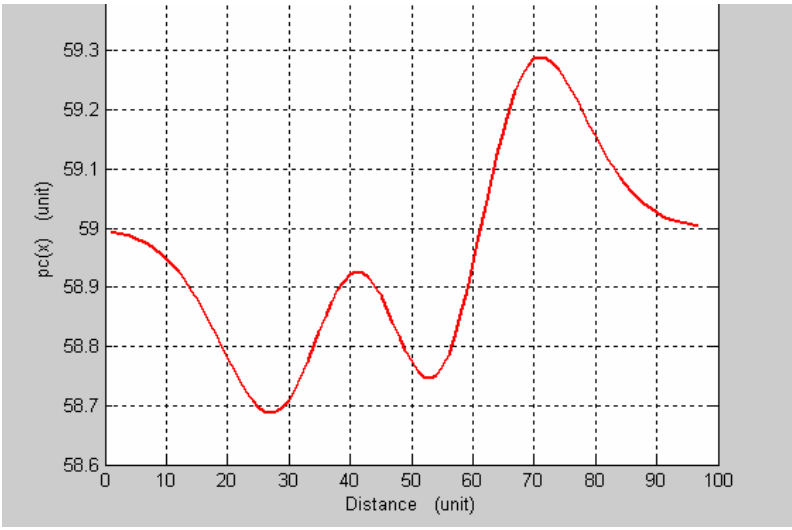

Figure (A-12): Center of mass in x-direction relative to the reference frame.

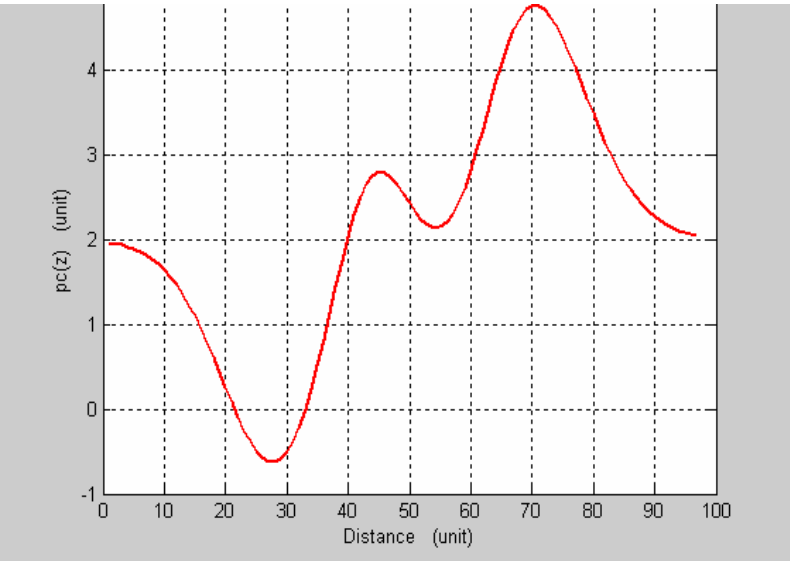

Figure (A-13): Center of mass in z-direction relative to the reference frame.

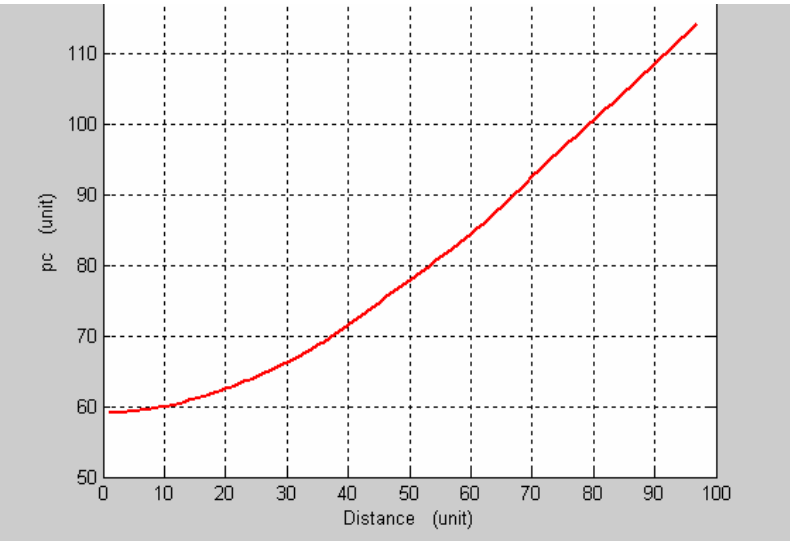

Figure (A-14): Center of mass distance magnitude relative to the reference frame.

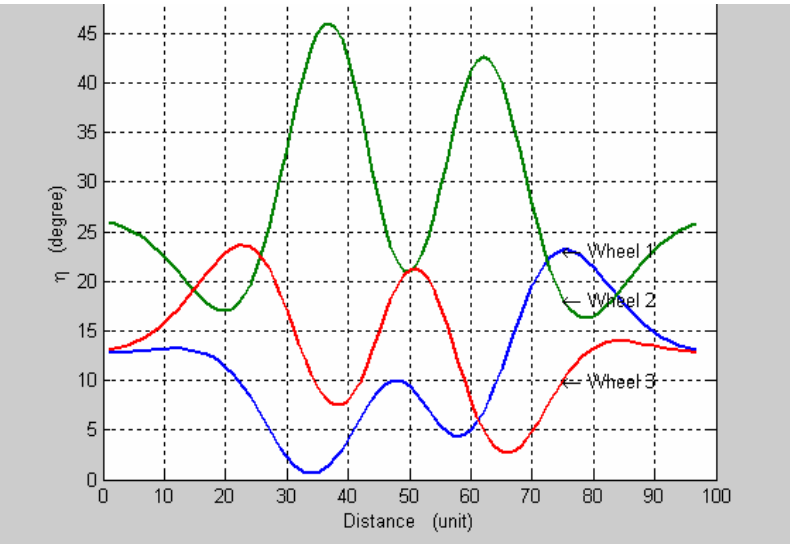

Figure (A-15): A combined graph of three-wheel mobile robot stability margin at the three wheels.

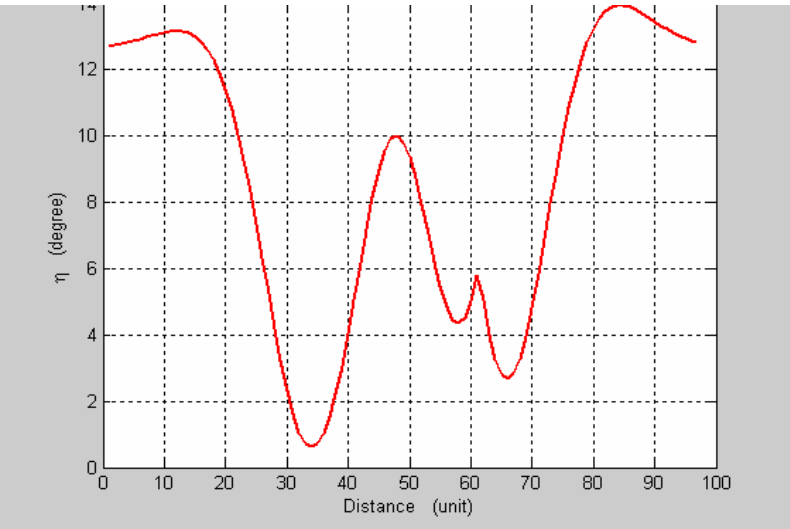

Figure (A-16): The minimum stability margin for the all three wheels.

B: Graphs of three-wheel mobile robot (two wheels on the rear side and one wheel on the front side).

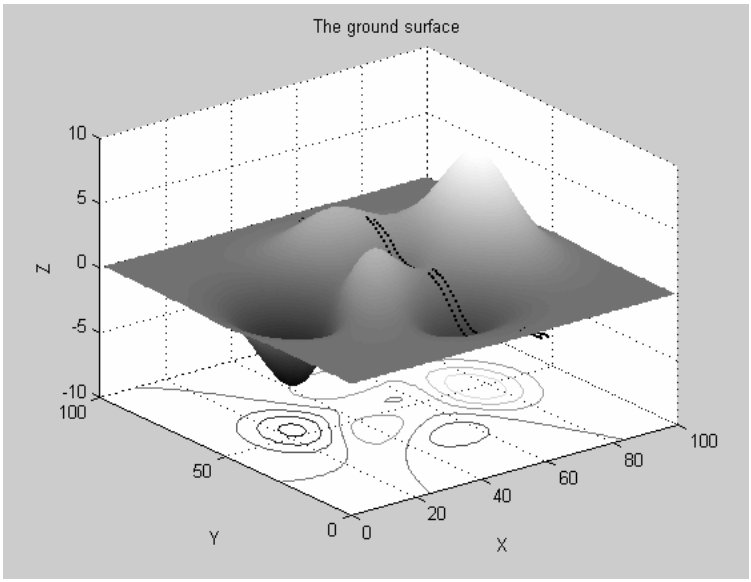

Figure (B-1): A rough terrain with a shown track of three-wheel mobile robot.

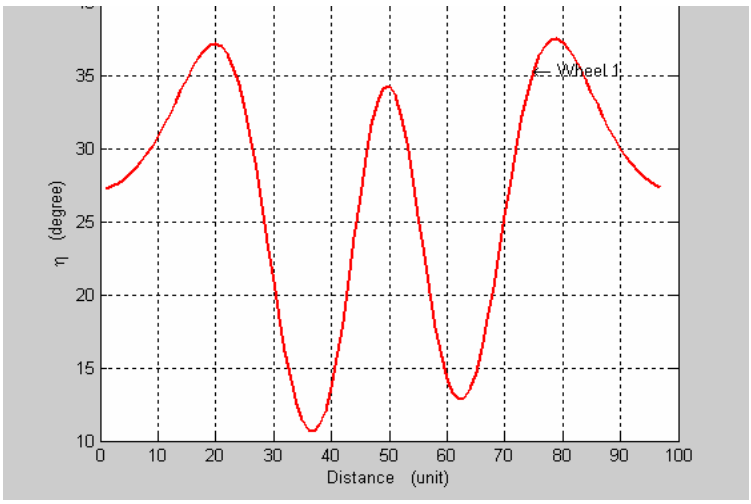

Figure (B -2): Three-wheel mobile robot stability margin according to wheel 1.

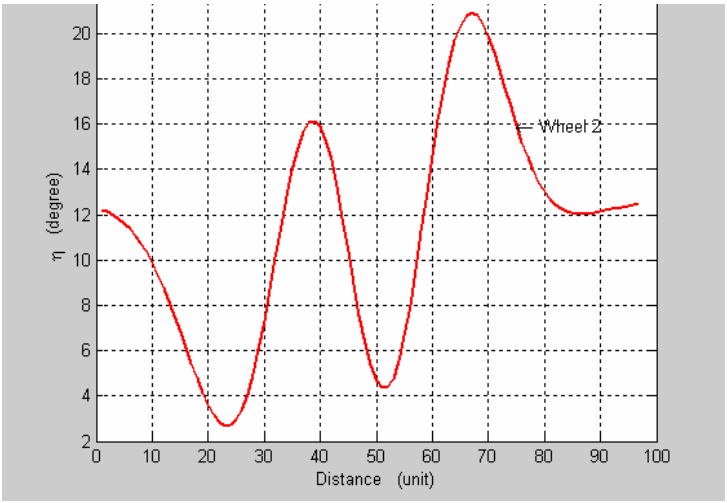

Figure (B -3): Three-wheel mobile robot stability margin according to wheel 2.

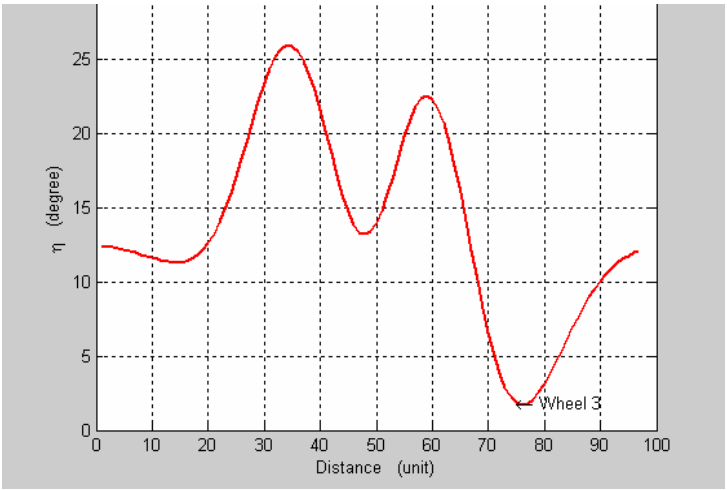

Figure (B -4): Three-wheel mobile robot stability margin according to wheel 3.

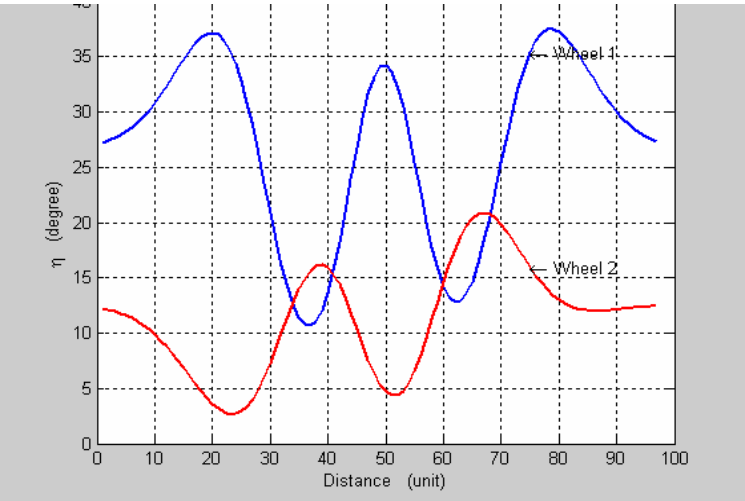

Figure (B -5): A combined graph of three-wheel robot stability margin at wheels 1 and 2.

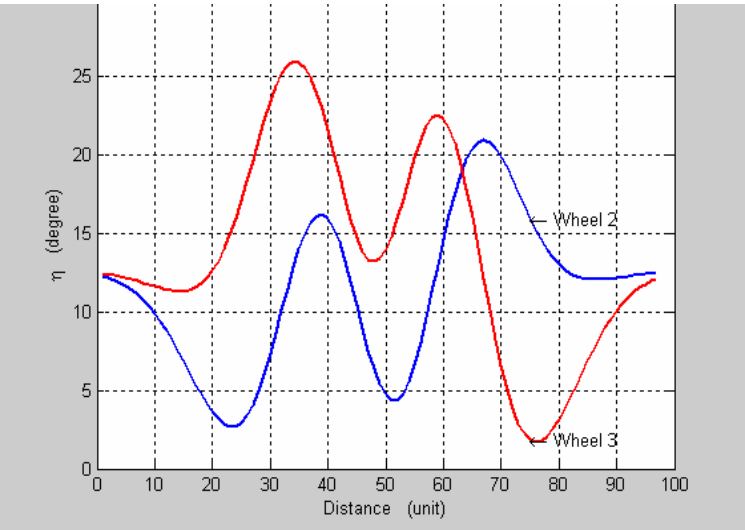

Figure (B -6): A combined graph of three-wheel robot stability margin at wheels 2 and 3.

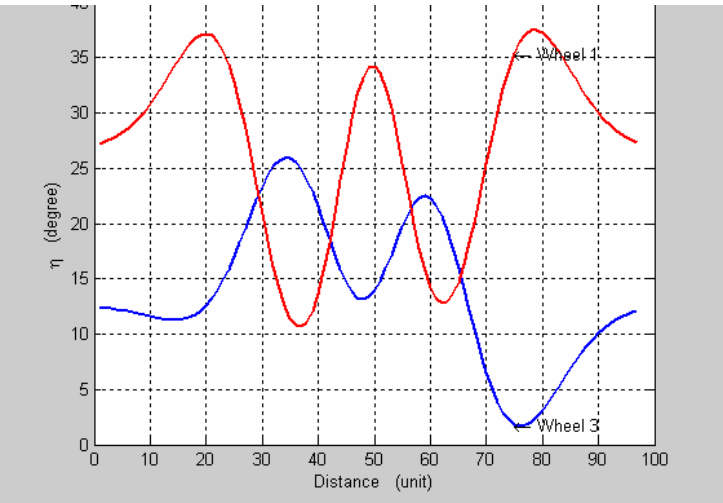

Figure (B -7): A combined graph of three-wheel robot stability margin at wheels 3 and 1.

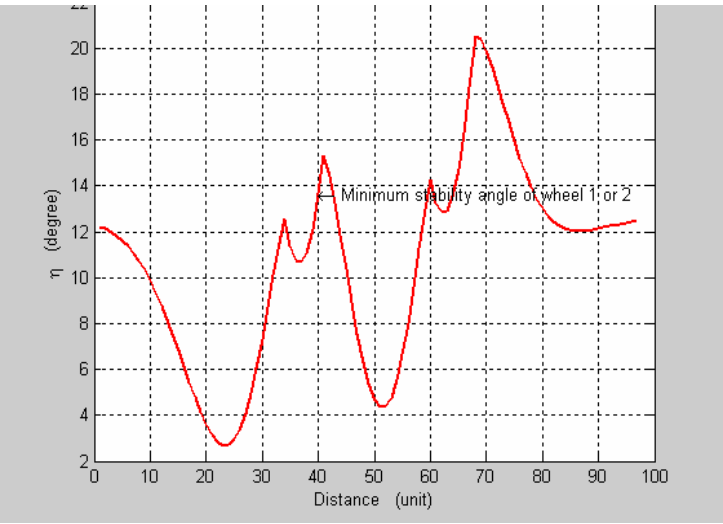

Figure (B -8): The minimum stability margin for the wheels 1 and 2.

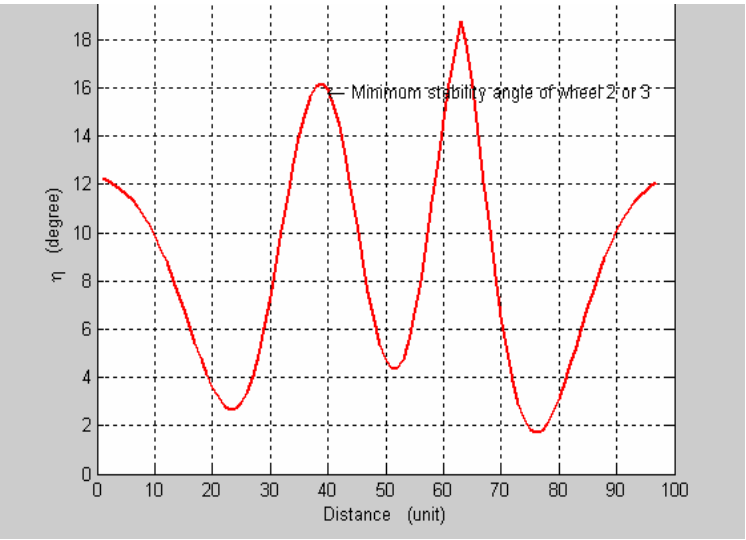

Figure (B -9): The minimum stability margin for the wheels 2 and 3.

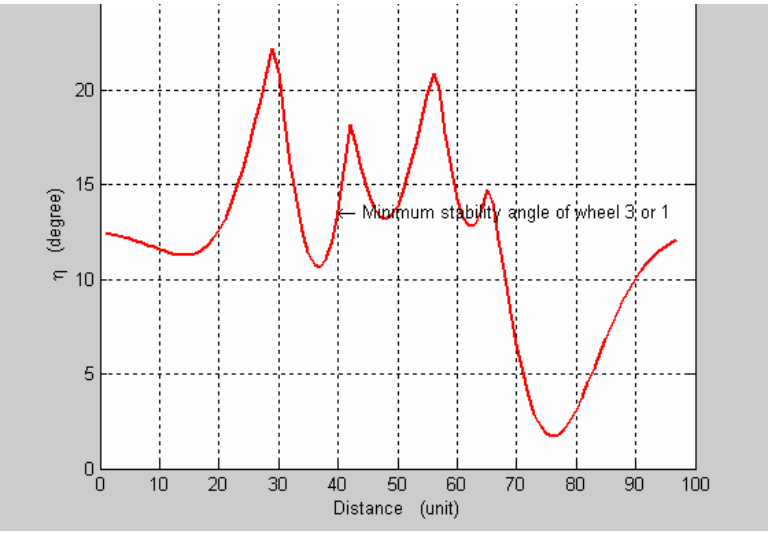

Figure (B -10): The minimum stability margin for the wheels 3 and 1.

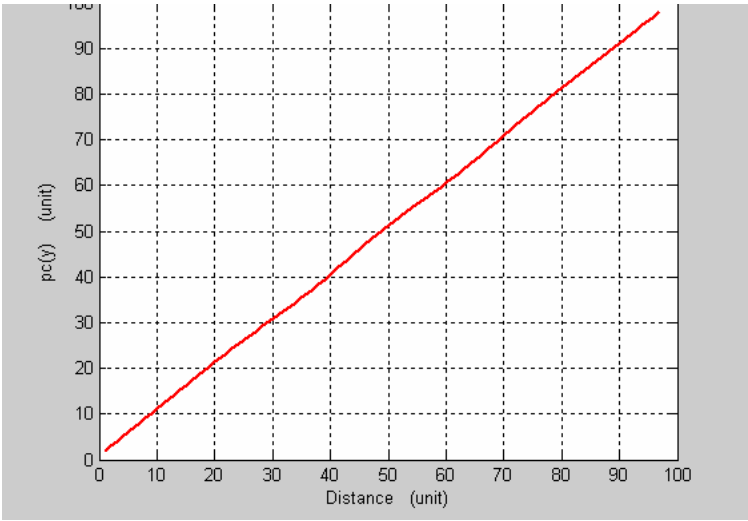

Figure (B -11): Center of mass in y-direction relative to the reference frame.

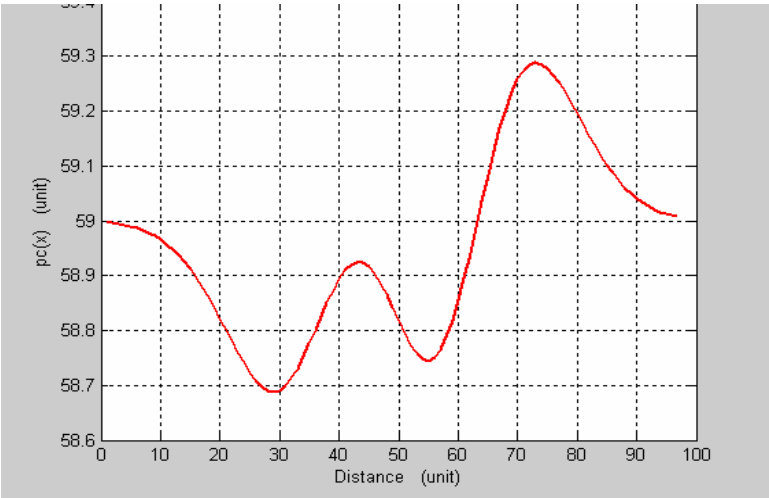

Figure (B -12): Center of mass in x-direction relative to the reference frame.

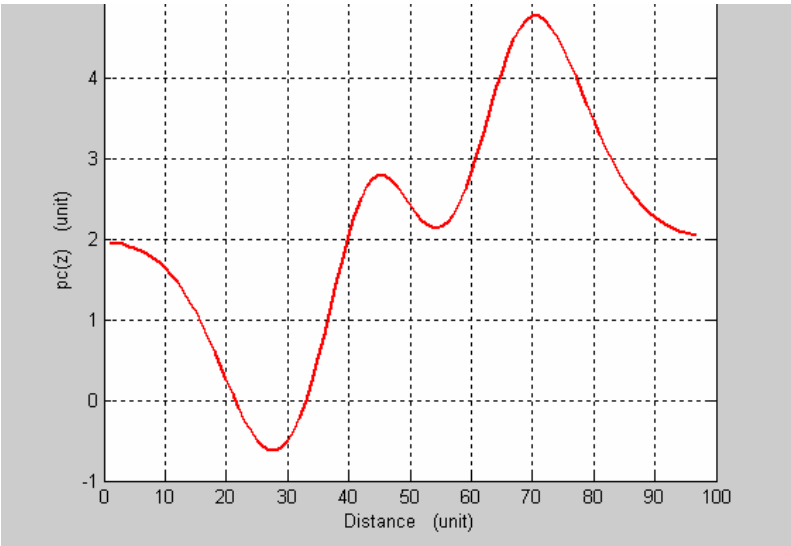

Figure (B -13): Center of mass in z-direction relative to the reference frame.

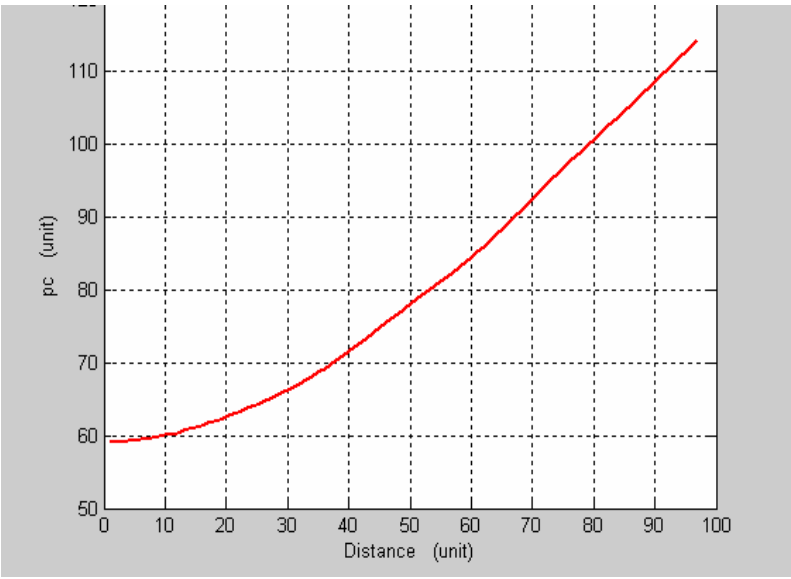

Figure (B -14): Center of mass distance magnitude relative to the reference frame.

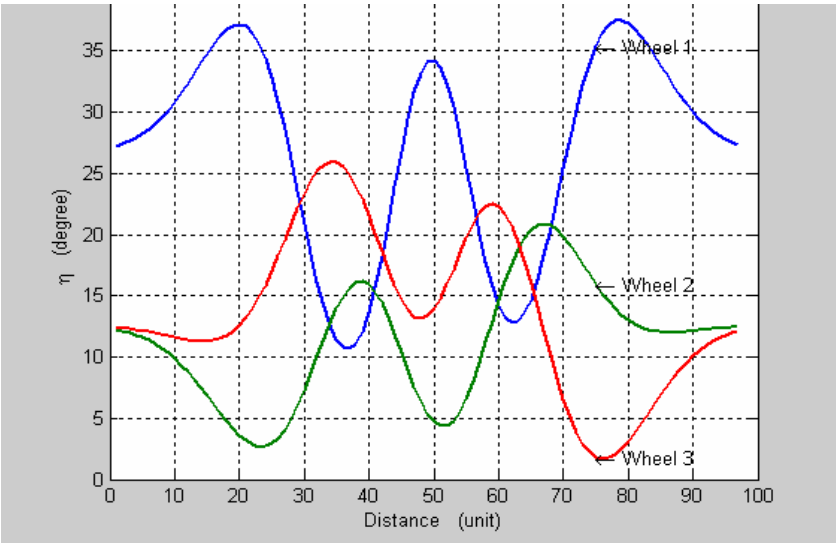

Figure (B -15): A combined graph of three-wheel mobile robot stability margin at the three wheels.

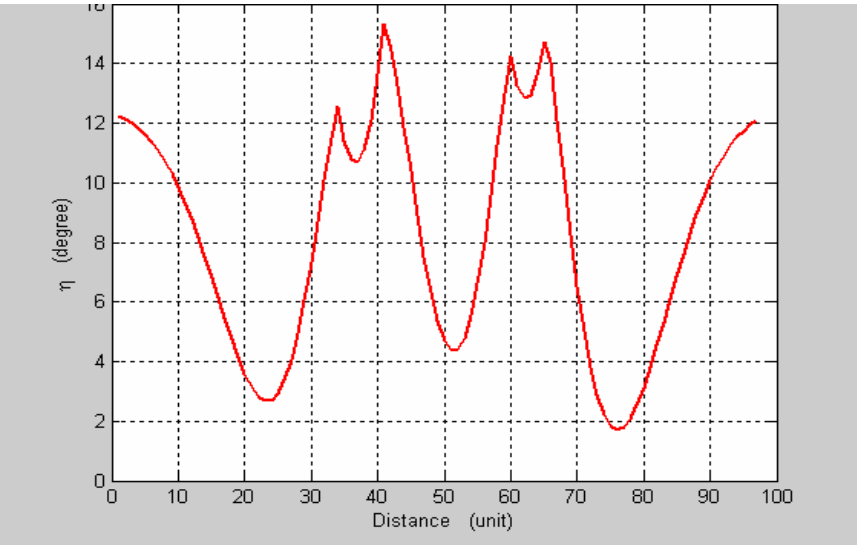

Figure (B -16): The minimum stability margin for the all three wheels.

الاتزان الحركي لروبوت سيار متحرك على أرض وعرة

اعداد
أمجد ابراهيم مساد

المشرف
د.خلدون طهبوب

المشرف المشارك
د.موسى عبدالله

ملخص

أصبحت الروبوتات السيارة تستخدم بشكل متزايد للتحرك على الأراضي الوعرة، وتستخدم هذه الروبوتات في استكشاف الكواكب والإستطلاعات العلمية والأغراض العسكرية وأعمال المساعدة والإنقاذ. ويلاحظ أن هذه الروبوتات تتعرض أثناء حركتها لحالة من عدم الإتزان الحركي الناتج عن وعورة الأرض والتضاريس مما يعرضها في بعض الأحيان الى الإنقلاب وبالتالي عدم تأدية المهام الموكلة إليها بشكل ملائم.

إن هذا البحث يدرس ويحدد عملية الإتزان الحركي لهذه الروبوتات، وتقوم هذه الرسالة على دراسة بعض العوامل والمتغيرات التي تؤثر بشكل مباشر على آلية الإتزان، وهذه العوامل مبنية على تقييم مدى تأثير ميلان الأسطح ومقدار ارتفاع مركز الكتلة للروبوت عن سطح الأرض بالإضافة الى دراسة تأثير عدد العجلات وتوزيعها الهندسي على الأرض.

من أجل منع تعثر و وقوع الروبوت والمحافظة على الاتزان، تم افتراض وجود بندول مقلوب (Invert Pendulum) ومتواجد عند مركز الكتلة للروبوت بحيث يعمل على تغيير مركز الكتلة عند فقدان الاتزان.

لقد تمّ عمل برنامج محاكاة (simulation) عن طريق جهاز الحاسوب لتمثيل المعادلات الرياضية (model) بالشكل الأنسب وذلك باستخدام ملفات ال (Simulink) الخاصة بالبرمجة داخل برنامج ال (MATLAB) مع ملاحظة أن المعادلات الرياضية مأخوذة من أبحاث سابقة. كما تمّ عمل أراضي افتراضيّة وبأبعاد الفضاء الثلاثة بحيث تحاكي الأسطح الواقعية على الأرض الى حد كبير.

إنّ تحديد مقدار الإتزان مبنيّ على أساس حساب مقدار زاوية محصلة القوى (Force-Angle Stability Measure). حيث أنّ القوى بالمحصلة تمرّ من خلال مركز الكتلة للروبوت، لقد تمّ بحث مقدار الإتزان الحركي على روبوت متحرك ذو أربع عجلات وثلاث عجلات، كما تمّ تطبيق العديد من الأسطح المائلة والأراضي الوعرة وحتى الأسطح المستوية وجعل الروبوت يتحرك عليها. لقد كانت نتائج المحاكاة جيدة وذات فعالية، ويمكن تطبيق البرنامج على أرض الواقع وذلك من خلال بناء نموذج فيزيائي ومادي.

وبشكل عام، تمّ الحكم على الروبوت السيّار بصورة كبيرة من خلال حساب أقل إتزان حاصل على كلّ من العجلات الأربعة أو الثلاثة للروبوت. وكانت النتيجة الرئيسية تفيد بأن مقدار الإتزان الحركي ينخفض عندما يقلّ عدد عجلات الروبوت (و ذلك حسب توزيع هندسي مناسب لهذه العجلات على الأرض) وعندما يزيد مقدار الإرتفاع عن سطح الأرض وزيادة ميلان الأسطح.